



To Study and Evaluate the Interacting Partners of SERRATE in
Arabidopsis thaliana.

Dissertation

von der Fakultät für Mathematik und Naturwissenschaften

der Carl von Ossietzky Universität Oldenburg

zur Erlangung des Grades und Titels eines

Doktors der Naturwissenschaften

(Dr. rer. nat.)

angenommene Dissertation von

Frau. Shruti Sameer Pande

Geboren am 09.04.1994 in Jalgaon, Indien

Oldenburg

2022

Gutachter: Prof. Dr. Sascha Laubinger

Zweitgutachter: Prof. Dr. Dirk Albach

Tag der Disputation: 30.09.2022

**Success is not final,
Failure is not fatal,
It is the courage to continue that counts.**

-Winston Churchill

Erklärung



Hiermit versichere ich, dass ich die vorliegende Arbeit selbstständig verfasst und nur die angegebenen Hilfsmittel verwendet habe. Außerdem versichere ich, dass ich die allgemeinen Prinzipien wissenschaftlicher Arbeit und Veröffentlichung, wie sie in den Leitlinien guter wissenschaftlicher Praxis der Carl von Ossietzky Universität Oldenburg festgelegt sind, befolgt habe.

Oldenburg, den _____

Acknowledgements

The presented dissertation was carried out in Carl von Ossietzky Universität Oldenburg under the supervision of Prof. Dr. Sascha Laubinger. I would like to thank each and every person for their kind support and help to make this dream a reality.

I express my sincere gratitude towards Prof. Sascha Laubinger for giving me the opportunity to work in his wonderful lab. Thank you professor, for being very enthusiastic, cheerful, and helping me become the scientist I am. Thank you for being so kind and supportive throughout my time in the lab. It has been a pleasure learning all the new techniques and scientific values from you.

I also express my sincere gratitude to Prof. Dr. Dirk Albach for kindly agreeing to act as my second reviewer. Thank you so much for your valuable time and support. Furthermore, I would like to thank my third reviewer for their time and support. Your valuable comments and suggestions will be helpful for me to become a better scientist.

Additionally, I would like to thank every member of the Laubinger lab for sharing all the good experiences with me throughout my PhD. A special thanks to Svea, this PhD wouldn't have been possible without you. I am sincerely thankful for the relentless emotional support that you provided. Next, I would like to thank Sandra for being my constant lab partner and helping me write *zusammenfassung*. Thank you for being there for every stupid question I asked, all the happy dances, ice cream breaks and all the times you helped me go through the difficult phases of this PhD. I would also like to thank Emese for believing in me and pushing me to finish the PhD. Additionally, I would like to thank Udo, Anchillie, Joachim, Tamara, and Manon for being the best colleagues. It was fun having you guys in the lab and going on all the falafel parties. I would like to specially thank Joachim for analysing the RNA seq data in this study. I would also like to thank all the students Johanna, Alina, Amanda, Anton, Joon, Karina, Svenja, Imke and Carolin who have helped me advance in my experiments as well as contributing to the fun times we had in the lab. A special thanks to Thilo for being my SERRATE lab partner.

I would like to sincerely thank members of AG Albach, Prof. Albach and Prof. Laubinger for helping me be a part of the collaborative work which lead to a fine publication. Additionally, I would like

to thank members of AG Nolte and AG Nothwang for allowing me to use the instruments in their lab. I would also like to extend my gratitude towards to administrative department of IBU for helping me with all the bureaucratic work.

A big thank you to all my friends Shreya, Jaagni, Utkarsh, Indraani, Shreyas, Bhavishya, Neelkanth and Yoga for being sane at times as well as insane most of the times, fun, crazy, supportive and my second family in this foreign country. I call this my second home because of you guys. Cheers to all the crazy times, all the vacations and tons of food that we ate together. All these good times helped me push through the hard parts of the PhD.

I would also like to sincerely thank my parents, my sister, and my in-laws for believing in me. You guys are the reason I have managed to achieve the goals that we had planned together. Last but not the least, I would like to thank my husband Saurabh for being my constant unconditional support. Thank you for sharing some of the best times with me as well as being my strong pillar in the difficult times.

P.S. I sincerely apologize if I have forgotten anyone and would also like to extend my gratitude towards their help and support.

Table of Contents

| | |
|---|----|
| Erklärung..... | 4 |
| Acknowledgements..... | 5 |
| List of Figures and Tables | 10 |
| Abbreviations..... | 13 |
| Summary..... | 16 |
| Zusammenfassung | 18 |
| 1 Introduction..... | 20 |
| 1.1 SERRATE, an intrinsically disordered protein, has multiple functions <i>in Arabidopsis thaliana</i> | 20 |
| 1.2 Transcription factors are transcriptional regulators shaping the life cycle of organisms | 23 |
| 1.3 ALFIN1-LIKE proteins are plant specific stress regulatory proteins involved in transcriptional repression | 23 |
| 1.4 IAA32 and IAA34 are non-canonical transcriptional repressors..... | 24 |
| 1.5 TOE1 and TOE2, targets of miRNA172 are repressors of flowering | 25 |
| 1.6 Regulation of flowering in <i>Arabidopsis thaliana</i> | 28 |
| 1.7 Aim of this work..... | 30 |
| 2 Results and Discussion..... | 31 |
| 2.1 IP-MS analysis reveals SE interacts with six out of seven ALFIN1-LIKE proteins..... | 31 |
| 2.1.1 Yeast two hybrid and co-immunoprecipitation assays confirm interaction of AL and SE..... | 32 |
| 2.1.2 <i>al4 al5 al6 al7</i> mutant generation via CRISPR-Cas9 method revealed redundant functions among ALFIN1-LIKE proteins | 34 |

| | | |
|-------|--|----|
| 2.2 | Y2H transcription factor library screening revealed SE binds to 57 different TFs | 38 |
| 2.2.1 | Y2H and Co-IP assay corroborates interaction of TOEs and IAA34 with SE..... | 38 |
| 2.2.2 | <i>se-1 toe1-2 toe2-1</i> mutant shows defects in leaf initiation, leaf morphology, shorter juvenile phase, and an early flowering phenotype | 42 |
| 2.2.3 | <i>toe1-2 toe2-1 se-1</i> depicts serrated leaf, reduced leaf size and a slower leaf initiation rate | 42 |
| 2.2.4 | <i>toe1-2 toe2-1 se-1</i> has a significantly shorter juvenile phase | 45 |
| 2.2.5 | TOEs are epistatic to SE for flowering time | 45 |
| 2.2.6 | TOE1 and TOE2 do not influence the transcription of <i>MIRNA156</i> and processing of pri-miRNA156 | 47 |
| 2.2.7 | Expression profile of miR156-targets <i>SPL3</i> and <i>SPL10</i> | 49 |
| 2.2.8 | Expression profile of <i>MIRNA172A</i> and levels of miR172a/b. | 51 |
| 2.2.9 | Transcriptomic analysis of <i>se-1, toe1-2 toe2-1</i> and <i>toe1-2 toe2-1 se-1</i> | 53 |
| 3 | Conclusion | 55 |
| 4 | Outlook:..... | 58 |
| 5 | Materials and Chemicals..... | 59 |
| 6 | Methods | 60 |
| 6.1 | Molecular biological methods | 60 |
| 6.1.1 | Polymerase Chain Reaction (PCR)..... | 60 |
| 6.1.2 | Gateway cloning:..... | 61 |
| 6.1.3 | Transformation of <i>Escherichia coli</i> and <i>Agrobacterium tumefaciens</i> | 61 |
| 6.1.4 | Yeast two hybrid assay | 62 |
| 6.1.5 | Co-Immunoprecipitation | 63 |
| 6.1.6 | SDS-PAGE and Western blotting..... | 64 |
| 6.1.7 | Isolation of total RNA and cDNA preparation | 64 |

| | | |
|--------|--|-----|
| 6.1.8 | Quantitative PCR (qPCR)..... | 65 |
| 6.1.9 | RNA library preparation, sequencing, and data analysis | 66 |
| 6.1.10 | Generation of CRISPR-Cas9 mutants | 67 |
| 6.2 | Plant based methods | 70 |
| 6.2.1 | Plant Growth conditions..... | 70 |
| 6.2.2 | Floral dip..... | 70 |
| 6.2.3 | <i>Nicotiana benthamiana</i> leaf infiltration | 70 |
| 6.2.4 | Crossing of plants | 71 |
| 6.2.5 | Selection of transgenic plants..... | 71 |
| 6.2.6 | Phenotypic analyses | 71 |
| 7 | References | 73 |
| 8 | Supplementary Data | 86 |
| 9 | Curriculum Vitae | 102 |

List of Figures and Tables

| | |
|--|----|
| Figure I 1: A summary of SE with its direct interaction partners and their diverse roles in plant development and transcriptional regulation..... | 22 |
| Figure I 2: Summary of the functions of TOE1 and TOE2 in <i>A. thaliana</i> | 27 |
| Figure I 3: A simplified summary of the regulation of flowering. Environmental and endogenous cues are integrated leading to activation of florigen <i>FT</i> . <i>FT</i> then triggers a cascade of events where multiple floral meristem-determining proteins and floral organ identity proteins are activated. | 29 |
| Figure R 1: Yeast two hybrid assay showing SE directly interacts with all seven ALFIN1-LIKE proteins..... | 32 |
| Figure R 2: Co-immunoprecipitation assay showing AL4, AL5 and AL7 interact with SE in planta. | 33 |
| Figure R 3: Generation of CRISPR-Cas9 mutants for ALFIN1-LIKE protein family. | 35 |
| Figure R 4: Gel electrophoresis images of genotyping PCR for <i>al</i> CRISPR mutants..... | 36 |
| Figure R 5: Alignment of gDNA sequences of <i>AL4</i> and <i>AL7</i> with sequenced amplicon..... | 37 |
| Figure R 6: Yeast two hybrid assay showing SE directly interacts with TOE1, TOE2 and IAA34... | 40 |
| Figure R 7: Co-IP studies show TOE1 and IAA34 interact with SE in planta. | 41 |
| Figure R 8: Phenotype of WT, <i>se-1</i> , <i>toe1-2 toe2-1</i> and <i>toe1-2 toe2-1 se-1</i> plants under long day condition. | 44 |
| Figure R 9: Phase transition and flowering time experiments..... | 46 |
| Figure R 10: Expression profile of pri-miRNA156a and levels of miR156 analysed using qPCR. ... | 48 |
| Figure R 11: Expression profile of <i>SPL3</i> and <i>SPL10</i> transcripts using qPCR..... | 50 |
| Figure R 12: Expression profile of <i>MIRNA172A</i> and levels of miR172a/b transcripts in leaves analysed using qPCR. | 52 |
| Figure R 13: Venn diagrams from RNA-seq data | 54 |
| Figure R 14: Hypothetical model of SE involved in transcription regulation via interaction with TFs..... | 57 |

| | |
|---|----|
| Supplementary Figure 1: Western blot images showing the Input and Co-IP for AL1, AL2 and AL4. | 86 |
| Supplementary Figure 2: Western blot images showing the Input and Co-IP for AL3. These images are the full images for Figure 2. | 87 |
| Supplementary Figure 3: Western blot images showing the Input and Co-IP for AL5, AL6 and AL7. These images are the full images for Figure 2. | 88 |
| Supplementary Figure 4: Complete western blot images showing the Input and Co-IP. These images are the full images for Figure 7. A) images of Co-IP from TOE1 B) Images of Co-IP from IAA34. | 89 |
| Supplementary Figure 5: Western blot images from tobacco leaves transformed with vectors containing TOE2-mRFP and SE-HA. | 90 |
| Supplementary Figure 6: Leaf initiation rate. | 91 |
| Supplementary Figure 7: Line graph showing the relative expression of genes and miRNAs. | 92 |
| Supplementary Figure 8: Venn diagrams of DEGs in <i>se-1</i> , <i>toe1-2</i> <i>toe2-1</i> and triple mutant. | 93 |
| | |
| Table R 1: List of AL proteins purified with SE complex. | 31 |
| | |
| Table M 1: PCR mix. All volumes are in μL | 60 |
| Table M 2 PCR program | 61 |
| Table M 3: Antibiotics list. | 62 |
| Table M 4 PCR program for cDNA synthesis of miRNA using stemloop oligonucleotides. | 65 |
| Table M 5: qPCR reaction mixture and program. | 66 |
| Table M 6: Reaction mixture and incubation cycle for cloning sgRNAs into shuttle vectors. | 68 |
| Table M 7: Reaction mixture and incubation cycle for cloning shuttle vectors into destination vector. | 69 |

Supplementary table 1: No of days until bolting for WT, *se-1*, *toe1-2 toe2-1* and *toe1-2 toe2-1 se-1*. 94

Supplementary table 2: List of primers used in the study..... 98

Supplementary Table 3: List of transformants generated in this study. List of mutants used in this study. 99

Supplementary table 4: List of constructs generated in this study. 101

Abbreviations

| | |
|----------|--|
| °C | Degree Celsius |
| ~ | approximately |
| AD | Activation domain |
| ADE | Adenine |
| AL | ALFIN1-LIKE |
| ATP | Adenosine Triphosphate |
| BD | Binding domain |
| bp | Base pairs |
| cDNA | Complementary Deoxyribonucleic acid |
| CHIP | Chromatin immunoprecipitation |
| Col-0 | Columbia-0 |
| Co-IP | Co-immunoprecipitation |
| CSM | Complete supplement mixture |
| Ct | Cycle threshold |
| DEG | Differentially expressed genes |
| dNTP | Deoxyribonucleotide triphosphate |
| EAR | Ethylene responsive element binding factor-associated Amphiphilic Repression |
| F | Forward (primer) |
| FAST | Fluorescence accumulating seed technology |
| FC | Fold change |
| HA | Hemagglutinin |
| HIS | histidine |
| hr | hours |
| IAA32/34 | INDOLE3 ACETIC ACID 32/34 |
| IP-MS | Immunoprecipitation- mass spectrometry |
| KB | Kilo base pairs |
| KDa | Kilo Dalton |

| | |
|-----------|--|
| LB | Lysogeny Broth |
| LiAc | Lithium Acetate |
| min | minutes |
| miRNA | Micro Ribonucleic acid |
| mRFP | Monomeric Red Fluorescence Protein |
| MS | Murashige Skoog |
| No. | number |
| n.s. | Not significant |
| PAM | protospacer adjacent motif |
| PBS | Phosphate buffered saline |
| PCR | Polymerase chain reaction |
| PEG | Polyethylene Glycol |
| primiRNA | Primary micro-Ribonucleic acid |
| qPCR | Quantitative Polymerase chain reaction |
| R | Reverse (primer) |
| RNA seq | Ribonucleic acid sequencing |
| RT | Room Temperature |
| s | seconds |
| ss-DNA | Single strand Deoxyribonucleic acid |
| SD | Standard deviation |
| SDS-PAGE | Sodium dodecyl sulphate polyacrylamide gel |
| SE | SERRATE |
| Ser2/Ser5 | Serine 2/ Serine 5 |
| sgRNA | Single guide Ribonucleic acid |
| T-DNA | Transfer Deoxyribonucleic acid |
| TOE1/2 | TARGET OF EARLY ACTIVATION TAGGED 1/2 |
| TPM | Transcripts per kilobase million |
| -WL | Without Tryptophan, Leucine |
| -WLH | Without Tryptophan, Leucine, Histidine |

| | |
|-------|---|
| -WLHA | Without Tryptophan, Leucine, Histidine, Adenine |
| WT | Wild type |
| w/v | weight /volume |
| Y2H | Yeast two Hybrid |
| YPDA | Yeast peptone dextrose adenine |

Summary

SERRATE is a multifunctional protein mainly studied for its role in miRNA biogenesis. It has two intrinsically disordered regions and thus can act as a scaffold and bind to numerous proteins. Recent studies revealed an unprecedented role of SE in transcriptional regulation of protein coding genes. It binds to a subset of majorly intronless genes and enhances their expression. Previous information hinted that SE possibly binds to these loci via protein-protein interactions. This study aims at investigating the multiple interacting partners of SE mainly focusing on transcription factors (TFs). Immunoprecipitation-mass spectrometry (IP-MS) and yeast two hybrid (Y2H) library screening of transcription factors were performed to obtain a list of interacting partners.

Y2H library screening revealed that SE directly binds to 57 TFs from multiple families. Additionally, IP-MS indicated it binds to the ALFIN1-LIKE protein family involved in stress regulation. To confirm these interactions, yeast two hybrid assays followed by co-immunoprecipitation (Co-IP) was performed. The Y2H assay revealed all seven ALFIN1-LIKE proteins directly bind to SE. Furthermore, it also directly interacts with TOE1, TOE2 from the AP2-like family and IAA34 from the IAA/AUX family. Co-IP experiments demonstrated that SE binds to AL4, AL5, AL7, TOE1 and IAA34 *in planta*.

Attempts were made to investigate the functional role of SE interacting with TFs. For this, CRISPR-Cas mutants for *ALFIN1-LIKE* genes were generated. The *al4 al5 al6 al7* mutant revealed a strong redundancy among all the proteins of this family. Apart from this, functional role of SE and TOEs was studied. *se-1* and *toe1-2 toe2-1* showed defects in leaf initiation rate, leaf morphology and phase transition and had an early flowering phenotype. A triple mutant generated by crossing *se-1* and *toe1-2 toe2-1* demonstrated defects in leaf initiation rate, leaf morphology and phase transition which were mainly due to an additive effect of *se-1* and *toe1-2 toe2-1*. Interestingly, the triple mutant exhibited no difference in flowering time compared to the double mutant. This indicates that *TOEs* are epistatic to *SE*.

Expression profiles of *MIRNA156A/172A*, levels of mature miR156a/miR172a/b and their respective targets in mutants revealed SE and TOEs independently affect phase transition by influencing miR156 processing and modulating levels of *SPLs* respectively. No changes in miR172a/b showed neither SE nor TOEs affect its abundance and indicate that they might be acting downstream of miR172 in terms of flowering. Global RNA sequencing analysis revealed a significant overlap of differentially expressed genes (DEGs) between *se-1* and *toe1-2 toe2-1*. These DEGs included upregulated flowering-related genes which act downstream of *FLOWERING LOCUS T*.

Zusammenfassung

SERRATE ist ein multifunktionales Protein, das hauptsächlich wegen seiner Rolle bei der miRNA-Biogenese untersucht wurde. Es besitzt zwei intrinsisch ungeordnete Regionen und kann daher als Gerüstprotein dienen und an zahlreiche Proteine binden. Jüngste Studien haben gezeigt, dass SE bei der Transkriptionsregulierung von proteinkodierenden Genen eine bisher nicht gekannte Rolle spielt. Es bindet an eine Untergruppe von weitgehend intronlosen Genen und verstärkt deren Expression. Frühere Informationen deuteten darauf hin, dass SE möglicherweise über Protein-Protein-Wechselwirkungen an diese Loci bindet. Ziel dieser Studie ist es, die vielfältigen Interaktionspartner von SE zu untersuchen, wobei der Schwerpunkt auf Transkriptionsfaktoren (TFs) liegt. Um eine Liste der interagierenden Partner zu erhalten, wurden Immunpräzipitation-Massenspektrometrie (IP-MS) und ein Screening von Hefe-Zwei-Hybrid-Library (Y2H) von Transkriptionsfaktoren durchgeführt.

Das Y2H-Library Screening ergab, dass SE direkt an 57 TFs aus mehreren Familien bindet. Zusätzlich zeigte die IP-MS, dass es an die ALFIN1-LIKE-Proteinfamilie bindet, die an der Stressregulierung beteiligt ist. Zur Bestätigung dieser Wechselwirkungen wurden Hefe-Zwei-Hybrid-Assays mit anschließender Co-Immunopräzipitation (Co-IP) durchgeführt. Der Y2H-Assay zeigte, dass alle sieben ALFIN1-LIKE-Proteine direkt an SE binden. Darüber hinaus interagiert es auch direkt mit TOE1, TOE2 aus der AP2-like Familie und IAA34 aus der IAA/AUX-Familie. Co-IP-Experimente zeigten, dass SE *in planta* an AL4, AL5, AL7, TOE1 und IAA34 bindet.

Es wurde versucht, die funktionelle Rolle von SE in Wechselwirkung mit TFs zu untersuchen. Zu diesem Zweck wurden CRISPR-Cas-Mutanten für *ALFIN1-LIKE* Gene erzeugt. Die Mutante *al4 al5 al6 al7* zeigte eine starke Redundanz zwischen allen Proteinen dieser Familie. Darüber hinaus wurden die funktionellen Rollen von SE und den TOEs untersucht. *se-1* und *toe1-2 toe2-1* zeigten Defekte bei der Blattinitiationsrate, der Blattmorphologie und dem Phasenübergang und hatten eine frühere Blütezeit. Eine Dreifachmutante, die durch Kreuzung von *se-1* und *toe1-2 toe2-1* erzeugt wurde, wies Defekte bei der Blattinitiationsrate, der Blattmorphologie und dem Phasenübergang auf, die hauptsächlich auf einen additiven Effekt von *se-1* und *toe1-2 toe2-1* zurückzuführen waren. Interessanterweise wies die Dreifachmutante im Vergleich zur

Doppelmutante keinen Unterschied in der Blütezeit auf. Dies deutet darauf hin, dass *TOEs* epistatisch zu *SE* sind.

Die Expressionsprofile von *MIRNA156A/172A*, der Gehalt an reifen miR156a/miR172a/b und ihrer jeweiligen Targets in den Mutanten zeigten, dass *SE* und *TOEs* den Phasenübergang unabhängig voneinander beeinflussen, indem sie die miR156-Verarbeitung beeinflussen bzw. den Gehalt an SPLs modulieren. Keine Veränderungen bei miR172a/b zeigten, dass weder *SE* noch *TOEs* die Menge von miR172 a/b beeinflussen, was darauf hindeutet, dass sie in Bezug auf die Blüte möglicherweise stromabwärts von miR172 wirken. Die Analyse der globalen RNA-Sequenzierung ergab eine signifikante Überschneidung von differentiell exprimierten Genen (DEGs) *zwischen se-1 und toe1-2 toe2-1*. Zu diesen DEGs gehörten hochregulierte, mit der Blüte zusammenhängende Gene, die stromabwärts von *FLOWERING LOCUS T* wirken.

1 Introduction

1.1 SERRATE, an intrinsically disordered protein, has multiple functions *in Arabidopsis thaliana*

SERRATE (SE), a C2H2-type zinc finger protein, is highly conserved among plants, drosophila as well as animals (Prigge & Wagner, 2001; Sabin et al., 2009; Wilson et al., 2008). It is a multifunctional protein, majorly studied for its role in miRNA biogenesis (Lobbes et al., 2006; Yang et al., 2006a). Earlier reports suggested that SE directly influences the enzymatic activity of DICER-LIKE 1 (DCL1) promoting maturation of miRNA from primary miRNA (Dong et al., 2008; Iwata et al., 2013). Recent studies clarified that SE rather acts as a scaffold to recruit HYPONASTIC LEAVES 1 (HYL1) and DCL1 into the Dicer bodies by mediating liquid-liquid phase separation (Xie et al., 2021). SE also regulates the degradation of pri-miRNA by directly interacting with zinc knuckle proteins ZCCHC8A/ZCCHC8B, components of the nuclear exosome targeting (NEXT) complex (Bajczyk et al., 2020a). Moreover, SE binds to CHROMATIN REMODELLING FACTOR 2 (CHR2), ATPase subunit of SWI/SNF complex (switch/sucrose non-fermentable). SE-CHR2 attenuate miRNA accumulation by remodelling secondary structure of pri-miRNA (Z. Wang et al., 2018). Thus, SE is involved in both attenuation/degradation of pri-miRNAs upstream of the microprocessor activity as well as promoting maturation of miRNAs.

In addition to its role in miRNA processing, SE along with the CAP BINDING COMPLEX (CBC) contributes to alternative splicing of pre-mRNA (Laubinger et al., 2008; Raczynska et al., 2014). It also regulates transposable elements (TE) expression by binding to histone methyltransferases ATXR5/6 (Ma et al., 2018). A human ortholog of SE, ARSENIC RESISTANCE PROTEIN 2 (ARS2), contributes to certain aspects of RNA metabolism like RNA transport, 3' end formation, biogenesis of non-coding RNA and RNA stability (Gruber et al., 2012; Hallais et al., 2013; Melko et al., 2020).

Taken together, SE can perform a wide range of functions by interacting with multitude of proteins (Figure I 1). Further structural analysis of SE and ARS2 revealed unstructured regions at the N and C terminal, indicating SE might be an intrinsically disordered protein (IDP) (Machida et

al., 2011; Schulze et al., 2018; Lin Wang et al., 2022). Due to its intrinsic property of conformation flexibility, IDPs can act as a scaffold for adherence of multiple proteins (Fung et al., 2018). Thus, SE/ARS2 shows an ability to bind to a wide range of proteins involved in diverse functions in plants as well as in animals.

A recent study demonstrated an unexpected and pivotal role of SE in transcriptional regulation of protein coding genes. SE associates with approx. 1000 genes which are majorly intronless or intron poor (Speth et al., 2018). It has been observed across kingdoms that intron containing genes have a higher expression as introns tend to enhance the expression of its gene. Thus, intronless genes are poorly expressed (Le Hir et al., 2003). In contrast to this trend, a subset of SE-associated intronless genes showed enhanced expression. This enhancement of transcription was mainly due to the association of SE with Ser2 and Ser5 phosphorylated RNA Polymerase II complex during transcriptional pausing and elongation respectively. SE-associated intronless genes were majorly stress regulatory proteins. This indicated yet another possible novel role of SE in stress regulation. Upon further investigation of transcriptome of SE-target genes, a significant proportion of genes were upregulated in *se-1* mutant. Consequently, it indicates SE could also act as a transcriptional repressor (Speth et al., 2018).

This raises a very interesting question: what are the trans-regulating factors that interact with SE and recruit it at these specific Arabidopsis loci? One of the major DNA binding proteins involved in transcriptional regulation are transcription factors (TFs). This research aims to investigate if SE could interact with TFs to mediate transcriptional regulation of protein coding genes.

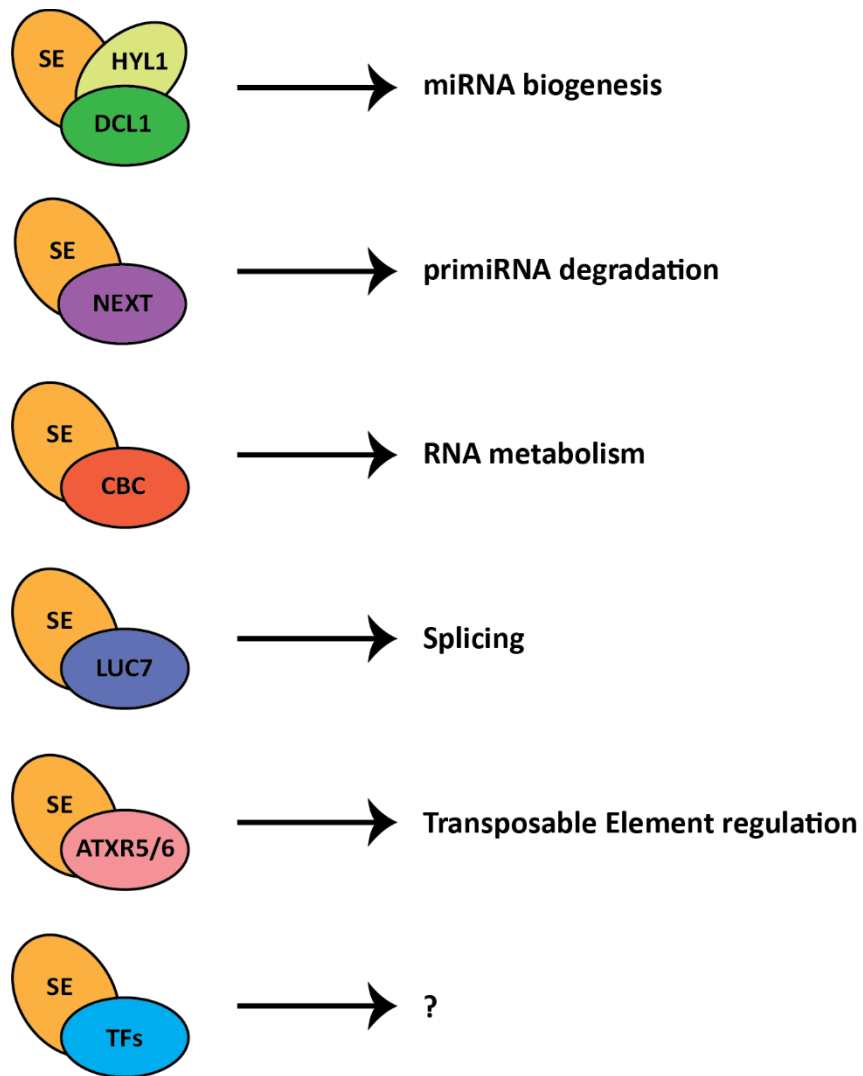


Figure I 1: A summary of SE with its direct interaction partners and their diverse roles in plant development and transcriptional regulation.

1.2 Transcription factors are transcriptional regulators shaping the life cycle of organisms

Transcription factors are proteins which regulate cellular processes by directly binding to specific conserved DNA sequences, generally in the promoter region of genes. TFs are considered to play a central role in evolution of species (Doebley, 1993). A typical plant TF contains a DNA binding domain, a nuclear localization signal, an oligomerization region and a transcriptional regulation domain (L. Liu et al., 1999). TFs are categorized into families according to the conserved functional domain and/or the conserved DNA sequence to which it binds. They have the ability to interact with other transcription factors, chromatin remodellers, and transcriptional machinery, etc. Based on their functional domain or their interacting partners, TFs can both activate or repress transcription of genes as well as regulate the rate of transcription (Dai et al., 2013).

In this research, a few families of TFs *viz.* ALFIN1-LIKE, IAA/AUX, and AP2-like family will be studied in further detail. Representative TFs from these families are specifically transcriptional repressors and are involved in diverse plant functions.

1.3 ALFIN1-LIKE proteins are plant specific stress regulatory proteins involved in transcriptional repression

ALFIN1-LIKE (AL) proteins are seven plant specific TFs belonging to the plant homeodomain (PHD) finger protein family. *A. thaliana* AL proteins have approx. 50-60% amino acid sequence identity to *alfalfa* AL1, hence the name alfin1-like (Wei et al., 2015). They have two conserved domains, PHD at the C terminal and PAL (PHD associated AL) domain at the N terminal (Molitor et al., 2014; Wei et al., 2015). PHD enables AL proteins to bind to H3K4me2/me3 (active transcription state) and act as readers of these histone post-translational modifications (Liang et al., 2018). AL proteins, specifically AL2, AL6 and AL7 interact with Polycomb Repressive Complex 1 (PRC1) core components AtBMI1b and AtRING1a (Molitor et al., 2014). PRC1 establishes a repressive chromatin state by docking at H3K27me3 and subsequently monoubiquitinating H2A (Simon &

Kingston, 2009). Thus, AL proteins in alliance with PRC1 complex, initiate a switch from the H3K4me active state to the H3K27me repressive state of transcription. This switch of transcriptional state occurs during seed germination and results in repressing of seed development-related genes (Molitor et al., 2014).

Additionally, AL4, AL5, AL6 and AL7 bind to the SWI/SNF2 RELATED 1 (SWR1) complex which mainly catalyses the exchange of H2A-H2B nucleosome with H2A.Z-H2B dimer. Inclusion of H2A.Z into the chromatin affects nucleosome structure stability. SWR1 complex plays a pivotal role in DNA damage repair, stress regulation, and flowering time (Aslam et al., 2019). AL5 is also directly involved in the abiotic stress response by binding to certain genes having a negative regulatory role and repressing their transcription (Wei et al., 2015). Additionally, AL6 induces root elongation when the plant faces phosphate starvation (Chandrika et al., 2013). On the contrary, AL7 plays a negative role in salt stress tolerance (Song et al., 2013). Thus, taken together AL proteins are mainly involved in transcriptional repression, and it may occur via PRC1 by inducing a chromatin state switch. They are also majorly involved in stress regulation having different roles. In this study, interaction of these plant specific stress regulatory AL proteins and SE will be tested. These interactions would hint towards a novel role of SE in stress regulation.

1.4 IAA32 and IAA34 are non-canonical transcriptional repressors

IAA32 and IAA34 belong to the IAA/AUX family of proteins. This family is known as early auxin response proteins and act as transcriptional repressors by interacting with AUXIN RESPONSIVE FACTORS (ARF) (Chandrika et al., 2013). Most proteins belonging to IAA/AUX family contain 4 typical conserved domains. Domain I is identified as the repressor EAR domain. Domain II is the auxin degron which plays a role in rapid protein turnover, and it also contains a bipartite nuclear localisation signal (NLS). Domain III includes the amphipathic $\beta\alpha$ -fold which is similar to DNA recognition motif and domain IV contains another NLS and an acidic region (Luo et al., 2018). Bioinformatic analysis revealed that IAA32 and IAA34 are the most divergent among the IAA/AUX family and do not contain domain II (Shimizu-Mitao & Kakimoto, 2014). A recent study demonstrated a role of IAA32 and IAA34 in maintaining the apical hook phenotype in seedlings of *A. thaliana*. Apical hook formation is important to prevent damage to the shoot apical

meristem while the seedling grows out of soil. Accumulation of auxin at the concave side of apical hook causes cleavage of TRANSMEMBRANE KINASE I (TMK1). C terminal of this cleaved TMK1 specifically interacts with and phosphorylates IAA32 and IAA34. Phosphorylation stabilizes these proteins thus repressing growth-related genes. (Cao et al., 2019). In this study, direct interaction of the non-canonical IAA and SE will be investigated.

1.5 TOE1 and TOE2, targets of miRNA172 are repressors of flowering

TARGET OF EARLY ACTIVATION TAGGED1 and 2 (TOE1 and TOE2) are transcription factors belonging to the AP2-like family. These proteins contain two putative DNA-binding APETALA2 (AP2) domains, an EAR-like motif (EARL) and a conserved miRNA172 binding sequence (Kim et al., 2006). Both the TOEs and other 4 members of the AP2-like family are targets of miRNA172 and are translationally inhibited (Aukerman & Sakai, 2003; Wu et al., 2009). TOE1 and TOE2 are mainly floral repressors but also play a critical role at multiple stages of the plant growth. They are expressed in a spatiotemporal manner with higher expression in the early stages of plant leading to a gradual decrease in the latter stages. This gradual decrease is mainly due to the age dependent increase in mature miRNA172 (Figure I 2A) (Aukerman & Sakai, 2003; Wu et al., 2009).

miRNA172b-TOE1/2 play a novel role in regulating the ontogeny of plant innate immunity at the seedling stage. Innate immunity response is induced by activating FLAGELLIN SENSING 2 (FLS2) which in turn triggers a cascade of events. Highly expressed TOEs directly bind to the promoter region of *FLS2* gene and inhibit its activity at the seedling stage. This decrease in *FLS2* expression is possibly due to an energy trade off between development and immunity. With increase in plant age, *FLS2* expression increases and strengthens the innate immunity response. (Figure I 2A) (Zou et al., 2018, 2020).

With progression of plant from seedling to juvenile stage, miRNA172-TOEs play a critical role in determining the juvenile epidermal identity of the plant. Production of trichomes on the abaxial side of the leaf is considered as marker for vegetative phase change (from juvenile to adult). TOEs promote the juvenile stage by inhibiting growth of trichome on the abaxial side of the leaf. This is carried out by direct interaction to KAN1. The KAN1-TOE complex then binds to the promoter region of *GLN1*, a gene necessary for trichome initiation, and represses its transcription (Long

Wang et al., 2019). Additionally miRNA172-TOE1/2 is important for the cytokinin-dependent regulation of vegetative phase change (Werner et al., 2021).

In reproductive stage of the plant, activity of TOE1/2 is regulated according to the circadian rhythm to ensure optimal vegetative development followed by flowering. TOE1/2 show an increased expression in the early morning and late afternoon under long day conditions. This enables the interaction of TOEs to CONSTANS (CO) and destabilizes CO protein. Thus, CO is unable to bind to *FLOWERING LOCUS T (FT)* leading to repression of its transcription. Additionally, TOEs also directly bind to *FT* gene and repress its transcription. Both these mechanisms prevent precocious flowering in the early morning till the appropriate daylight threshold has been reached in long day conditions (Figure I 2B) (B. Zhang et al., 2015a). Another level of floral regulation is via the CRYPTOCHROME (CRY) proteins. Blue light triggers the binding of CRY2 with TOE1 and TOE2. This in turn promotes the dissociation of TOE and CO rendering it free to bind to FKF1. CO-FKF1 forms a stable complex and promote the expression of *FT*. Furthermore, association of CRY2 and TOEs prevents TOEs from binding to *FT* directly (Figure I 2B) (Du et al., 2020).

To summarise, TOEs are transcriptional repressors which ensure proper vegetative growth before transitioning into next stage of development. Initially by preventing trichome formation on the abaxial side of leaves, TOEs ensure adequate development of plant in the juvenile stage. In the reproductive stage, it binds to different proteins and *FT* gene to inhibit precocious flowering in early morning. This ensures proper development and growth of the vegetative parts and ascertain that appropriate daylight threshold has reached for successful reproduction. Additionally, it also plays a novel role in the ontogeny of plant innate immunity. This study aims at testing the interaction of SE with TOEs and elucidating their functional role in plant development.

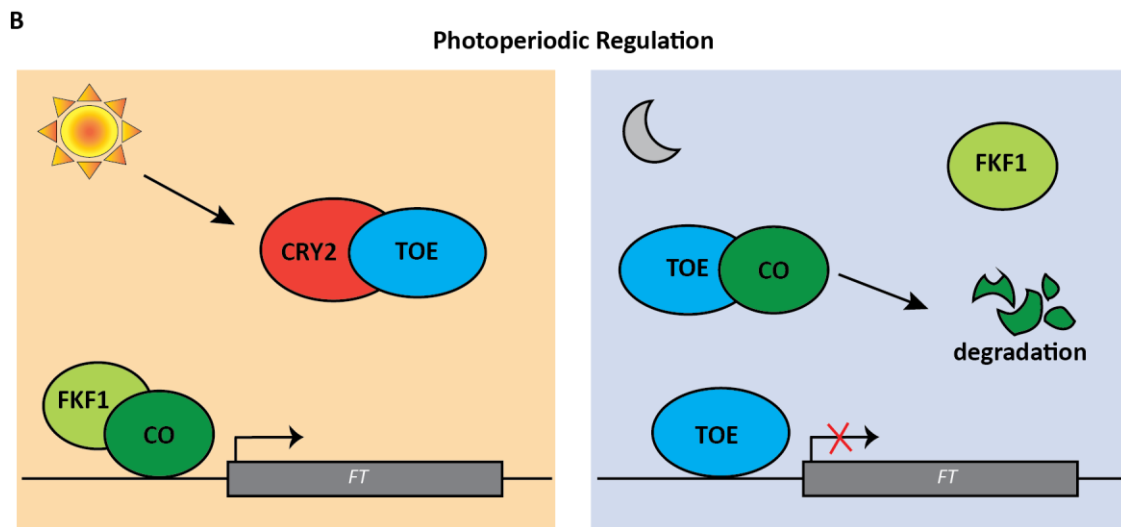
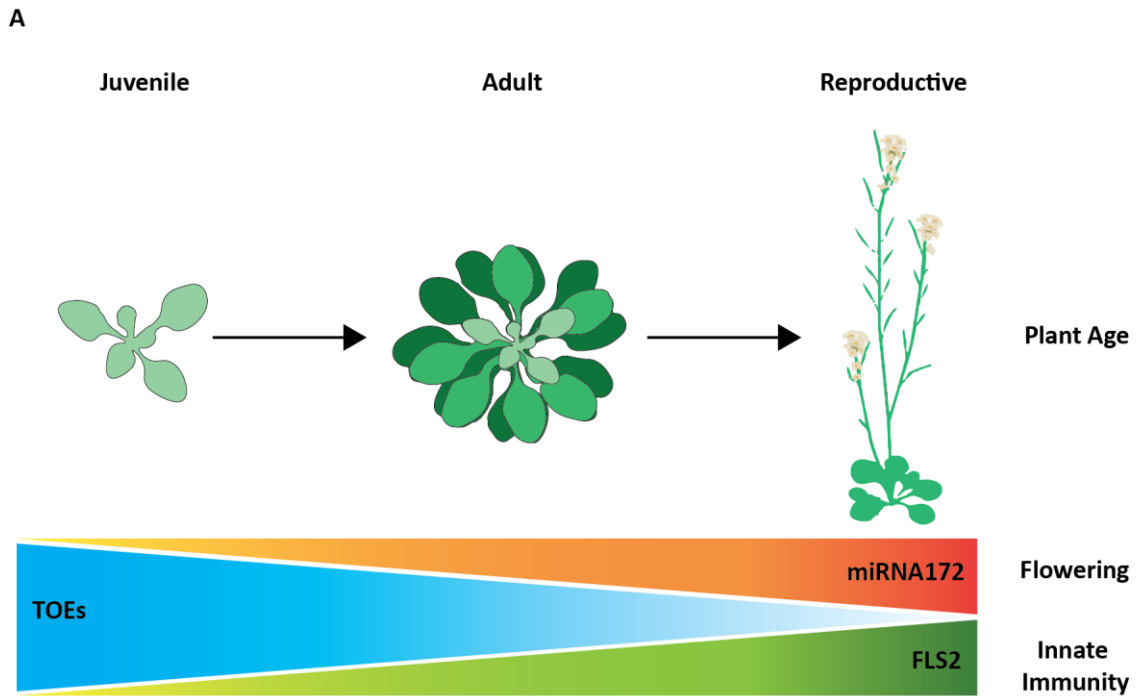


Figure I 2: Summary of the functions of TOE1 and TOE2 in *A. thaliana*.

A) Model showing abundance of TOEs throughout the plant life cycle leading to phase change and development of innate immunity. B) Model showing role of TOEs in flowering and repression of *FT*. Image of Arabidopsis plant adapted from biorender.com and edited using Adobe Photoshop 2022.

1.6 Regulation of flowering in *Arabidopsis thaliana*

Reproduction is an essential process for continuation and survival of species. In plants, the transition from vegetative to reproductive stage starts by formation of the inflorescence meristem followed by floral organ development. This transition takes place by production of the florigen FLOWERING LOCUS T (FT) which is transcribed in the companion cells of leaves and then transported to the shoot apical meristem (SAM). Transcription, translation and transport of FT and its homologues is tightly controlled and takes place by integrating environmental signals such as daylight, temperature, nutrients etc., along with endogenous cues like plant age (Chen et al., 2018; Schmid et al., 2003; Wigge et al., 2005). As mentioned earlier, flowering is induced only when the plant has reached its optimum vegetative growth. This is ensured by a combination of miRNA and its target TFs. With progression of plant age, miRNA172 levels increase leading to a translational inhibition of TOEs and its homologues (Aukerman & Sakai, 2003; Long Wang et al., 2019; B. Zhang et al., 2015b). This in turn reverses the repression of *FT* by TOEs and induces flowering (Figure I 3) (B. Zhang et al., 2015a). Similarly, external cues like photoperiodic signals also directly affects the transcription of *FT* via the central regulator *CO*. mRNA abundance of *CO* is directly influenced by circadian clock genes and accumulates in the late afternoon. Additionally, photoreceptor *CRY2* stabilises *CO* protein thus inducing *FT* expression (Putterill et al., 1995; B. Zhang et al., 2015b). Vernalization is also known to speed up flowering in *A. thaliana*. Vernalization inhibits floral repressor *FLOWERING LOCUS C (FLC)* which leads to activation of *FT*. All these pathways are also interlinked and affect each other (Figure I 3). Thus, the plant ensures a total conducive environment is available and then initiates flowering.

Production and transport of FT to SAM triggers a cascade of events. FT along with FD, a bZIP transcription factor, activates *SOC1 (SUPPRESSOR OF CONSTANS1)*, *LFY (LEAFY)*, *SWEET10*, etc (Andrés et al., 2020; Valverde et al., 2004). These genes then further activate floral meristem identity genes like *AP1 (APETALA1)*, *CAL (CAULIFLOWER)*, *FUL (FRUITFULL)* and floral organ determination genes.

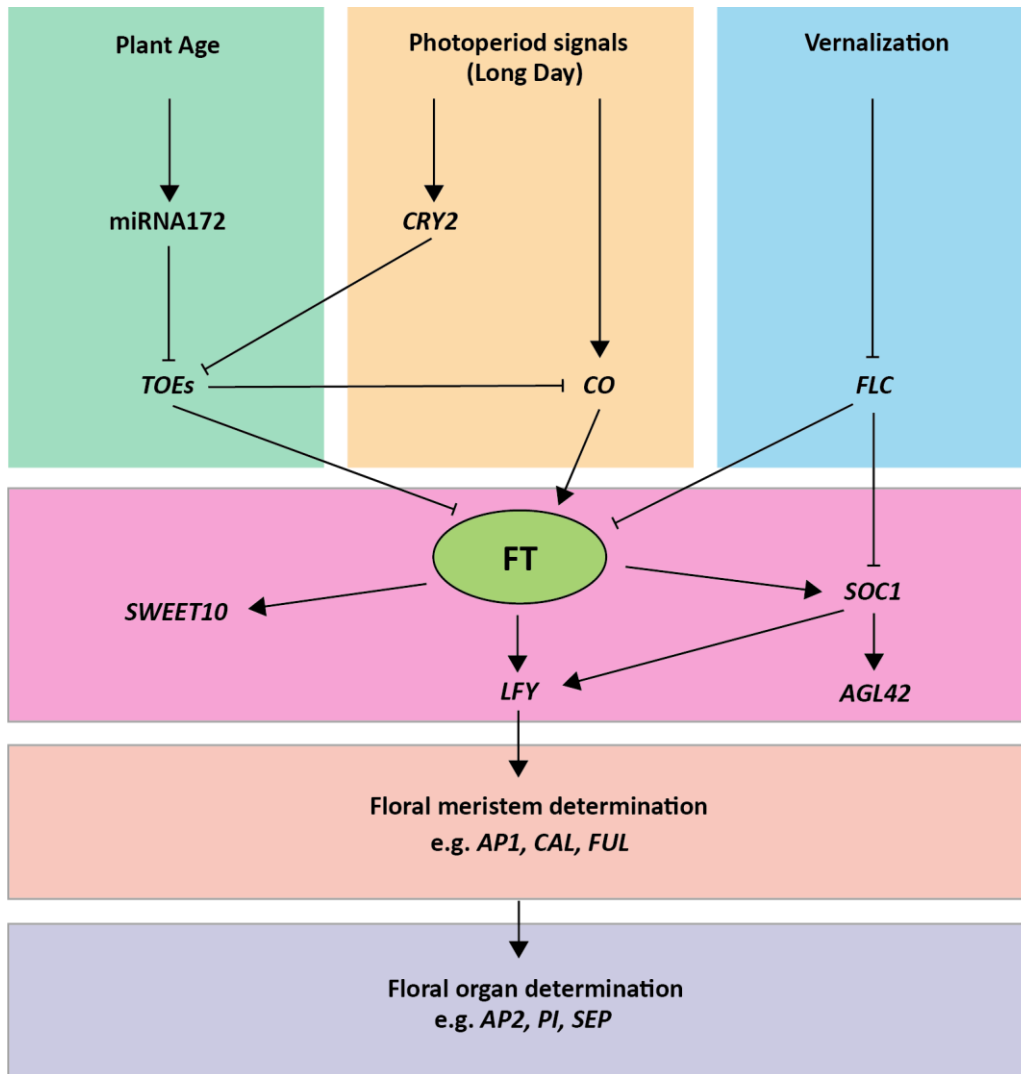


Figure I 3: A simplified summary of the regulation of flowering. Environmental and endogenous cues are integrated leading to activation of florigen *FT*. *FT* then triggers a cascade of events where multiple floral meristem-determining genes and floral organ identity genes are activated.

1.7 Aim of this work

SERRATE, is a multifunctional protein mainly studied for its role in miRNA biogenesis. Recent publications have given evidence that SE is an intrinsic disorder protein (IDP) and has an ability to bind to multiple proteins thus acting as a scaffold. Additionally, the publication by Speth et al., showed an unprecedented role of SE in transcription regulation of intronless genes. This regulation speculatively is carried out via protein-protein interactions.

Hence, this study aims at identifying interacting partners of SE especially focusing on transcription factors (TFs). This could aid in elucidating if TFs are the trans-regulatory factors involved in recruiting SE to a subset of intronless genes. Additionally, it would help in discovering other unknown remarkable functions of SE. To identify interacting partners, two methods *viz.* Immunoprecipitation-mass spectrometry (IP-MS) and yeast two hybrid library screening would be used. The IP-MS method would aid in isolating the whole interactome of SE, while yeast two hybrid library screening would focus on direct interaction of TFs with SE. Interaction of SE with candidate TFs obtained from these methods would then be reconfirmed by yeast two hybrid assay. Furthermore, these proteins would be expressed in *N. benthamiana* leaves followed by co-immunoprecipitation to check *in planta* interactions.

In the second part, the functional role of these interactions would be studied in *A. thaliana* by generating CRISPR-Cas9 mutants or by crossing T-DNA insertion lines. Phenotypic analysis would be carried out where the basic morphology, leaf initiation rate, phase transition and flowering time would be characterized. This research will shed light on the multiple interacting partners of SE and will lead to discovering new roles of SE in transcriptional regulation.

2 Results and Discussion

In order to identify proteins interacting with SE, two of the popular, reliable, and standard techniques were used in this research. The first was immunoprecipitation-mass spectrometry (IP-MS) technique which granted a way of discovering the entire interactome of SE while yeast-two-hybrid (Y2H) library screening provided a method to study direct interacting partners.

2.1 IP-MS analysis reveals SE interacts with six out of seven ALFIN1-LIKE proteins

Immunoprecipitation followed by mass spectrometric analysis provided a precise and quantitative way of studying large network of proteins interacting with SE. For this, mass spectrometry data from Speth et al (unpublished) and Bajczyk et al., 2020 were utilised. Speth et al., performed this experiment by immunoprecipitating SE and its interactome by using SE-specific antibody. While Bajczyk et al., used transgenic lines overexpressing AtSE:FLAG in the background of *se-1*. They then used antibody against FLAG tag and isolated SE and its multiple interacting partners. Both these analyses exhibited SE binds to proteins from the microprocessor complex, cap binding complex and the NEXT complex. Additionally, the data hinted that SE interacts with multiple stress regulatory proteins. Among these were six ALFIN1-LIKE (AL) plant specific transcription factors which are mainly known to be involved in abiotic stress response (Chandrika et al., 2013; Tao et al., 2018; Wei et al., 2015) (Table R 1).

| Protein | Reference |
|---------|--|
| AL2 | Speth et al. unpublished |
| AL3 | Speth et al. unpublished ; (Bajczyk et al., 2020b) |
| AL4 | Speth et al. unpublished |
| AL5 | (Bajczyk et al., 2020) |
| AL6 | Speth et al. unpublished |
| AL7 | Speth et al. unpublished ; (Bajczyk et al., 2020b) |

Table R 1: List of AL proteins purified with SE complex.

2.1.1 Yeast two hybrid and co-immunoprecipitation assays confirm interaction of AL and SE

Proteins binding to SE reported by IP-MS analysis could be a direct or indirect interaction. Thus, to test direct binding of ALFIN1-LIKE proteins, yeast-two-hybrid assay was performed. UAS-GAL4 system (Upstream Activator Site- GAL4) was used for this experiment where the GAL4 protein is split to separate the binding domain (BD) and activation domain (AD) (Fields & Song, 1989). SE was translationally fused to BD and ALFIN1-LIKE 1-7 were translationally fused with AD. Interaction between SE and AL proteins would allow the reconstituted GAL4 protein to bind to UAS. This would consequently activate the downstream histidine reporter gene which promotes the growth of yeast on media devoid of this amino acid (CSM-WLH). Yeast grown on CSM-WLH plates confirmed all seven ALFIN1-LIKE proteins directly bind to SE. Cells grown on CSM-WL media were used as a spotting control indicating that these cells contained both pGADT7 and pGBKT7 vectors. Spotting of AL1-7-AD with empty BD vector and SE-BD with empty AD vector was used as a negative control. These controls did not show any growth on CSM-WLH plates. Interaction of CBP20 with SE was used as a positive control which correctly showed cells growing on CSM-WLH media (Figure R 1).

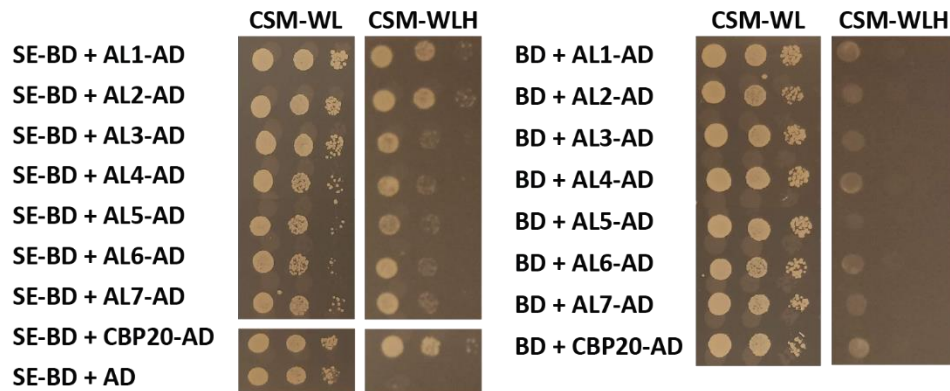


Figure R 1: Yeast two hybrid assay showing SE directly interacts with all seven ALFIN1-LIKE proteins.

Left panel shows test interactions while right panel shows negative controls. CSM-WL is used as a spotting control. CSM-WLH is the interaction test. 10-fold serial dilution is spotted from left to right. Three spotting replicates from at least two independent yeast transformations were performed.

The next logical step was to verify these interactions in a plant-based system. Transiently expressing proteins in *N. benthamiana* (tobacco) leaves followed by co-immunoprecipitation and immunoblotting is an interim and fast way of studying protein-protein interactions in planta. For this, vector expressing AL proteins translationally fused to mRFP tag and SE translationally fused to HA tag was used. Except for AL3, all other proteins were strongly expressed in tobacco leaves (Figure R 2 and Supplementary Figure 2). A strong band in Co-IP for AL1, AL2 and AL4 to AL7 compared to respective inputs indicated an affirmative immunoprecipitation. A positive interaction with SE was observed in Co-IP for AL4, AL5 and AL7 (Figure R 2, Supplementary Figure 1 and Supplementary Figure 3). No band was observed in IP control where mRFP and SE-HA were co-expressed. This experiment clearly demonstrates the ability of SE to bind to multiple proteins from the ALFIN1-LIKE family. Additionally, it gave a clear indication that SE can interact with several proteins involved in gene regulation and a speculative involvement in stress regulation.

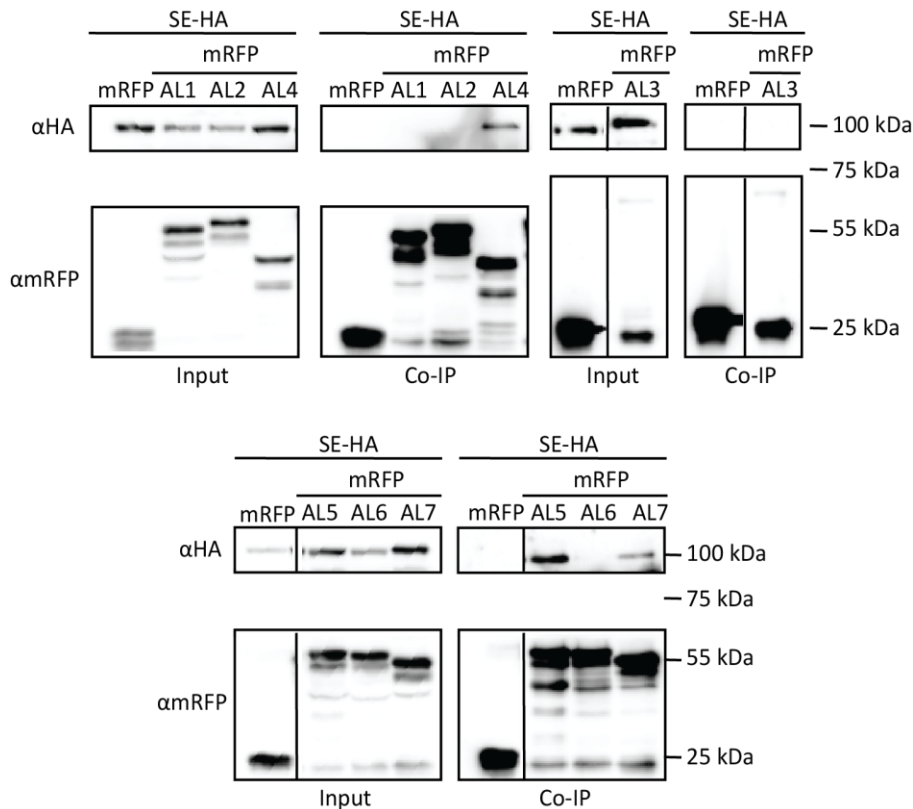


Figure R 2: Co-immunoprecipitation assay showing AL4, AL5 and AL7 interact with SE in planta. Western blot images of mRFP-AL1-7 and SE-HA in transiently expressed *N. benthamiana* leaves. All experiments were carried out with at least duplicate infiltrations and triplicate Co-IP.

2.1.2 *al4 al5 al6 al7* mutant generation via CRISPR-Cas9 method revealed redundant functions among ALFIN1-LIKE proteins

After demonstrating direct interaction of AL4, AL5 and AL7 with SE in tobacco, the aim was to study the functional role of these interactions in *A. thaliana*. The first step towards this goal was to generate mutants of the above-mentioned genes. Multiple approaches to generate a quadruple mutant were employed. This included using CRISPR-Cas9 technology in the background of a double T-DNA insertion mutant. *AL4* and *AL7* genes were mutated in *al5 al6* background (Wei et al., 2015). *al6* mutant was included as *AL6* and *AL7* are phylogenetically related (Liang et al., 2018). sgRNAs targeting the 5' and 3' of the coding region for both the genes were designed and cloned into destination vector (Figure R 3A and Supplementary table 2). *al5 al6* double mutant were then transformed with these destination vectors via *Agrobacterium* mediated transformation. Post-herbicide resistance selection, genotyping of T1 generation yielded heterozygous mutations in both genes (Figure R 4A). FAST screening was performed on T2 generation seeds yielding progeny without Cas9 construct. This ensured no further simultaneous deletions occurring in the somatic tissue, making it easier for genotyping. PCR amplification and sequencing of *AL4* gene in T2 generation showed a deletion of 1278 bp yielding *al4 al5 al6* triple mutant (Figure R 4C and Figure R 5C). Genotyping of T3 generation of another independent line revealed a deletion of 352 bp in *AL4* gene and 300 bp deletion in *AL7* causing a frameshift mutation for the quadruple mutant (Figure R 4D, Figure R 5A and B). Despite mutating 4 out of 7 genes, there was no significant quantifiable phenotypic difference among WT, double, triple, and quadruple mutants (Figure R 3B). This suggests a strong redundancy among all ALFIN1-LIKE proteins. Previous publications have generated double mutants with observable phenotype only after stress induction (Molitor et al., 2014; Wei et al., 2015).

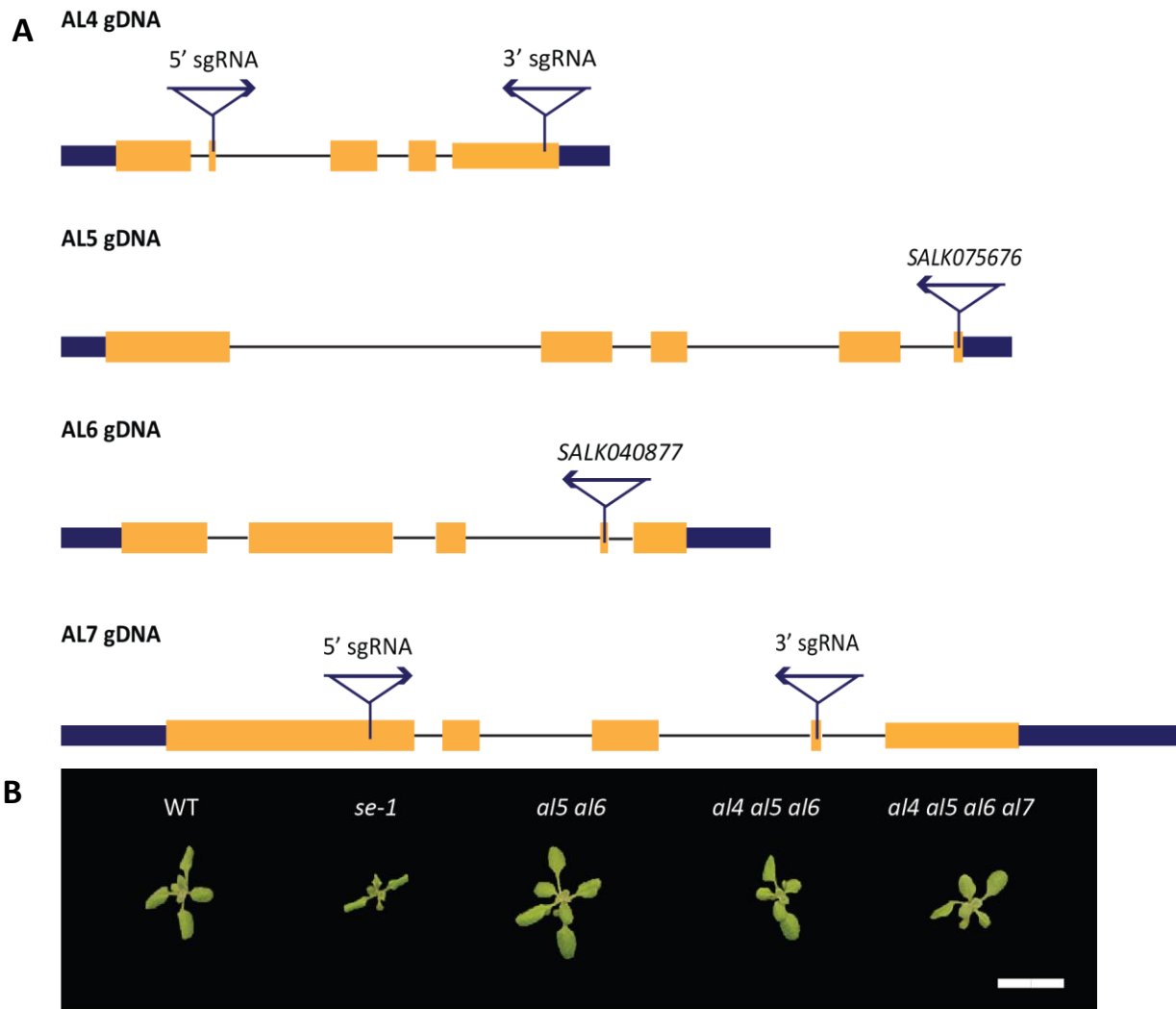


Figure R 3: Generation of CRISPR-Cas9 mutants for ALFIN1-LIKE protein family.

A) Diagrammatic representation of gDNA with the position of sgRNAs and SALK T-DNA insertions. *AL4* gDNA with the sites of 5' and 3' sgRNA located in the 2nd and the 5th exon. *AL5* gDNA with the T-DNA (SALK075676) insertion position in the 5th exon. *AL6* gDNA with the T-DNA (SALK040877) insertion position in the 4th exon. *AL7* gDNA with the sites of 5' and 3' sgRNA located in the 1st and the 4th exon. Left blue bar is 5'UTR and right blue bar is 3' UTR. Yellow bars indicate exons and intersperse black lines denote introns. Diagram drawn to scale. B) Comparative morphology of 10-day old WT, *se-1*, *al5 al6*, *al4 al5 al6*, *al4 al5 al6 al7* seedlings grown under long day conditions. Scale bar 2 cm.

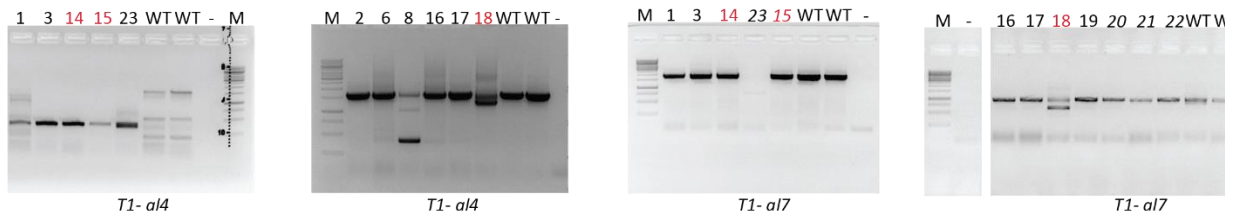
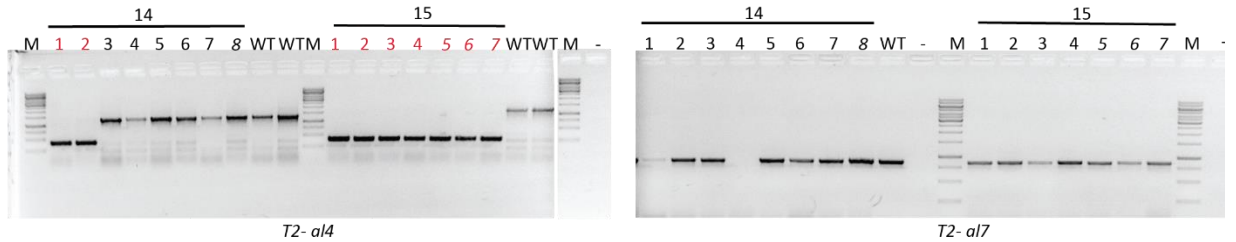
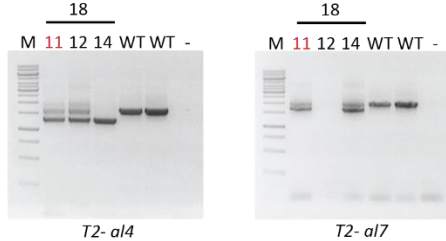
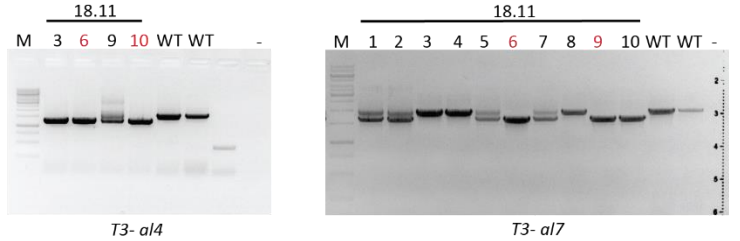
A**B****C****D**

Figure R 4: Gel electrophoresis images of genotyping PCR for *al* CRISPR mutants.

A) T1 generation genotyping. Plant number 14 15 and 18 displaying multiple bands or deletions were used for further genotyping B) T2 generation genotyping resulting in *al4 al5 al6* mutants. Plants 14.1, 14.2 and 15.1-7 show deletion in *al4* but WT like band for *AL7* gene. C) T2 generation genotyping for *al4 al5 al6 al7* mutants resulted in heterozygous mutations in *al4* and *al7*. Plants 18.11 was used for further genotyping. D) T3 generation plants genotyped for *al4 al5 al6 al7* mutants. Plant number 18.11.6 and 18.11.9 were used for further analysis. Plant numbers marked in red were used for further genotyping. – is water control. M stands for marker which was Generuler 1KB plus ladder.

2.2 Y2H transcription factor library screening revealed SE binds to 57 different TFs

SE has the ability of binding to a subset of intronless genes and consequently modulating gene expression (Speth et al., 2018). Interaction of SE with ALFIN1-LIKE proteins gave a strong indication of transcription factors being the mediators of this process. To strengthen this hypothesis, a library of TFs was screened that potentially could directly bind to SE. This screening process was executed by using the golden standard technique to study protein-protein interaction, yeast-two-hybrid library screening. Unlike IP-MS, this technique ensured the procurement of a list of TFs that directly bind to SE and not as a part of a complex.

SE was used as a bait to screen a library of 1200 different TFs by Geyer et al., (unpublished, master thesis). Out of these, 57 different TFs directly bind to SE. Further analysis of these TFs revealed they belong to multiple families with diverse functions ranging from stress regulation to plant growth and development.

2.2.1 Y2H and Co-IP assay corroborates interaction of TOEs and IAA34 with SE

To further substantiate the results obtained from the library screening, candidate proteins from four different families were re-tested individually using yeast-two-hybrid assay. These families included the AP2/ERF, IAA/AUX, MYB and WRKY family which are involved in diverse functions in plant development. Apart from CSM-WLH plates, cells were also spotted on CSM-WLHA plates, a stringent interaction condition which is additionally devoid of adenine. TOE2 from the AP2/ERF family was selected as it showed the highest interaction frequency with SE in the yeast two hybrid library screening. TOE2 was translationally fused to the BD part of GAL4 while SE was fused to AD. Transformation of yeast with these vectors followed by spotting on CSM-WL, CSM-WLH and CSM-WLHA plates revealed a strong and direct interaction of TOE2 and SE (Figure R 6A). As TOE1 and TOE2 have very similar structures and have previously shown overlapping functions (Aukerman & Sakai, 2003), binding of TOE1 with SE was also tested using the same strategy. Growth of yeast cells was observed not only on CSM-WLH plates but also on CSM-WLHA plates. Thus, as speculated, TOE1 also showed a strong interaction with SE (Figure R 6). This further hinted to test other TOE related proteins, SCHNARCHZAPFEN (SNZ), and SCHLAFMÜTZE (SMZ)

(Kim et al., 2006). Surprisingly, SNZ did not bind to SE (Appeldorn et al., unpublished bachelor thesis). TOE1 and TOE2 play an important role as transcriptional repressors at multiple stages of the plant development and ensure proper growth of vegetative as well as reproductive stage of the plant (Aukerman & Sakai, 2003). Thus, the direct interactions between TOE1, TOE2 and SE could indicate a novel role of SE in transcriptional regulation via transcription factors.

Subsequently, interaction of IAA34 and IAA32 from the IAA/AUX family with SE were tested. This family of proteins are known as early auxin response proteins and act as transcriptional repressors by interacting with AUXIN RESPONSIVE FACTORS (ARF) (Chandrika et al., 2013). IAA34 was also among the transcription factors with a high interaction frequency. Yeast two hybrid assay indicated binding of IAA34 with SE (Figure R 6A) but not with IAA32 (Appeldorn et al, bachelor thesis, unpublished). This interaction with IAA34 indicated a possible role of SE in plant development via auxin signalling.

Furthermore, MYBC1 from MYB family and WRKY49 from WRKY family were tested. MYBC1 has the competency to negatively regulating freeze tolerance (Zhai et al., 2010), while WRKY family is known to be involved in pathogen defence, senescence and trichome development (Eulgem et al., 2000). MYBC1 and WRKY49 did not indicate a direct binding to SE (Figure R 6B). To summarize these results, three candidate TFs from two different families directly associate with SE. This data provided a positive inclination towards examining the role of the alliance of TFs with SE in planta and investigating the role of SE in gene repression.

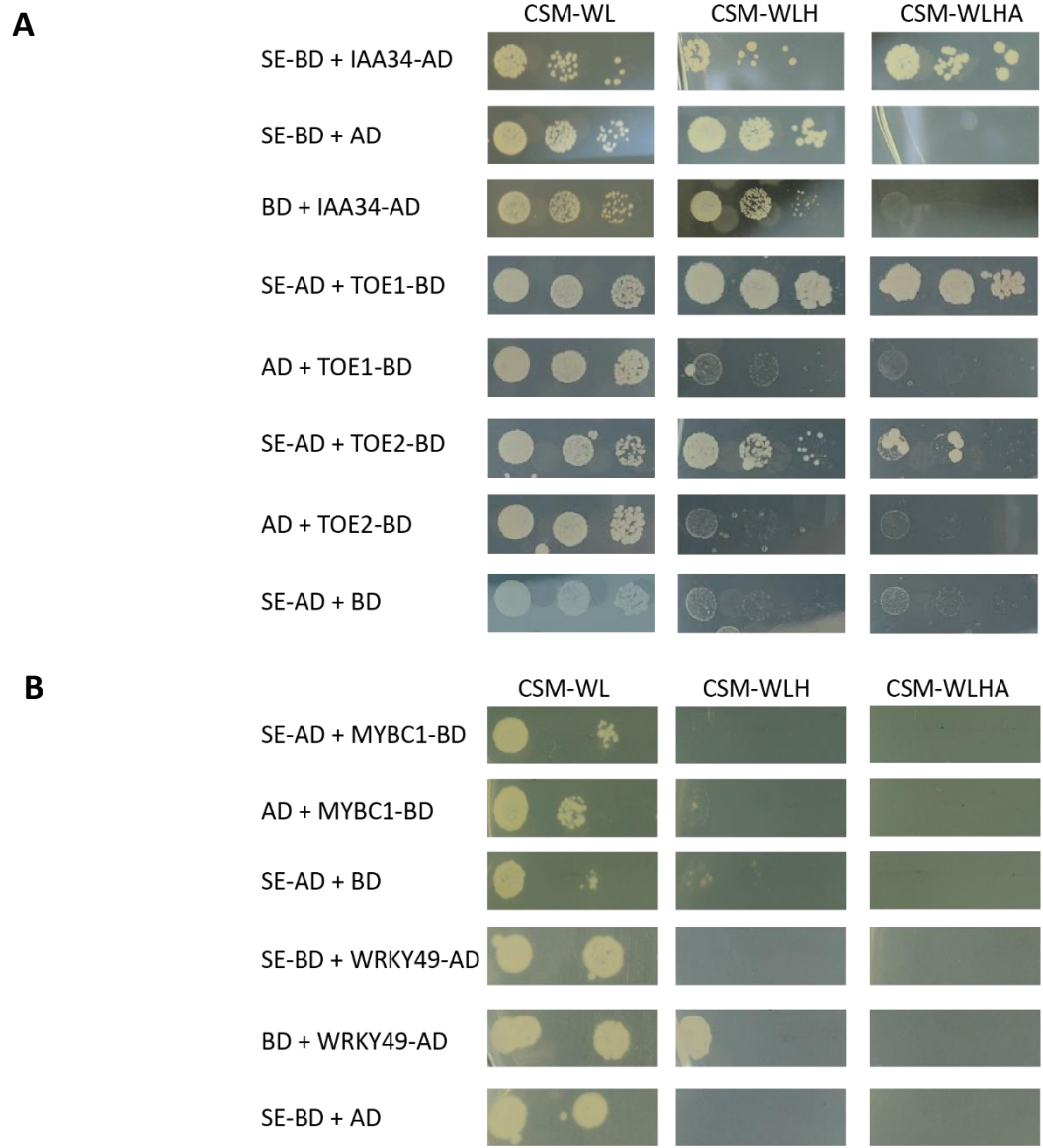


Figure R 6: Yeast two hybrid assay showing SE directly interacts with TOE1, TOE2 and IAA34. CSM-WL is used as a spotting control. CSM-WLH and CSM-WLHA are the interaction test. 10-fold serial dilution is spotted from left to right. Three spotting replicates from at least two independent yeast transformations were performed.

After verifying direct interactions, co-immunoprecipitation experiments were performed for TOE1, TOE2 and IAA34 with SE in tobacco. SE was translationally fused to HA and TFs to mRFP tag. These proteins were transiently expressed in tobacco and co-immunoprecipitation experiments were performed. A band in input indicated a well expressed TOE1-mRFP and mRFP-IAA34 protein in *N. benthamiana* system (Figure R 7A and B and Supplementary Figure 4). TOE2 was not well expressed in tobacco leaves possibly due to mRFP tag interfering with proper folding of the protein leading to protein degradation (Supplementary Figure 5). Cloning different isoforms of *TOE2* or gDNA of *TOE2* with different tags could be used for future experiments. In the case of TOE1 and IAA34, a band in the Co-IP from mRFP was observed indicating affirmative immunoprecipitated protein. A positive interaction was observed for both TOE1 and IAA34 with SE (Figure R 7A and B). This demonstrated the ability of SE to directly associate with transcription factors from different families. TOE1 and IAA34 both are transcriptional repressors, indicating a speculative repressive role of SE.

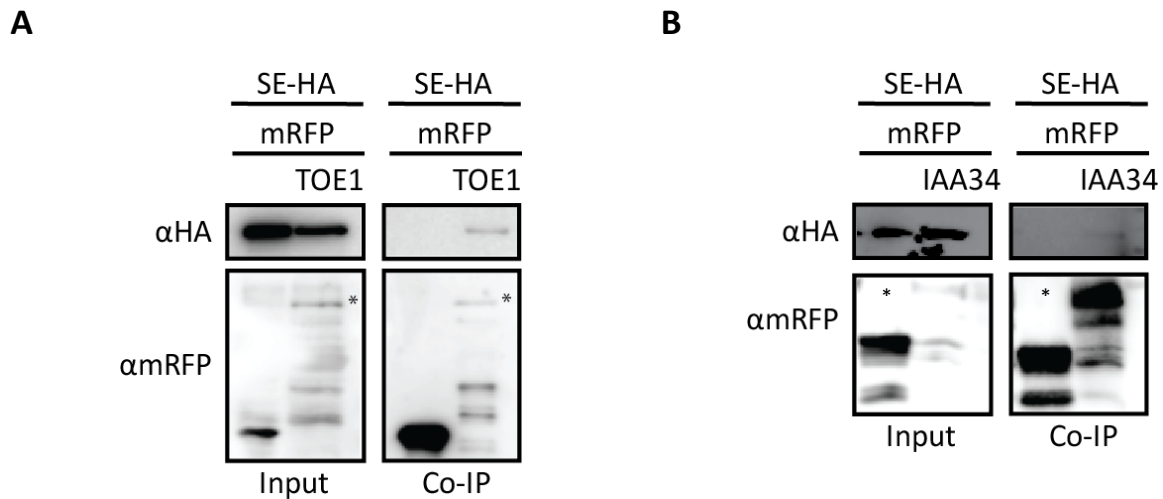


Figure R 7: Co-IP studies show TOE1 and IAA34 interact with SE in planta.

A) Western blot images showing TOE1 binding to SE and B) IAA34 weakly binding to SE.* indicates band for TOE1-mRFP and B) mRFP-IAA34. Antibody against HA was used to detect SE and antibody against mRFP was used to detect TOE1 and IAA34. Images were edited using Adobe Illustrator 2022.

2.2.2 *se-1 toe1-2 toe2-1* mutant shows defects in leaf initiation, leaf morphology, shorter juvenile phase, and an early flowering phenotype

To test the functional relationship of SE with TOEs and IAA34 *in vivo*, genetic interaction studies were performed. *iaa32 iaa34* mutant is being generated using CRIPSR-Cas9 technology via the strategy mentioned above (Section 2.1.2). *toe1-2 toe2-1* (double mutant) was obtained from Schmid Lab, Umea (SALK_069677 for *toe1-2* and SALK_065370 for *toe2-1*). A triple mutant was generated by crossing *se-1* and *toe1-2 toe2-1*. The phenotype of *toe1-2 toe2-1 se-1* (triple mutant) showed pleiotropic defects like small and serrated leaves, retarded plant growth and early flowering phenotype (Figure R 8A). To quantify these observations, experiments to check phase transition, leaf size, leaf initiation rate and flowering time were performed.

2.2.3 *toe1-2 toe2-1 se-1* depicts serrated leaf, reduced leaf size and a slower leaf initiation rate

Leaves of the triple mutant displayed strong *se-1*-like characteristics with size of the adult leaf considerably smaller than *se-1*. In general, first adult leaf area of *se-1* and *toe1-2 toe2-1* were substantially smaller than WT but not significantly different from each other (Figure R 8B and D, Figure R 9D). Interestingly, the leaf size of the triple mutant was significantly smaller than that of *se-1* and *toe1-2 toe2-1*. This hints towards an additive effect of mutation in SE and TOEs with respect to the leaf size.

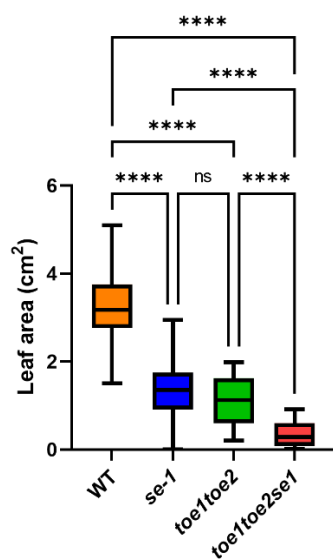
SE previously has shown to have an influence on the leaf production rate (Prigge & Wagner, 2001). Consequently, the leaf initiation rate for WT and all the mutants was checked where number of leaves were counted every two days until flowering occurred. *se-1* showed a slower leaf production rate (~67%) as opposed to WT (Figure R 8C and E, Supplementary Figure 6: Leaf initiation rate.). This has been shown by published data by Prigge & Wagner, 2001. Similarly, *toe1-2 toe2-1* also depicted a slower leaf growth rate (~84%), but not as delayed as *se-1*. Concomitantly, growth rate of the triple mutant was also significantly lower (~53%) (Figure R 8C and E). This indicates an additive effect of mutation in SE and TOEs. Overall, the phenotype

reduced leaf size and slower leaf production of *se-1* and *toe1-2 toe2-1* is independent and additive effect.

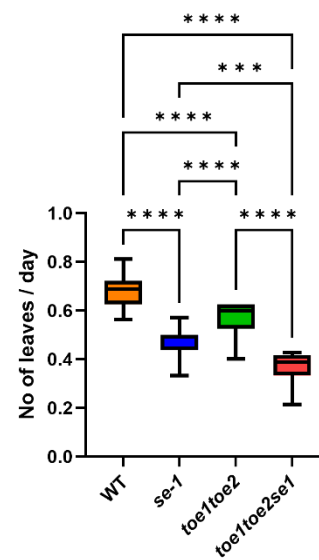
A



B



C



D

| Genotype | Average leaf area (cm ²) |
|---------------------------|--------------------------------------|
| WT | 3.2 ± 0.84 |
| <i>se-1</i> | 1.33 ± 0.64 |
| <i>toe1-2 toe2-1</i> | 1.11 ± 0.51 |
| <i>toe1-2 toe2-1 se-1</i> | 0.33 ± 0.26 |

E

| Genotype | Leaf initiation rate (days) |
|---------------------------|-----------------------------|
| WT | 0.68 ± 0.07 |
| <i>se-1</i> | 0.50 ± 0.05 |
| <i>toe1-2 toe2-1</i> | 0.57 ± 0.06 |
| <i>toe1-2 toe2-1 se-1</i> | 0.36 ± 0.06 |

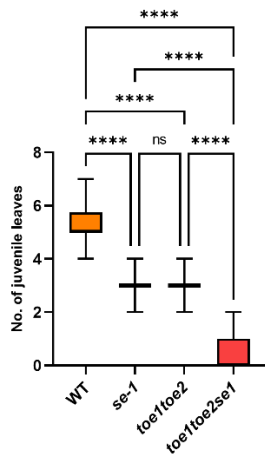
Figure R 8: Phenotype of WT, *se-1*, *toe1-2 toe2-1* and *toe1-2 toe2-1 se-1* plants under long day condition. A) Picture of bolted plants at day 28 showing differences in the flowering time. B) Box plot depicting leaf area in cm². C) Box plot showing leaf initiation rate measured by counting number of leaves per number of days until flowering. D) Table listing average leaf area ± SD. E) Table listing leaf initiation rate ± SD. ANOVA test was performed on B) and C) followed by Tukey post-hoc test for multiple comparison. ****<P 0.0001, ***<P 0.001, n.s. not significant.

2.2.4 *toe1-2 toe2-1 se-1* has a significantly shorter juvenile phase

Phase transition from juvenile to adult towards reproductive stage is majorly influenced by the combination of miRNA156, miRNA172 and their respective targets (Wu et al., 2009) which is regulated by SE (Yang et al., 2006a). Additionally, TOEs influence the cytokinin response to vegetative phase change (Werner et al., 2021). To further clarify the influence of these three genes in combination, phase transition in WT and mutants was tested. For this, plants were grown on soil under long day conditions and leaves without trichomes on the abaxial side were counted (juvenile leaves). *se-1* and *toe1-2 toe2-1* showed a substantial decrease in the number of juvenile leaves compared to WT but no significant difference between the length of juvenile phase among both the mutants (Figure R 9A, B and D). In case of the triple mutant, the juvenile phase was shorter than *se-1* and double mutant (Figure R 9A, B and D). From this data it appears that the length of the juvenile phase in *se-1* and *toe1-2 toe2-1* is an additive effect.

2.2.5 TOEs are epistatic to SE for flowering time

Transitioning from vegetative to reproductive stage is one of the most crucial and well controlled pathways. TOE1 and TOE2 are known flowering repressors, preventing early onset of flowering (Aukerman & Sakai, 2003). With this prior knowledge, flowering time was assessed in *toe1-2 toe2-1 se-1* mutant. *se-1* showed a reduced number of rosette leaves as compared to WT (Figure R 9C, D). Even though this translates to early flowering, *se-1* plants flower ~2-3 days later than WT (Supplementary table 1). This might be due to the delay in the leaf production observed (in section 2.2.3). *toe1-2 toe2-1* as expected, flowered significantly early than WT and *se-1*. Interestingly, *toe1-2 toe2-1 se-1* also displayed early flowering but was not significantly different from *toe1-2 toe2-1* (Figure R 9C, D). This indicates epistasis of TOEs over SE and hinted towards both these proteins in alliance modulating flowering time.

A**B**

| Genotype | Number of juvenile leaves |
|---------------------------|---------------------------|
| WT | 5.1 ± 0.7 |
| <i>se-1</i> | 2.9 ± 0.6 |
| <i>toe1-2 toe2-1</i> | 3.0 ± 0.5 |
| <i>toe1-2 toe2-1 se-1</i> | 0.5 ± 0.7 |

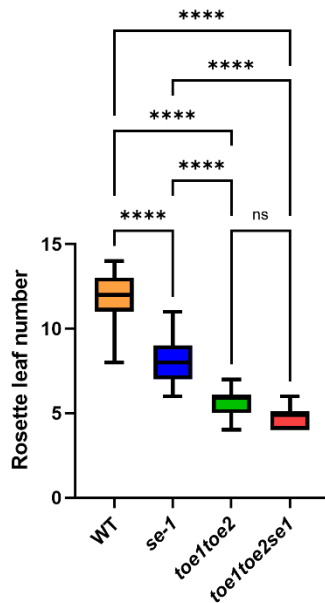
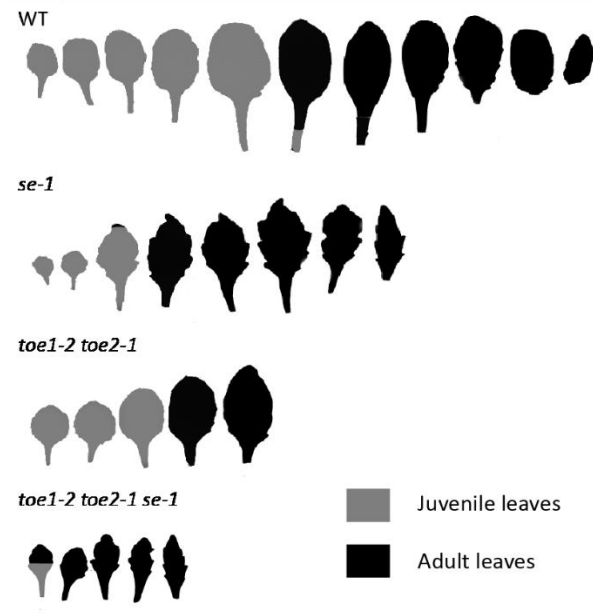
C**D**

Figure R 9: Phase transition and flowering time experiments.

A) Box plot showing a short juvenile phase length in *se-1*, *toe1-2 toe2-1* and *toe1-2 toe2-1 se-1* mutant.

B) Table showing average number of juvenile leaves ± SD. C) Box plot showing the flowering time of WT and mutants by counting rosette leaf number. D) Leaf morphology of WT, *se-1*, *toe1-2 toe2-1* and triple mutant. Scale bar: 1cm. Scanned images were edited using Adobe Photoshop 2022. A), B) and C) 20 plants from each genotype were used in every experiment. Two experimental replicates were performed. A) and C) ANOVA test was performed followed by Tukey post-hoc test for multiple comparison. ****<math>P < 0.0001</math>, n.s. not significant.

2.2.6 TOE1 and TOE2 do not influence the transcription of *MIRNA156* and processing of pri-miRNA156

miR156 is necessary for continuation of the early vegetative (juvenile) phase and is crucial for transitioning from early vegetative to late vegetative phase (adult). Its expression is highest at the juvenile phase and reduces with progression of the age of plant (Wu et al., 2009). As seen earlier, *se-1* and *toe1-2 toe2-1* both have a shorter juvenile phase than WT. Concomitantly, transcription of *MIRNA156* and processing of pri-miRNA156 in the early vegetative, late vegetative, and reproductive stages of the plant was examined.

To conduct this experiment, leaves were harvested at different developmental stages of WT and mutants. Based on the phase transition experiment (section 2.2.4) developmental stages were defined as follows: leaves 1 and 2 were harvested as early vegetative phase, leaves 4, 5 and 6 as late vegetative phase and reproductive phase was defined by newest two rosette leaves harvested when the plants started flowering. Similar experiment was also conducted with harvested shoot apices of plants at the aforementioned developmental stage. RNA was isolated from these leaves, followed by cDNA synthesis and qPCR. Pri-miRNA156a level in *se-1* was significantly higher than WT in the early vegetative phase (Figure R 10A). This corroborates well with published data, where *se-1* shows accumulation of pri-miRNAs due to defects in miRNA biogenesis pathway (Yang et al., 2006b). In contrast, *toe1-2 toe2-1* showed no difference in expression compared to WT, indicating no influence of TOEs on *MIRNA156A* transcription. Thus it shows efficient processing of the short-lived pri-miRNAs in *toe1-2 toe2-1* (Marzi et al., 2016). Interestingly, *toe1-2 toe2-1 se-1* also depicted an increase in the *MIRNA156* expression but to a lesser extent than *se-1* (Figure R 10A).

The expression trend in late vegetative and reproductive phase remained approximately the same as early vegetative phase for *MIRNA156A* among all the mutants and WT (Figure R 10B, C). As expected, there was an overall decrease in the expression levels in *se-1* and *toe1-2 toe2-1 se-1* with progression of age of the plants (Supplementary Figure 7A). These results indicate, accumulation of pri-miRNA156 is majorly due to *se-1* and not due to *toe1-2 toe2-1*.

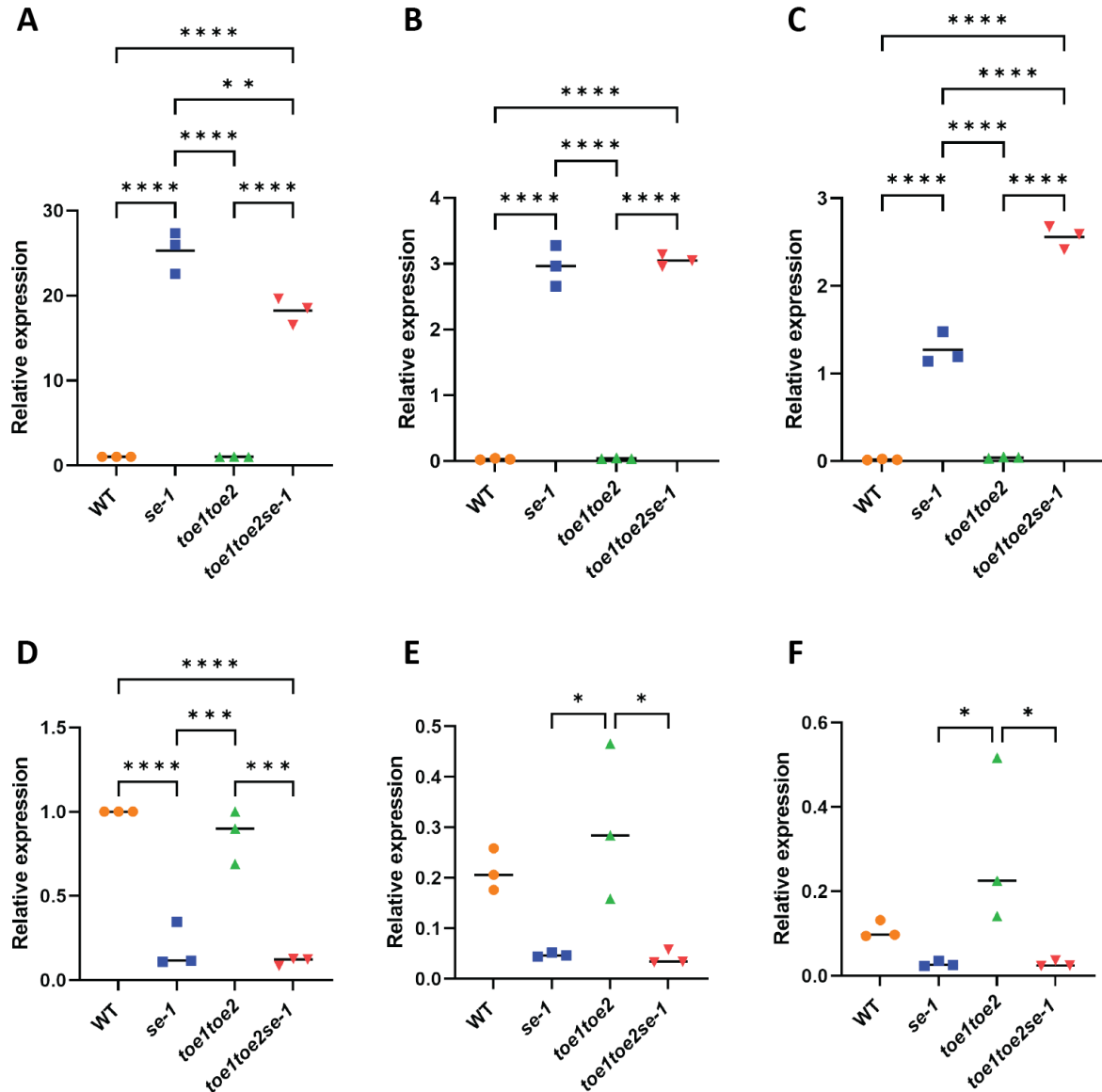


Figure R 10: Expression profile of *MIRNA156a* and levels of miR156 analysed using qPCR. Relative expression of *MIRNA156a* in A) early vegetative B) late vegetative and C) reproductive phase of plant. Relative expression of miR156 in D) early vegetative E) late vegetative and F) reproductive phase of plant. qPCR was performed using 3 individual biological replicates with 2 technical replicates. Value of WT early vegetative phase was denoted as 1. Horizontal line in between the individual values denotes the average of all 3 replicates. ANOVA test was performed followed by Tukey post-hoc test for multiple comparison. ****<math>P < 0.0001</math>, ***<math>P < 0.001</math>, **<math>P < 0.01</math>, *<math>P < 0.05</math>, n.s. not significant.

With regards to the levels of miR156, *toe1-2 toe2-1* did not show significant difference than WT in early vegetative (Figure R 10D), late vegetative (Figure R 10E) or reproductive phase (Figure R 10F). This indicates no influence of TOEs on the processing of pri-miRNA156 to produce mature miR156. miR156 levels in *se-1* and triple mutant were substantially lower than WT and double mutant in early vegetative phase (Figure R 10D). It was only negligibly lower than *toe1-2 toe2-1* in late vegetative (Figure R 10E) and reproductive stage (Figure R 10F). This clearly is due to the miRNA processing defects observed in *se-1* (Yang et al., 2006b). No significant difference was observed between WT and *se-1, toe1-2 toe2-1 se-1* in late vegetative and reproductive phase. The levels of miR156 gradually decreased in WT and *toe1-2 toe2-1* throughout the life cycle of the plant. With respect to *se-1* and the triple mutant, there was only a minor non-significant decrease over time (Supplementary Figure 7B). Thus, unlike SE, TOE1 and TOE2 are not involved in either the transcription of *MIRNA156A* or processing of pri-miRNA156. This indicates that TOEs might regulate the length of the juvenile phase by affecting downstream processes of miR156 regulation.

2.2.7 Expression profile of miR156-targets *SPL3* and *SPL10*

Downstream of miR156 are the targets SQUAMOSA PROMOTER BINDING PROTEIN-LIKE (*SPL*) proteins which mediate the transition from juvenile (early vegetative) to adult (late vegetative) and then to reproductive stage of the plant. Reduction in miR156, promotes the transcription of *SPLs* aiding in developmental transition (Wu & Poethig, 2006; Xu et al., 2016). Thus, expression of *SPL3* and *SPL10* in the early vegetative, late vegetative, and reproductive stage of WT and the mutants were analysed.

Expression of *SPL3* transcript was lower in WT and *toe1-2 toe2-1* than in *se-1 and toe1-2 toe2-1 se-1* in the early vegetative phase (Figure R 11A). This could be due to substantially low amount of miR156 in *se-1* and triple mutant (Figure R 10D). With progression of age of the plant, overall expression in WT and *se-1* gradually increased in late vegetative (Figure R 11B) and in reproductive (Figure R 11C) phase as expected. Curiously, the expression in *toe1-2 toe2-1* increased substantially than WT in late vegetative as well as reproductive phase, leading it almost similar to *se-1* (Supplementary Figure 7C). This indicates TOEs negatively regulate *SPL3*.

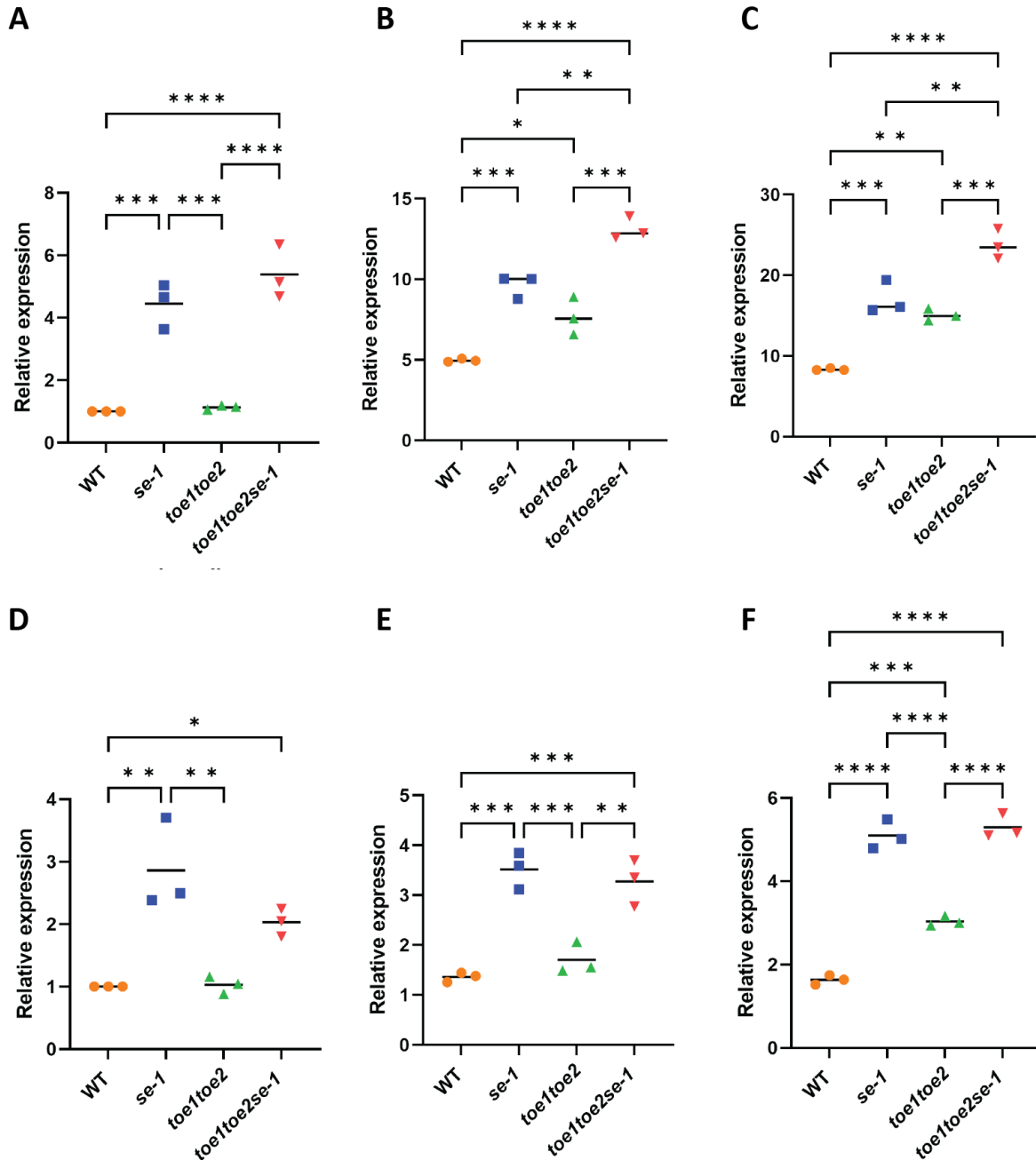


Figure R 11: Expression profile of *SPL3* and *SPL10* transcripts using qPCR. Relative expression of *SPL3* in A) early vegetative B) late vegetative and C) reproductive phase of plant. Relative expression of *SPL10* in D) early vegetative E) late vegetative and F) reproductive phase of plant. qPCR was performed using 3 individual biological replicates with 2 technical replicates. Value of WT early vegetative phase was denoted as 1. Horizontal line in between the individual values denotes the average of all 3 replicates. ANOVA test was performed followed by Tukey post-hoc test for multiple comparison. ****<math>P < 0.0001</math>, ***<math>P < 0.001</math>, **<math>P < 0.01</math>, *<math>P < 0.05</math>, n.s. not significant.

Consequently, the expression in *toe1-2 toe2-1 se-1* for the late vegetative and reproductive stage was additively higher than in *se-1* and *toe1-2 toe2-1* (Figure R 11B, C).

Transcripts of *SPL10* in *se-1* was higher than WT and double mutant in early vegetative phase (Figure R 11D), probably due to low levels of miR156. In the late vegetative phase, there was a significant increase in expression of *SPL10* in *se-1* and triple mutant (Figure R 11E). Conversely in the reproductive stage, expression in the double mutant also considerably increased than WT (Figure R 11F) indicating *SPL10* is also negatively regulated by TOEs (Supplementary Figure 7D).

To summarize this data, TOE1 and TOE2 negatively influence *SPL3* in late vegetative and reproductive phase and *SPL10* only in the reproductive stage. Data from another study revealed TOE1 and TOE2 are sufficient to influence cytokinin response on vegetative phase change (Werner et al., 2021). Thus, acting downstream of miRNA156, TOEs modulate vegetative phase change, while SE regulates phase change via biogenesis of miR156.

2.2.8 Expression profile of *MIRNA172A* and levels of miR172a/b.

To further investigate the functional role of SE and TOEs in *A. thaliana*, the expression pattern of *MIRNA172A* and levels of miR172a/b was studied. miRNA172a-e are known flowering time regulators by translationally inhibiting floral repressors AP2-like proteins (Aukerman & Sakai, 2003). Contrary to miRNA156, expression of miRNA172 increases with the age of the plant (Wu et al., 2009).

Expression of *MIRNA172A* was significantly higher in *se-1* and triple mutant compared to WT and *toe1-2 toe2-1* in early vegetative (Figure R 12A), late vegetative (Figure R 12B) and reproductive stage (Figure R 12C). This might be due to the inability of *se-1* to process pri-miRNAs into mature miRNAs. Overall, the expression in *se-1* and triple mutant increased gradually from early vegetative to reproductive stage indicating transcriptional upregulation (Supplementary Figure 7E). This indicated TOEs do not influence the transcription of *MIRNA172A*.

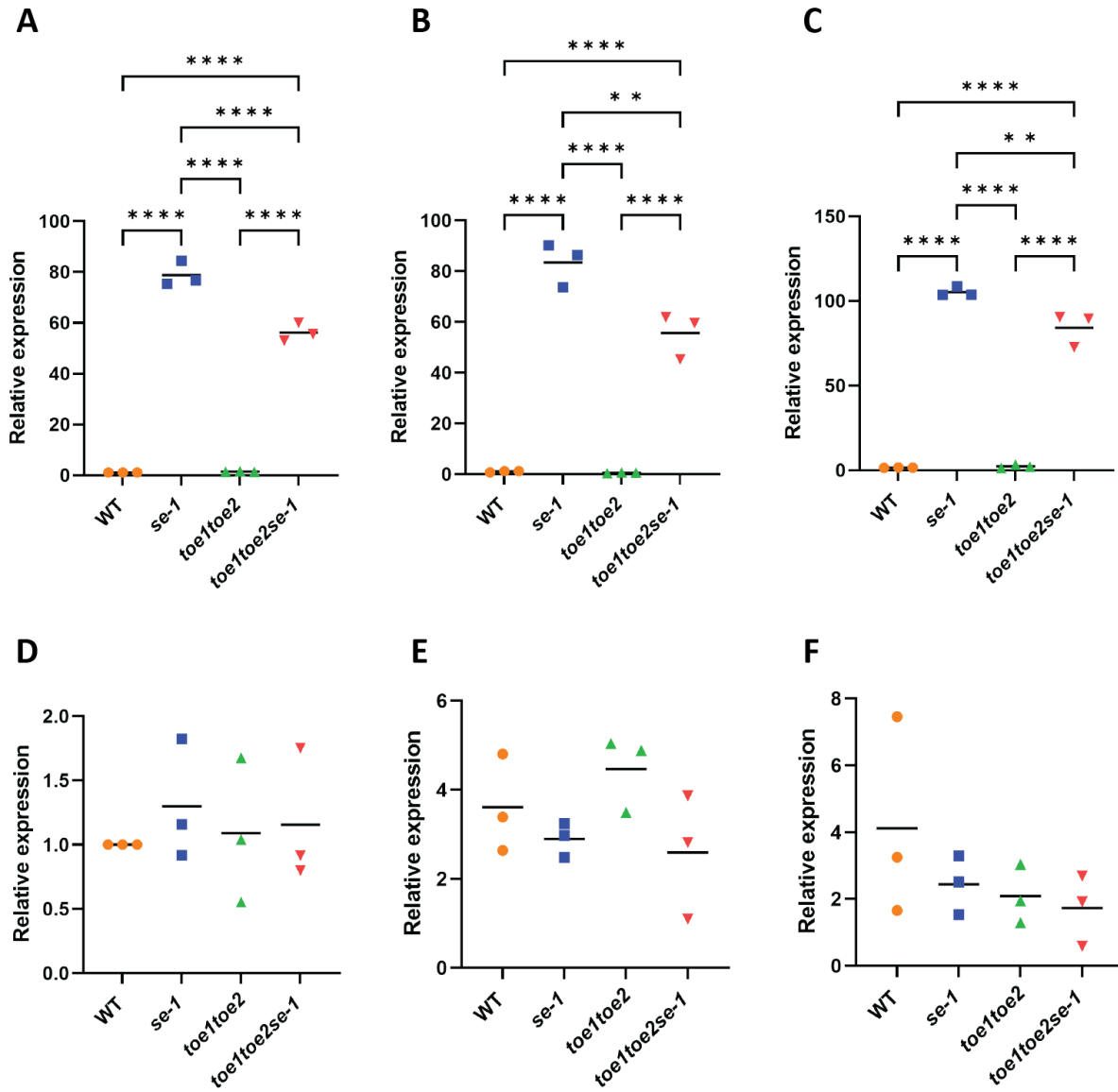


Figure R 12: Expression profile of *MIRNA172A* and levels of miR172a/b transcripts in leaves analysed using qPCR.

Relative expression of *MIRNA172A* in A) early vegetative B) late vegetative and C) reproductive phase of plant. Relative expression of miR172a/b in D) early vegetative E) late vegetative and F) reproductive phase of plant. qPCR was performed using 3 individual biological replicates with 2 technical replicates. Value of WT early vegetative phase was denoted as 1. Horizontal line in between the individual values denotes the average of all 3 replicates. ANOVA test was performed followed by Tukey post-hoc test for multiple comparison. ****<math>P < 0.0001</math>, ***<math>P < 0.001</math>, **<math>P < 0.01</math>, *<math>P < 0.05</math>, n.s. not significant.

Strikingly, the level of miR172a/b was different than expected. There was no significant difference between WT, *se-1*, double and the triple mutant in either early vegetative (Figure R 12D), late vegetative (Figure R 12E) or reproductive phase (Figure R 12F). This could be due to multiple possibilities like *se-1* being a hypomorphic mutant might not affect the processing of all miRNAs. A previous study shows no significant difference in the mature miRNA172 in WT and *se-1* (Laubinger et al., 2008). Another possibility is that miRNA172b isoform is massively abundant than miRNA172a (Ó'Maoiléidigh et al., 2021). This data indicates that TOEs do not directly influence expression of *MIRNA172A* or processing of pri-miRNA172. While *se-1* accumulates *MIRNA172A* but might not affect the processing of other isoforms of miRNA172.

It has been demonstrated that TOEs directly bind to the promoter of *FT* (*FLOWERING LOCUS T*), repressing its transcription (B. Zhang et al., 2015b). Further experiments to check *FT* expression in WT and mutants by harvesting leaves at multiple timepoints throughout the day would aid in investigating if alliance of TOEs and SE modulate *FT* expression and consequently influences flowering time.

2.2.9 Transcriptomic analysis of *se-1*, *toe1-2 toe2-1* and *toe1-2 toe2-1 se-1*

To further investigate a global role of SE and TOEs, an RNA sequencing experiment was performed on WT and mutant seedlings grown under continuous light conditions. Differentially expressed genes (DEGs) were identified between WT and mutants with log₂ fold change > ± 1 and adjusted p value < 0.05. In *se-1*, 1606 genes were differentially expressed. Out of these, 874 genes were upregulated while 732 genes were downregulated (Figure R 13 and Supplementary Figure 8). While in *toe1-2 toe2-1*, 151 genes were differentially expressed including 98 upregulated and 53 downregulated genes (Figure R 13 and Supplementary Figure 8D and E). Comparatively lesser number of DEGs in double mutant indicate that TOEs influence only certain pathways that affect the expression of a small subset of genes. There was a significant overlap of 77 genes between the DEGs in *se-1* and *toe1-2 toe2-1* ($p < 4.811e-52$) (Figure R 13). The number of DEGs in *toe1-2 toe2-1 se-1* were 1724 (Supplementary Figure 8A), out of which 1143 genes were upregulated (Supplementary Figure 8B), and 581 genes were downregulated (Supplementary Figure 8C).

Previous study by Speth et al., has demonstrated the ability of SE to bind to a subset of intronless genes and consequently enhancing their expression. This led to the hypothesis that TOEs, being transcription factors, aid in binding of SE to a subset of genes and modulate their expression. Thus, overlap between the list of SE-binding genes and DEGs from *toe1-2 toe2-1* was checked. No significant overlap was observed among these subsets ($p < 0.154$). This indicates, TOE1 and TOE2 might be few of the many transcription factors interacting with SE possibly aiding in its binding to a subset of genes. The list of genes that were differentially expressed in *se-1* and the double mutant were further examined. Among the upregulated genes in *se-1* as well as *toe1-2 toe2-1* (Supplementary Figure 8D), a subset of genes were flowering responsive genes, functioning downstream of FT (e.g. *TSF1*, *SRS7*, *SWEET10*, *AGO9*, *FUL*, etc). This upregulation hinted towards SE and TOEs negatively influencing flowering responsive genes in early stages of the plant growth. Consequently, SE and TOEs could prevent precocious flowering. Further experiments to confirm the upregulation of these genes by qPCR in *se-1* and *toe1-2 toe2-1* seedlings would aid in studying this hypothesis.

Taken together, SE demonstrated the ability to directly interact with numerous TFs from multiple families like AL, IAA34 and TOEs. TOEs and SE independently influence the leaf morphology of the plant as well as juvenile phase length. Furthermore, TOEs and SE in alliance have a role on flowering regulation and might influence the gene repression of FT activated genes in the early vegetative phases seen by the DEGs in both *se-1* and *toe1-2 toe2-1*.

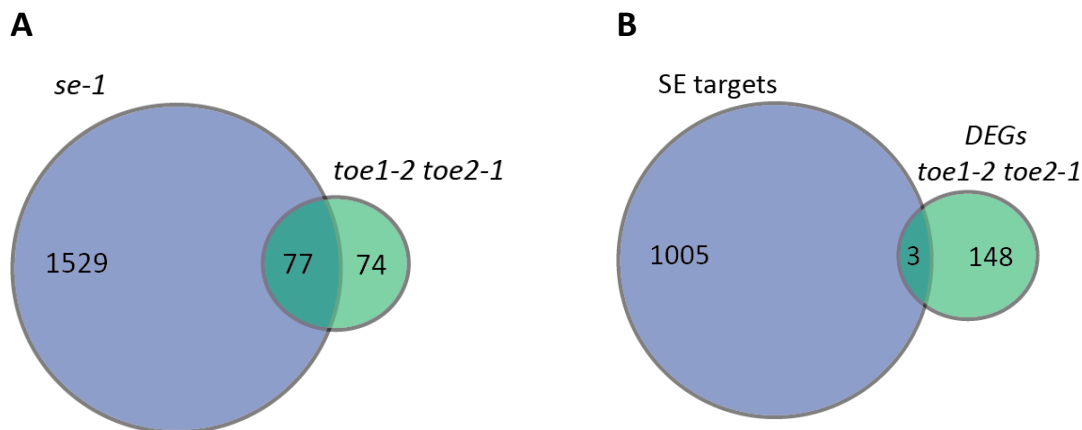


Figure R 13: Venn diagrams from RNA-seq data

A) Overlap of DEGs from *se-1* and *toe1-2 toe2-1* B) Overlap of SE targets (Speth et al., 2018) and DEGs from *toe1-2 toe2-1*. Log₂ fold change > ±1 and adjusted p value < 0.05.

3 Conclusion

SERRATE is a zinc finger protein equipped with multiple functions. This study revealed the ability of SE as an intrinsically disordered protein (IDP) to directly bind to a wide range of transcription factors (TFs) from multiple families. These transcription factors have diverse roles ranging from stress regulation, hormonal signalling to flowering time regulation (Figure R 14A). TFs that directly interact with SE are known transcriptional repressors. This unfurls a new avenue for SE, where it has the ability to negatively regulate genes via these repressors. Consequently, this study supports published data by Speth et al., 2018 where SE has a role in transcriptional regulation. Direct interaction of SE with three out of seven ALFIN1-LIKE proteins was demonstrated by independent experiments including IP-MS, yeast two hybrid assay and co-immunoprecipitation. ALFIN1-LIKE proteins are transcriptional repressors involved in stress regulation. Generation of quadruple *al* mutant indicated redundancy among all ALFIN1-LIKE proteins. Generating a septuple mutant would aid in studying the speculative stress regulatory role of SE and ALFINS.

Furthermore, yeast two hybrid library screening identified 57 different TFs directly binding to SE. Confirmatory yeast two hybrid assay revealed direct interaction of TOE1, TOE2 from the AP2-like family and IAA34 from the IAA/AUX family with SE. Concurrently, all these proteins contain canonical EAR motif or EAR-like motif.

The interaction studies further led to analysis of the functional relationship of TOE1, TOE2 and SE in *A. thaliana*. *toe1-2 toe2-1 se-1* mutant exhibited defects in leaf morphology and leaf initiation rate which are controlled by SE and TOEs independently. Additionally, an additive effect of *se-1* and *toe1-2 toe2-1* was seen in the triple mutant when studying phase transition (from early vegetative to late vegetative). Further, expression analysis of *MIRNA156*, miRNA156, *SPL3* and *SPL10* was performed. This experiment confirmed SE influences phase transition by aiding in miRNA156 processing. On the contrary, TOEs do not influence miRNA levels, but modulate *SPL3* and *SPL10* transcript levels in late vegetative and reproductive phase. *toe1-2 toe2-1 se-1* also showed an early flowering phenotype similar to *toe1-2 toe2-1*. This suggests TOEs are epistatic to SE in flowering time regulation. No changes in miR172 levels were observed in *se-1* and *toe1-*

2 *toe2-1* mutant indicating both these genes regulate flowering by modulating genes downstream of miRNA172. Transcriptomic analysis of *se-1* and *toe1-2 toe2-1* seedlings revealed, 77 genes differentially expressed in both the mutants. Out of these genes, a subset of FT-activated, flowering related genes were upregulated in seedlings of both the mutants. Previous publication showed TOEs directly bind to *FT* gene and repress its transcription (Zhang et al., 2015b). To conclude this study, a hypothetical model was generated (Figure R 14B) where a temporal role of SE in *FT* regulation can be speculated. SE and TOEs in alliance bind to *FT* and repress its expression in the early phase of plant. This in turn represses *FT-activated* genes in the early vegetative or juvenile phase, preventing precocious flowering. With progressing age of the plant, miRNA172 represses TOEs (Aukerman & Sakai, 2003). Correspondingly, transcription of *FT* occurs which promotes flowering. Thus, SE ensures plant gains competency to enter reproductive phase.

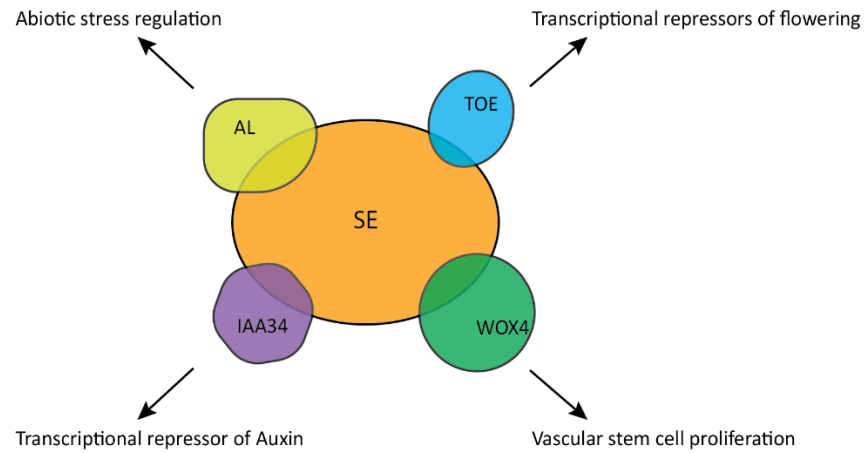
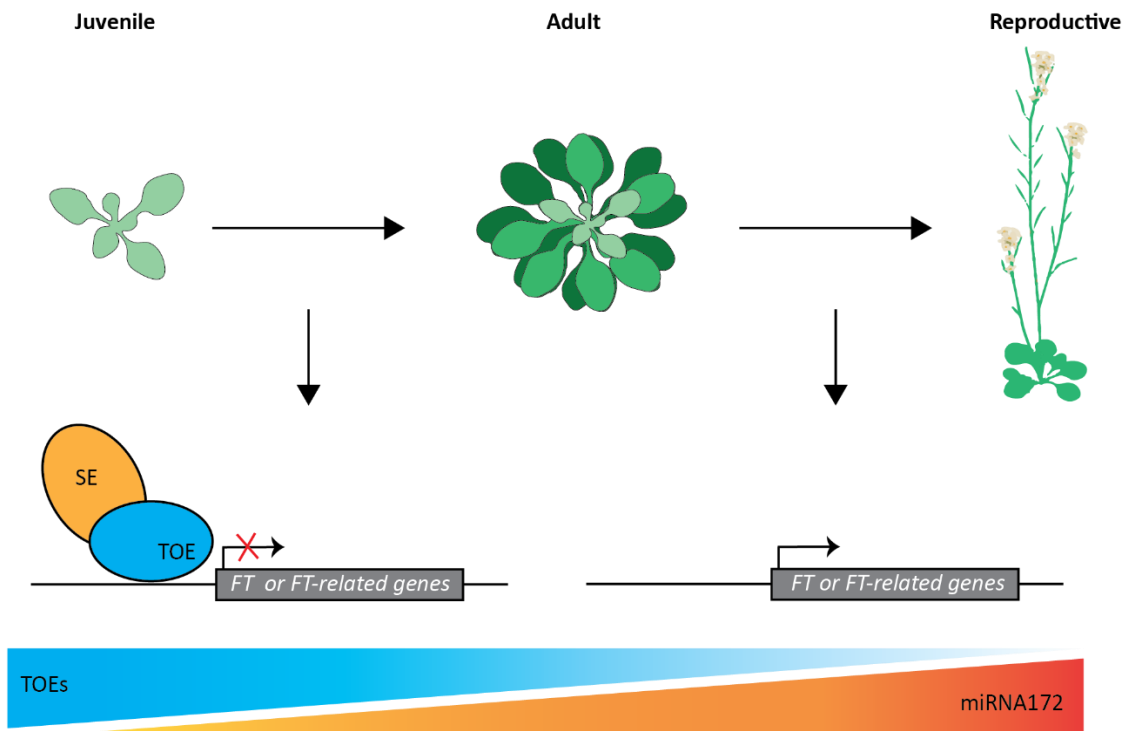
A**B**

Figure R 14: Hypothetical model of SE involved in transcription regulation via interaction with TFs. A) SE directly binds to TOE1, TOE2, AL4, AL5, AL7, IAA34 thus regulating transcription of multiple genes. B) Hypothetical model of SE and TOEs binding to *FT* or *FT*-related genes in the early vegetative phase and repressing its transcription. On the contrary, in the reproductive phase depletion of TOEs lead to transcriptional activation of *FT*. Image of *A. thaliana* plant adopted from biorender.com. Image generated using Adobe Illustrator and Photoshop.

4 Outlook:

To further study the functional role of SE interacting with multiple transcription factors, phenotypic and transcriptomic studies of other TF knockout lines and *se* mutant can be performed. Generation of septuple *alpin1-like* mutant would aid in studying the speculative role of SE in stress regulation.

To test the hypothesis, whether SE and TOEs prevent precocious flowering in early vegetative stage of the plant, multiple experiments can be performed. Firstly, expression of *FT* in different phases of the plant with plant material harvested especially at dawn, where *FT* shows an expression peak or highest expression in WT can be analysed in *se-1*, double and triple mutant. Additionally, upregulation of FT-activated genes in early vegetative phase of *se-1* and *toe1-2 toe2-1* needs to be confirmed by qPCR. Previous literature suggests TOEs bind to *FT* gene. CHIP-qPCR (Chromatin immunoprecipitation-qPCR) of SE in *toe1-2 toe2-1* background would aid in understanding if SE and TOEs in alliance bind to *FT* or other flowering related genes and modulate its expression.

5 Materials and Chemicals

For PCR amplification Dream Taq polymerase or Phusion High Fidelity DNA Polymerase from ThermoFisher Scientific was used. For entry vector cloning, pCR8/GW/TOPO TA Cloning Kit from Invitrogen was used. Further cloning into destination vector was carried out using Gateway™ LR Clonase™ II from Invitrogen. Purification of amplicon from gel was carried out using GeneJet Gel extraction kit from ThermoFisher Scientific. Plasmid isolation was carried out using GeneJet Gel plasmid isolation kit from ThermoFisher Scientific. For all transformations *E. coli* strain NEB5 α and *Agrobacterium* strain GV3101 was used. For yeast transformations, AH109 strain was used. mRFP magnetic beads from Chromotek were used for co-immunoprecipitation. Isolation of total RNA was carried out using RNeasy Plant Mini kit from Qiagen. Isolation of miRNA was carried out using Direct-zol RNA Microprep Kit from Zymo Research. For cDNA synthesis, RevertAid First strand cDNA synthesis Kit from ThermoFisher Scientific was used. qPCR was carried out using 2X Maxima SYBR Green Master Mix from ThermoFisher Scientific and CFX384 qPCR machine from Bio-Rad Laboratories Inc. mRNA library preparation for RNA sequencing was carried out using Poly(A) mRNA magnetic isolation module (NEB #7490) and NEBNext Ultra II RNA library kit with Sample purification beads (NEB #7775).

6 Methods

6.1 Molecular biological methods

6.1.1 Polymerase Chain Reaction (PCR)

For successful primer design, Primer-Blast (NCBI) was used. All oligonucleotides used in this study are listed in Supplementary table 2. Amplification of genes for genotyping was carried out using Homemade Taq polymerase or Dream Taq DNA Polymerase (ThermoFisher Scientific™). Amplification of genes for cloning was carried out using Phusion™ High-Fidelity DNA Polymerase (ThermoFisher Scientific™) (Table M 1). PCR were performed using cycler Peqstar (Peqlab Biotechnology AG, Erlangen, Germany). PCR program used is mentioned in Table M 2.

| Homemade Taq | | Dream Taq Polymerase | | Phusion Polymerase | |
|--------------------------|------|--------------------------|------|--------------------------|------|
| 10x Taq Buffer | 2 | 10x Dream Taq Buffer | 2 | 5x HF Buffer | 4 |
| dNTP (2mM) | 0.5 | dNTP | 2 | dNTP (2mM) | 0.5 |
| Forward Primer (10mM) | 0.5 | Forward Primer (10mM) | 0.5 | Forward Primer (10mM) | 0.5 |
| Reverse Primer (10mM) | 0.5 | Reverse Primer (10mM) | 0.5 | Reverse Primer (10mM) | 0.5 |
| Polymerase | 1 | Polymerase (5U/ μ L) | 0.1 | Polymerase (2U/ μ L) | 0.3 |
| DNA | 1 | DNA | 1 | cDNA | 0.5 |
| H ₂ O | 14.5 | H ₂ O | 13.9 | H ₂ O | 13.7 |
| Total volume | 20 | Total volume | 20 | Total volume | 20 |

Table M 1: PCR mix. All volumes are in μ L.

| | Homemade Taq | Dream Taq | Phusion Polymerase |
|----------------------|--------------|--------------|--------------------|
| Initial denaturation | 94°C 1 min | 95°C 1 min | 98°C 30 sec |
| Denaturation | 94°C 10 sec | 95°C 30 sec | 98°C 10 sec |
| Annealing | 55°C 30 sec | 55°C 30 sec | 60°C 30 sec |
| Elongation | 72°C 1min/kb | 72°C 1min/kb | 72°C 10sec/kb |
| Final Elongation | 72°C 10 min | 72°C 5 min | 72°C 5 min |
| Storage | 25°C ∞ | 25°C ∞ | 25°C ∞ |

Table M 2 PCR program

6.1.2 Gateway cloning:

For expression of tagged proteins, cDNA of the gene of interest was PCR amplified. Amplicon was excised from 1% gel after gel electrophoresis and purified using GeneJet Gel extraction kit (ThermoFisher Scientific). A-tailing was performed by incubating 17 μ L purified DNA with PCR mastermix (2 μ L of 10x Taq Buffer, 0.5 μ L of dNTP (2mM), 0.5 μ L of Taq Polymerase) at 72°C for 10 mins. A-tailed insert was then subcloned in pCR8/GW/TOPO entry vector using pCR8/GW/TOPO™ TA Cloning Kit (Invitrogen) (2.3 μ L of A-Tailed PCR Product, 0.5 μ L of Salt Solution, 0.2 μ L TOPO vector). After confirming correct sequence by Sanger sequencing, entry vector was recombined with pGWB vectors (expression in plants) or pGADT7 and pGBKT7 vectors (expression in yeast) using Gateway™ LR Clonase™ II (Invitrogen).

6.1.3 Transformation of *Escherichia coli* and *Agrobacterium tumefaciens*

Constructs were transformed in *Escherichia coli* (*E. coli*) strain NEB5 α . 2.5 μ L of ligation mixture was added to 50 μ L of competent *E. coli* cells and incubated on ice for 5 mins. Subsequently cells were heat shocked at 42°C for 45 secs followed by cooling on ice for 2 mins. 400 μ L of Lysogeny Broth medium (LB medium, 10 g/L Tryptone, 5 g/L Yeast extract, 10 g/L NaCl) was added and cells were incubated at 37°C on a shaker (Eppendorf Thermomixer F2,0) for 1 hr. After a quick spin, cells were plated on LB agar media containing required antibiotic (Table M 3) and incubated at 37°C (New Brunswick Scientific™ Innova™ 42) overnight.

For plant transformations, plasmids were transformed in *Agrobacterium tumefaciens* strain GV3101. 5 µL of plasmid was added to 50 µL of competent *A. tumefaciens* cells and incubated for 20 mins on ice. Cells were frozen in liquid nitrogen for 1 min followed by heat shock treatment at 37°C for 4 mins. 100 µL of LB medium was supplemented to cells and incubated at 28°C on shaker (Eppendorf Thermomixer F2,0) for 3 hours. Cells were then plated on LB agar plates with Rifampicin (100 µg/mL), Gentamycin (50 µg/mL) and Spectinomycin (100 µg/mL) and incubated at 28°C (New Brunswick Scientific™ Innova™ 44) for 2 days.

| Antibiotic | Final concentration (<i>E. Coli</i>) (µg/mL) | Final concentration (<i>A. tumefaciens</i>) (µg/mL) | Stock (mg/mL) | Solvent |
|-----------------|---|---|------------------|------------------|
| Ampicillin | 100 | - | 100 | 50% EtOH |
| Chloramphenicol | 25 | 25 | 12.5 | 100% EtOH |
| Gentamycin | - | 50 | 40 | H ₂ O |
| Kanamycin | 25 | - | 25 | H ₂ O |
| Rifampicin | - | 100 | 50 | DMSO |
| Spectinomycin | 50 | 100 | 50 | H ₂ O |

Table M 3: Antibiotics list.

6.1.4 Yeast two hybrid assay

The UAS-GAL4 system for yeast two hybrid assay was used to study direct interaction of TFs with SE (Fields & Song, 1989). Auxotrophic markers (*HIS*, *ADE*) were used to check protein-protein interactions. cDNA fragments of TOE1, TOE2, IAA32, IAA34, WRKY49, and MYBC1 were cloned in pGBKT7 vector by using Gateway cloning method. cDNA fragments of AL1-7 were cloned in pGADT7 vector while cDNA fragment of SE was cloned in both the vectors. *Saccharomyces cerevisiae* AH109 cells were freshly grown in YPDA medium (2% w/v Peptone, 1% w/v Yeast extract, 2% w/v Glucose, 0,002% w/v Adenine, pH 6.5) at 30°C (New Brunswick Scientific™ Innova™ 42). Combinations of pGBKT7 and pGADT7 (one containing the TF and other SE) were co-transformed via the LiAc/ss-DNA/PEG transformation procedure (Parchaliuk et al., 1998). These cells were then grown at 30°C for 2 days on tryptophan and leucine deficient CSM plates

(CSM-WL, 0.17% w/v Yeast nitrogen base, 0.5% w/v Ammonium sulphate, 0.064% w/v CSM-WL, 2% w/v Glucose, 0.002% w/v Adenine, 2% w/v Agar oxoid, pH 5.8) (MP Biomedicals). Transformation with sterile H₂O was used as control. For interaction studies, 10-fold serial dilutions of transformed cells in 10% glycerol diluted in H₂O (sterile) were carried out. These serial dilutions were then spotted on CSM-WL, CSM-WLH (0.064% w/v CSM-WLH) and CSM-WLHA (0.064% w/v CSM-WLHA) plates and incubated at 30°C for 2-6 days. Spotting on CSM-WL was used as a control for the serial dilution. As negative control, a combination of respective empty vector with TFs or SE were co-transformed and spotted on CSM-WL, CSM-WLH and CSM-WLHA plates.

6.1.5 Co-Immunoprecipitation

Nicotiana benthamiana leaves were infiltrated with N terminally fused TFs with mRFP and C terminally fused SE with HA tag. After two days, leaves were harvested and ground into fine powder using liquid nitrogen. This powder was resuspended in 1 mL protein extraction buffer (50mM Tris-HCl pH7.5 adjusted at 4°C, 100mM NaCl, 0.5% Triton X-100, 10% Glycerol, 1mM PMSF, 50µM MG132, 2mM DTT, 10µM ZnSO₄, 1x cOmplete protease inhibitor cocktail, 1x plant protease inhibitor cocktail) and centrifuged at 16000 rcf for 10 mins at 4°C (Eppendorf Microcentrifuge 5424R). Supernatant was stored in a new tube and 50 µL was aliquoted as input. Remaining supernatant was added to washed RFP-trap magnetic beads (Chromotek GmbH) and incubated at 4°C on a rotating wheel for 1 hr. Using a magnetic stand, beads were washed with washing buffer (50mM Tris-HCl pH 7.5 adjusted at 4°C, 100mM NaCl, 10% Glycerol) 3 times and then resuspended in 2x Laemmli buffer (5x stock: 250mM Tris-HCl pH 6.8, 50% Glycerol, 10% SDS, 1mg/mL bromophenol blue). 2x Laemmli buffer was also added to input and all samples were heated at 80°C for 10 mins. Using a magnetic stand, supernatant from the IP fraction was transferred to a new tube and beads were discarded. Samples were then stored at -20°C or loaded on an SDS-PAGE gel for further analysis.

6.1.6 SDS-PAGE and Western blotting

SDS-PAGE Gel was cast with 7.5% or 10% resolving gel and 5% stacking gel. The gel was then assembled in the electrophoresis chamber filled with 1x SDS running buffer (2mM Tris base, 192mM Glycine, 1% SDS). 30 μ L of sample was loaded in the wells along with PAGERuler Prestained protein ladder. The gel was run at 300V, 25mA/gel until the dye reaches at the lower end of resolving gel. This gel was then sandwiched with Nitrocellulose membrane and Whatmann paper inside a protein transfer cassette. The cassette was placed in a blotting tank containing 1x transfer buffer (150mM Glycine, 20mM Tris base, 20% EtOH). Proteins were transferred on the membrane at 100V, 400mA for 1-2hrs. Subsequently, the membrane was stained with Ponceau S for 5 mins to visualize highly abundant proteins. It was then stored in 1x ROTI[®] block (Carl Roth GmbH) at 4°C overnight. For immunodetection, primary antibody (mRFP 1:2000 Chromotek GmbH, HA 1:3000 Agrisera) was mixed with 1% milk powder in 1x PBS (137mM NaCl, 2.7mM KCl, 8.1mM Na₂HPO₄, 1.4mM KH₂PO₄) and incubated with the membrane for 1.5 hrs at RT with continuous shaking. Nitrocellulose membrane was then washed 3 times in 1x PBS supplemented with 0.1% Tween-20. Successively, secondary antibody (Rabbit anti-mouse-HRP 1:5000 Agrisera, Goat anti-Rabbit-HRP 1:25000 Agrisera) resuspended in 1xPBS + 1% milk powder was added to the primed membrane and incubated for 1 hr at RT. Membrane was again washed 3 times with 1x PBS and 0.1% Tween-20. Signal was detected using ECL reagent kit (Advansta Inc.) and a CCD camera (Azure Biosystems c400). Images obtained were then edited using Adobe Illustrator 2022.

6.1.7 Isolation of total RNA and cDNA preparation

Isolation of total RNA was carried out using RNeasy Plant Mini kit (Qiagen). Isolation of miRNA was carried out using Direct-zol RNA Microprep Kit (Zymo Research). RNA concentration was measured using Nanodrop (DeNovix DS-11, ThermoFisher Scientific™). To check quality, diluted RNA was separated on a 1% agarose gel and visualized under UV light (Azure Biosystems c200).

For cDNA synthesis, RevertAid First strand cDNA synthesis Kit (ThermoFisher Scientific) was used. 0.5-1 μ g of total RNA was incubated with DNase I (1U/ μ L, ThermoFisher Scientific) for 30min at 37°C. 1 μ L of 50mM EDTA was added and incubated at 65°C for 10 mins to inactivate DNase I.

1 μ L of 100mM oligo-dT was added and mixture was incubated at 65°C for 5 mins. In case of cDNA synthesis for miRNA an additional 0.5 μ L of stemloop oligonucleotide mixture (4 different oligos with a concentration of 2mM each) was added.

For reverse transcriptase reaction, 1x RT buffer, 1mM dNTPs, 1x Ribo-Lock and 1U Revert-Aid was added to the mixture and incubated at 42°C for 60 mins followed by 5 mins at 70°C. For cDNA synthesis of miRNAs, a PCR cycle with the following program was used:

| Temperature | Time |
|-------------|---------|
| 16°C | 30 mins |
| 30°C | 30s |
| 42°C | 30s |
| 50°C | 1s |
| 85°C | 5 mins |

} 60 cycles

Table M 4 PCR program for cDNA synthesis of miRNA using stemloop oligonucleotides. cDNA was then stored at -20°C.

6.1.8 Quantitative PCR (qPCR)

qPCR was carried out using 2X Maxima SYBR Green Master Mix (ThermoFisher Scientific) and CFX384 qPCR machine (Bio-Rad Laboratories Inc.). For highly abundant transcripts, cDNA was diluted 1:5 in nuclease free water. 2-3 technical replicates and at least 3 biological replicates were carried out for each transcript analysed. For each oligonucleotide combination, a no template control was used. For quantification of relative expression of transcripts, *TUBULIN* was used as control housekeeping gene. qPCR reaction mixture and qPCR program used are listed in Table M 5. Ct values were determined using the threshold cycle method. For data analysis, $\Delta\Delta$ Ct method was used.

| qPCR reaction mixture | | qPCR program | | |
|--------------------------------|--------------|-----------------------------------|-------|----------------------------------|
| Reagent | Volume | Temperature | Time | |
| SYBR Green Mastermix (2x) | 5 μ L | 95°C | 5 min | |
| Forward Oligonucleotide (10mM) | 0.25 μ L | 95°C | 10s | } 40 cycles |
| Reverse Oligonucleotide (10mM) | 0.25 μ L | 55°C | 30s | |
| Template (different dilutions) | 1 μ L | 72°C | 30s | |
| | | | | Photometric measurement at 530nm |
| Nuclease free water | 3.5 μ L | 95°C | 30s | |
| Total | 10 μ L | 55°C to 95°C +1°C each step | 5s | Photometric measurement at 530nm |

Table M 5: qPCR reaction mixture and program.

6.1.9 RNA library preparation, sequencing, and data analysis

For RNA library preparation, 3 μ g of total RNA was treated with DNase I (1U/ μ L). DNase I treated RNA was then purified using RNA Clean and Concentrator Kit (Zymo Research). 1 μ g of purified total RNA was used to isolate mRNA using Poly(A) mRNA magnetic isolation module (NEB #7490). mRNA library was prepared using NEBNext Ultra II RNA library kit with Sample purification beads (NEB #7775). Index primers used for barcoding were NEBNext Multiplex Oligos for Illumina (Set1, 2 and 3). To check the size and quality of the library, samples were run on Bioanalyzer (Agilent 2100) using High Sensitivity DNA Kit (Agilent Technologies). Samples were pooled and mRNA library was sequenced using Illumina sequencing NovaSeq-PE150 (Novogene Co. Ltd.).

For data analysis, first step was to perform a quality control on the reads obtained. FastQC and MultiQC tools were used for quality check. Adaptor sequences were trimmed using Trim Galore. rRNA and tRNA reads were filtered using bowtie2 tool. Once the reads were quality controlled, trimmed and filtered, they were aligned to custom reference derived from atRTD2 transcriptome (R. Zhang et al., 2016). Salmon was used to quantify the expression of transcripts (Patro et al., 2017). TPM (transcript per kilobase million) abundance was measured using TXimport (Soneson

et al., 2016a). Differential expression analysis was performed using Deseq2 within R between WT/*se-1*, WT/*toe1-2toe2-1* and WT/*toe1-2 toe2-1 se-1* using the annotated file generated (adjusted $p < 0.05$ and \log_2 fold change $< \pm 1$) (Soneson et al., 2016b).

6.1.10 Generation of CRISPR-Cas9 mutants

CRISPR-Cas9 based multiple allele mutant generation protocol was adapted from Ordon and colleagues. (Ordon et al., 2020)

6.1.10.1 sgRNA selection

sgRNAs were selected using CRISPR-P V2.0 software (H. Liu et al., 2017) or CHOP-CHOP v3 software (Labun et al., 2019; Labun et al., 2016). The length of the sgRNA was 23-24 nucleotides (including overhangs 'attg' or 'aac' necessary for golden gate cloning) with a GC content of 40-60%. PAM sequence 'NGG' acted as anchoring point in the genome to design the sgRNA. The list of sgRNAs used and their targets is listed in Supplementary table 2.

6.1.10.2 Golden Gate cloning

Golden gate cloning was performed in two steps. Initially individual sgRNAs were cloned in shuttle vectors (pDGE331-342). The shuttle vectors were chosen based on number of sgRNAs to be used as mentioned by (Ordon et al., 2020). The details for reaction mixture and incubation period are mentioned in Table M 6: Reaction mixture and incubation cycle for cloning sgRNAs into shuttle vectors. NEB α cells were directly inoculated in liquid LB medium containing ampicillin (concentration mentioned in Table M 3). Following day, plasmids were isolated using GeneJET plasmid miniprep kit (ThermoFisher Scientific) and test digested using HindIII and XbaI (0.1 μ L of each enzyme, 1 μ L of 10x FD buffer, 3 μ L of plasmid, 5.8 μ L of H₂O).

| Reaction mixture | | Incubation cycle | |
|-----------------------------|---------|------------------|---------|
| Reagent | Volume | Temperature | Time |
| pDGE331-342 | 20 fmol | 37°C | 2 mins |
| Hybridized oligonucleotides | 50 fmol | 16°C | 5 mins |
| 10x Ligation buffer | 1 µL | 50°C | 10mins |
| 10x BSA (10mg/mL) | 1 µL | 80°C | 10 mins |
| Bpil | 0.5 µL | | |
| T4 DNA ligase (1U/ µL) | 0.5 µL | | |
| H ₂ O | | | |
| Total | 10 µL | | |

Table M 6: Reaction mixture and incubation cycle for cloning sgRNAs into shuttle vectors.

Second step was to clone multiple sgRNAs from the shuttle vector into the multiplex destination vector pDGE347. The details of reaction mixture and incubation period are mentioned in Table M 7. Ligated multiplex vector was then transformed into NEBα cells and plated on LB agar medium containing spectinomycin (concentration mentioned in Table M 3).

| Reaction mixture | | Incubation cycle | |
|------------------------|---------|------------------|---------|
| Reagent | Volume | Temperature | Time |
| pDGE347 | 20 fmol | 37°C | 2 mins |
| sgRNA shuttle vector | 20 fmol | 16°C | 5 mins |
| 10x Ligation buffer | 2 µL | 50°C | 10mins |
| 10x BSA (10mg/mL) | 2 µL | 80°C | 10 mins |
| Bpil | 1 µL | | |
| T4 DNA ligase (1U/ µL) | 1 µL | | |
| H ₂ O | | | |
| Total | 20 µL | | |

Table M 7: Reaction mixture and incubation cycle for cloning shuttle vectors into destination vector.

4-6 colonies were picked from the plates and grown in liquid medium. Following day, plasmid isolation was carried out as mentioned above. Plasmid was test digested with AatII and PacI enzymes. To ensure correct ligation of sgRNAs, vector was sequenced using Sanger sequencing (Eurofins GmbH). Confirmed vector was then transformed into *A. tumefaciens* and transformed into plants.

6.1.10.3 FAST screening

After selection of transgenic lines and genotyping for mutations in T1 or T2 generation, Cas9 free plants were selected using FAST screening method. FAST marker was expressed in transgenic plants under a seed coat specific promoter. Seeds which do not express FAST marker were selected using a fluorescence microscope. Seeds were viewed under a Brightfield light and mRFP filter (Alexa 568nm) using Leica DM5500B fluorescence microscope and cellSens imaging software. 15-20 non-fluorescent seeds were picked using a toothpick and then grown on soil.

6.2 Plant based methods

6.2.1 Plant Growth conditions

6.2.1.1 On soil

Arabidopsis thaliana seeds were stratified in 0.1% agarose at 4°C in dark for 2 days. Seeds were grown on soil in a CLF Plant Climatics growth chamber under long day conditions (16h light/8h dark) at 22°C or under continuous light conditions. For *Nicotiana benthamiana*, seeds were directly grown on soil without stratification.

6.2.1.2 On plates or liquid media

Seeds were sterilized under a clean bench (LaminAir® HB2472) by rinsing them in 80% EtOH and 0.05% Triton-X100 for 15 mins on a rotating wheel. Then they were washed with 100% EtOH. Seeds were grown on plates containing ½ MS media (2.15 g/L Murashige Skoog medium, 8 g/L Phytoagar, pH 5.7). After stratification at 4°C in dark for 2 days, plates were transferred to plant chamber (Percival Incubator) with continuous light conditions a 22°C. For seeds in liquid media, flasks were incubated at 130 rpm under continuous light at 22°C.

6.2.2 Floral dip

Agrobacterium tumefaciens was grown in LB medium containing Rifampicin, Gentamicin, and other necessary antibiotics (concentrations mentioned in Table M 3) overnight at 28°C. Freshly grown cells were then centrifuged at 3500 g for 10 mins at 4°C. Pelleted cells were resuspended in dipping solution (200 mL water, 10 g sucrose and 100 µL Silwet). Subsequently, flowering plants were dipped in this cell suspension for 1 min each. Overnight, plants were kept in dark and then moved to plant chamber the following day. (Clough & Bent, 1998)

6.2.3 *Nicotiana benthamiana* leaf infiltration

Agrobacterium tumefaciens containing the respective plasmid was grown in LB medium with Rifampicin, Gentamicin, and other necessary antibiotics (concentrations mentioned in Table M 3) overnight at 28°C. Following day, cells were centrifuged at 3500 g for 10 mins at 4°C. Cells were

resuspended in infiltration medium (10mM MgCl₂, 10mM MES pH 5.7, 100μM acetosyringone) and the OD_{600nm} was adjusted to 0.5. Cells suspension was incubated at RT for 3 hrs under shaking conditions. For ColP, cell suspensions with two different plasmids were mixed in 1:1 ratio. p19 plasmid was used to enhance the protein expression in leaves. Using a 1 mL syringe, cell suspension mixture was infiltrated through the abaxial side of the leaf. Infiltrated plants were kept in dark overnight and then moved to the plant chamber. Leaves were then harvested after two days for further processing.

6.2.4 Crossing of plants

3-4 closed flowers of *Arabidopsis thaliana* were emasculated by removing the stamen under dissection binocular (Zeiss STEMI SV8). 2-3 days later, emasculated flowers were pollinated using pollen from the crossing partner.

6.2.5 Selection of transgenic plants

BASTA selection was used to identify transgenic plants containing the CRISPR-Cas9 construct pDGE347. Seeds from floral dipped T0 generation were harvested and sterilized. Sterilized seeds were then sown on BASTA containing ½ MS medium. After 2 days of stratification, plates were moved to the plant chamber for approx. 10-15 days. BASTA resistant transgenic plants survived, which were then moved on soil.

6.2.6 Phenotypic analyses

To study phenotype of mutants, phase transition time (from juvenile to adult), leaf initiation rate, adult leaf size and flowering time was observed as explained below. Leaf morphology image was generated by arranging the leaves on a sheet of paper and scanning this sheet using Canon LiDe scanner.

6.2.6.1 Counting rosette leaf number for flowering time determination

Seeds were sown on soil and grown under long day conditions. Number of rosette leaves were counted once the plant started bolting. Minimum 20 plants per genotype were analysed. Experiment was conducted in duplicates.

6.2.6.2 Determining phase transition from juvenile to adult stage

To determine phase transition, first rosette leaf with formation of trichomes on the abaxial side was noted. Minimum 20 plants per genotype were examined. Experiment was conducted in duplicates.

6.2.6.3 Calculating leaf initiation rate

For calculating leaf initiation rate, number of rosette leaves formed were counted every two days up until bolting. Minimum 20 plants per genotype were examined. Experiment was conducted in duplicates.

6.2.6.4 Measuring leaf area

The width and length of the first adult leaf of each plant was measured using a scale. Average of 20 plants for each mutant and WT was counted. Experiment was conducted in duplicates.

7 References

- Andrés, F., Kinoshita, A., Kalluri, N., Fernández, V., Falavigna, V. S., Cruz, T. M. D., Jang, S., Chiba, Y., Seo, M., Mettler-Altmann, T., Huettel, B., & Coupland, G. (2020). The sugar transporter SWEET10 acts downstream of FLOWERING LOCUS T during floral transition of *Arabidopsis thaliana*. *BMC Plant Biology*, *20*(1), 1–14. <https://doi.org/10.1186/S12870-020-2266-0/FIGURES/5>
- Aslam, M., Fakher, B., Jakada, B. H., Cao, S., & Qin, Y. (2019). SWR1 Chromatin Remodeling Complex: A Key Transcriptional Regulator in Plants. *Cells*, *8*(12). <https://doi.org/10.3390/CELLS8121621>
- Aukerman, M. J., & Sakai, H. (2003). Regulation of Flowering Time and Floral Organ Identity by a MicroRNA and Its APETALA2-Like Target Genes. *The Plant Cell*, *15*(11), 2730–2741. <https://doi.org/10.1105/TPC.016238>
- Bajczyk, M., Lange, H., Bielewicz, D., Szewc, L., Bhat, S. S., Dolata, J., Kuhn, L., Szweykowska-Kulinska, Z., Gagliardi, D., & Jarmolowski, A. (2020a). SERRATE interacts with the nuclear exosome targeting (NEXT) complex to degrade primary miRNA precursors in *Arabidopsis*. *BioRxiv*, 2020.04.08.032003. <https://doi.org/10.1101/2020.04.08.032003>
- Bajczyk, M., Lange, H., Bielewicz, D., Szewc, L., Bhat, S. S., Dolata, J., Kuhn, L., Szweykowska-Kulinska, Z., Gagliardi, D., & Jarmolowski, A. (2020b). SERRATE interacts with the nuclear exosome targeting (NEXT) complex to degrade primary miRNA precursors in *Arabidopsis*. *Nucleic Acids Research*, *48*(12), 6839–6854. <https://doi.org/10.1093/nar/gkaa373>

Cao, M., Chen, R., Li, P., Yu, Y., Zheng, R., Ge, D., Zheng, W., Wang, X., Gu, Y., Gelová, Z., Friml, J., Zhang, H., Liu, R., He, J., & Xu, T. (2019). TMK1-mediated auxin signalling regulates differential growth of the apical hook. *Nature*, 1. <https://doi.org/10.1038/s41586-019-1069-7>

Chandrika, N. N. P., Sundaravelpandian, K., Yu, S. M., & Schmidt, W. (2013). ALFIN-LIKE 6 is involved in root hair elongation during phosphate deficiency in Arabidopsis. *New Phytologist*, 198(3), 709–720. <https://doi.org/10.1111/nph.12194>

Chen, D., Yan, W., Fu, L. Y., & Kaufmann, K. (2018). Architecture of gene regulatory networks controlling flower development in Arabidopsis thaliana. *Nature Communications* 2018 9:1, 9(1), 1–13. <https://doi.org/10.1038/s41467-018-06772-3>

Clough, S. J., & Bent, A. F. (1998). Floral dip: A simplified method for Agrobacterium-mediated transformation of Arabidopsis thaliana. *Plant Journal*, 16(6), 735–743. <https://doi.org/10.1046/j.1365-313X.1998.00343.x>

Dai, X., Sinharoy, S., Udvardi, M., & Zhao, P. X. (2013). PlantTFcat: An online plant transcription factor and transcriptional regulator categorization and analysis tool. *BMC Bioinformatics*, 14(1), 1–6. <https://doi.org/10.1186/1471-2105-14-321/FIGURES/3>

Doebley, J. (1993). Genetics, development and plant evolution. *Current Opinion in Genetics & Development*, 3(6), 865–872. [https://doi.org/10.1016/0959-437X\(93\)90006-B](https://doi.org/10.1016/0959-437X(93)90006-B)

Dong, Z., Han, M. H., & Fedoroff, N. (2008). The RNA-binding proteins HYL1 and SE promote

accurate in vitro processing of pri-miRNA by DCL1. *Proceedings of the National Academy of Sciences of the United States of America*, 105(29), 9970–9975. <https://doi.org/10.1073/PNAS.0803356105>

Du, S.-S., Li, L., Li, L., Wei, X., Xu, F., Xu, P., Wang, W., Xu, P., Cao, X., Miao, L., Guo, T., Wang, S., Mao, Z., & Yang, H.-Q. (2020). Photoexcited Cryptochrome2 Interacts Directly with TOE1 and TOE2 in Flowering Regulation. *Plant Physiology*, 184(1), 487–505. <https://doi.org/10.1104/PP.20.00486>

Eulgem, T., Rushton, P. J., Robatzek, S., & Somssich, I. E. (2000). The WRKY superfamily of plant transcription factors. *Trends in Plant Science*, 5(5), 199–206. [https://doi.org/10.1016/S1360-1385\(00\)01600-9](https://doi.org/10.1016/S1360-1385(00)01600-9)

Fields, S., & Song, O. K. (1989). A novel genetic system to detect protein-protein interactions. *Nature*, 340(6230), 245–246. <https://doi.org/10.1038/340245A0>

Fung, H. Y. J., Birol, M., & Rhoades, E. (2018). IDPs in macromolecular complexes: the roles of multivalent interactions in diverse assemblies. *Current Opinion in Structural Biology*, 49, 36. <https://doi.org/10.1016/J.SBI.2017.12.007>

Gruber, J. J., Olejniczak, S. H., Yong, J., LaRocca, G., Dreyfuss, G., & Thompson, C. B. (2012). Ars2 Promotes Proper Replication-Dependent Histone mRNA 3' End Formation. *Molecular Cell*, 45(1), 87–98. <https://doi.org/10.1016/J.MOLCEL.2011.12.020>

Hallais, M., Pontvianne, F., Andersen, P. R., Clerici, M., Lener, D., Benbahouche, N. E. H., Gostan,

- T., Vandermoere, F., Robert, M. C., Cusack, S., Verheggen, C., Jensen, T. H., & Bertrand, E. (2013). CBC–ARS2 stimulates 3'-end maturation of multiple RNA families and favors cap-proximal processing. *Nature Structural & Molecular Biology* 20:12, 20(12), 1358–1366. <https://doi.org/10.1038/nsmb.2720>
- Iwata, Y., Takahashi, M., Fedoroff, N. V., & Hamdan, S. M. (2013). Dissecting the interactions of SERRATE with RNA and DICER-LIKE 1 in Arabidopsis microRNA precursor processing. *Nucleic Acids Research*, 41(19), 9129–9140. <https://doi.org/10.1093/NAR/GKT667>
- Kim, S., Soltis, P. S., Wall, K., & Soltis, D. E. (2006). Phylogeny and Domain Evolution in the APETALA2-like Gene Family. *Molecular Biology and Evolution*, 23(1), 107–120. <https://doi.org/10.1093/MOLBEV/MSJ014>
- Labun, K., Montague, T. G., Gagnon, J. A., Thyme, S. B., & Valen, E. (2016). CHOPCHOP v2: a web tool for the next generation of CRISPR genome engineering. *Nucleic Acids Research*, 44(W1), W272–W276. <https://doi.org/10.1093/NAR/GKW398>
- Labun, K., Montague, T. G., Krause, M., Torres Cleuren, Y. N., Tjeldnes, H., & Valen, E. (2019). CHOPCHOP v3: expanding the CRISPR web toolbox beyond genome editing. *Nucleic Acids Research*, 47(W1), W171–W174. <https://doi.org/10.1093/NAR/GKZ365>
- Laubinger, S., Sachsenberg, T., Zeller, G., Busch, W., Lohmann, J. U., Ratsch, G., & Weigel, D. (2008). Dual roles of the nuclear cap-binding complex and SERRATE in pre-mRNA splicing and microRNA processing in Arabidopsis thaliana. *Proceedings of the National Academy of Sciences of the United States of America*, 105(25), 8795–8800. <https://doi.org/10.1073/pnas.0802493105>

- Le Hir, H., Nott, A., & Moore, M. J. (2003). How introns influence and enhance eukaryotic gene expression. *Trends in Biochemical Sciences*, *28*(4), 215–220. [https://doi.org/10.1016/S0968-0004\(03\)00052-5](https://doi.org/10.1016/S0968-0004(03)00052-5)
- Liang, X., Lei, M., Li, F., Yang, X., Zhou, M., Li, B., Cao, Y., Gong, S., Liu, K., Liu, J., Qi, C., & Liu, Y. (2018). Family-Wide Characterization of Histone Binding Abilities of PHD Domains of AL Proteins in *Arabidopsis thaliana*. *Protein Journal*, *37*(6), 531–538. <https://doi.org/10.1007/s10930-018-9796-4>
- Liu, H., Ding, Y., Zhou, Y., Jin, W., Xie, K., & Chen, L. L. (2017). CRISPR-P 2.0: An Improved CRISPR-Cas9 Tool for Genome Editing in Plants. *Molecular Plant*, *10*(3), 530–532. <https://doi.org/10.1016/J.MOLP.2017.01.003>
- Liu, L., White, M. J., & MacRae, T. H. (1999). Transcription factors and their genes in higher plants. *European Journal of Biochemistry*, *262*(2), 247–257. <https://doi.org/10.1046/J.1432-1327.1999.00349.X>
- Lobbes, D., Rallapalli, G., Schmidt, D. D., Martin, C., & Clarke, J. (2006). SERRATE: a new player on the plant microRNA scene. *EMBO Reports*, *7*(10), 1052–1058. <https://doi.org/10.1038/sj.embor.7400806>
- Luo, J., Zhou, J. J., & Zhang, J. Z. (2018). Aux/IAA Gene Family in Plants: Molecular Structure, Regulation, and Function. *International Journal of Molecular Sciences*, *19*(1), 86–113. <https://doi.org/10.3390/IJMS19010259>

- Ma, Z., Castillo-González, C., Wang, Z., Sun, D., Hu, X., Shen, X., Potok, M. E., & Zhang, X. (2018). Arabidopsis Serrate Coordinates Histone Methyltransferases ATXR5/6 and RNA Processing Factor RDR6 to Regulate Transposon Expression. *Developmental Cell*, 45(6), 769-784.e6. <https://doi.org/10.1016/j.devcel.2018.05.023>
- Machida, S., Chen, H.-Y., & Adam Yuan, Y. (2011). Molecular insights into miRNA processing by Arabidopsis thaliana SERRATE. *Nucleic Acids Research*, 39(17), 7828–7836. <https://doi.org/10.1093/nar/gkr428>
- Marzi, M. J., Ghini, F., Cerruti, B., De Pretis, S., Bonetti, P., Giacomelli, C., Gorski, M. M., Kress, T., Pelizzola, M., Muller, H., Amati, B., & Nicassio, F. (2016). Degradation dynamics of microRNAs revealed by a novel pulse-chase approach. *Genome Research*, 26(4), 554. <https://doi.org/10.1101/GR.198788.115>
- Melko, M., Winczura, K., Rouvière, J. O., Oborská-Oplová, M., Andersen, P. K., & Heick Jensen, T. (2020). Mapping domains of ARS2 critical for its RNA decay capacity. *Nucleic Acids Research*, 48(12), 6943–6953. <https://doi.org/10.1093/NAR/GKAA445>
- Molitor, A. M., Bu, Z., Yu, Y., & Shen, W. H. (2014). Arabidopsis AL PHD-PRC1 Complexes Promote Seed Germination through H3K4me3-to-H3K27me3 Chromatin State Switch in Repression of Seed Developmental Genes. *PLoS Genetics*, 10(1), 1004091. <https://doi.org/10.1371/journal.pgen.1004091>
- Ó'Maoiléidigh, D. S., Driel, A. D. van, Singh, A., Sang, Q., Bec, N. Le, Vincent, C., Olalla, E. B. G. de, Vayssières, A., Branchat, M. R., Severing, E., Gallegos, R. M., & Coupland, G. (2021). Systematic analyses of the MIR172 family members of Arabidopsis define their distinct roles

in regulation of APETALA2 during floral transition. *PLOS Biology*, 19(2), e3001043. <https://doi.org/10.1371/JOURNAL.PBIO.3001043>

Ordon, J., Bressan, M., Kretschmer, C., Dall'Osto, L., Marillonnet, S., Bassi, R., & Stuttman, J. (2020). Optimized Cas9 expression systems for highly efficient Arabidopsis genome editing facilitate isolation of complex alleles in a single generation. *Functional and Integrative Genomics*, 20(1), 151–162. <https://doi.org/10.1007/S10142-019-00665-4/FIGURES/5>

Parchaliuk, D., Daniel Gietz, R., Agatep, R., Kirkpatrick, R. D., Parchaliuk, D. L., & Woods, R. A. (1998). Transformation of *Saccharomyces cerevisiae* by the lithium acetate/single-stranded carrier DNA/polyethylene glycol (LiAc/ss-DNA/PEG) protocol Transformation of *Saccharomyces cerevisiae* by the lithium acetate/single-stranded carrier DNA/polyethylene glycol protocol. *Technical Tips Online*, 3. [https://doi.org/10.1016/S1366-2120\(08\)70121-1](https://doi.org/10.1016/S1366-2120(08)70121-1)

Patro, R., Duggal, G., Love, M. I., Irizarry, R. A., & Kingsford, C. (2017). Salmon provides fast and bias-aware quantification of transcript expression. *Nature Methods* 2017 14:4, 14(4), 417–419. <https://doi.org/10.1038/nmeth.4197>

Prigge, M. J., & Wagner, D. R. (2001). The arabidopsis serrate gene encodes a zinc-finger protein required for normal shoot development. *The Plant Cell*, 13(6), 1263–1279. <https://doi.org/10.1105/tpc.13.6.1263>

Putterill, J., Robson, F., Lee, K., Simon, R., & Coupland, G. (1995). The CONSTANS Gene of Arabidopsis Promotes Flowering and Encodes a Protein Showing Similarities to Zinc Finger Transcription Factors. *Cell*, 80, 847–857.

- Raczynska, K. D., Stepien, A., Kierzkowski, D., Kalak, M., Bajczyk, M., McNicol, J., Simpson, C. G., Szweykowska-Kulinska, Z., Brown, J. W. S., & Jarmolowski, A. (2014). The SERRATE protein is involved in alternative splicing in *Arabidopsis thaliana*. *Nucleic Acids Research*, *42*(2), 1224–1244. <https://doi.org/10.1093/nar/gkt894>
- Sabin, L. R., Zhou, R., Gruber, J. J., Lukinova, N., Bambina, S., Berman, A., Lau, C. K., Thompson, C. B., & Cherry, S. (2009). Ars2 Regulates Both miRNA- and siRNA- Dependent Silencing and Suppresses RNA Virus Infection in *Drosophila*. *Cell*, *138*(2), 340–351. <https://doi.org/10.1016/J.CELL.2009.04.045>
- Schmid, M., Uhlenhaut, N. H., Godard, F., Demar, M., Bressan, R., Weigel, D., & Lohman, J. U. (2003). Dissection of floral induction pathways using global expression analysis. *Development*, *130*(24), 6001–6012. <https://doi.org/10.1242/DEV.00842>
- Schulze, W. M., Stein, F., Rettel, M., Nanao, M., & Cusack, S. (2018). Structural analysis of human ARS2 as a platform for co-transcriptional RNA sorting. *Nature Communications*, *9*(1), 1701. <https://doi.org/10.1038/s41467-018-04142-7>
- Shimizu-Mitao, Y., & Kakimoto, T. (2014). Auxin Sensitivities of All *Arabidopsis* Aux/IAAs for Degradation in the Presence of Every TIR1/AFB. *Plant and Cell Physiology*, *55*(8), 1450–1459. <https://doi.org/10.1093/pcp/pcu077>
- Simon, J. A., & Kingston, R. E. (2009). Mechanisms of Polycomb gene silencing: knowns and unknowns. *Nature Reviews Molecular Cell Biology*, *10*(10), 697–708. <https://doi.org/10.1038/nrm2763>

- Soneson, C., Love, M. I., Robinson, M. D., & Floor, S. N. (2016a). *Differential analyses for RNA-seq: transcript-level estimates improve gene-level inferences [version 1; peer review: 2 approved]*. <https://doi.org/10.12688/f1000research.7563.1>
- Soneson, C., Love, M. I., Robinson, M. D., & Floor, S. N. (2016b). Differential analyses for RNA-seq: transcript-level estimates improve gene-level inferences. *F1000Research* 2015 4:1521, 4, 1521. <https://doi.org/10.12688/f1000research.7563.1>
- Song, Y., Gao, J., Yang, F., Kua, C. S., Liu, J., & Cannon, C. H. (2013). Molecular Evolutionary Analysis of the Alfin-Like Protein Family in *Arabidopsis lyrata*, *Arabidopsis thaliana*, and *Thellungiella halophila*. *PLoS ONE*, 8(7), 66838. <https://doi.org/10.1371/journal.pone.0066838>
- Speth, C., Szabo, E. X., Martinho, C., Collani, S., zur Oven-Krockhaus, S., Richter, S., Droste-Borel, I., Macek, B., Stierhof, Y. D., Schmid, M., Liu, C., & Laubinger, S. (2018). *Arabidopsis* RNA processing factor SERRATE regulates the transcription of intronless genes. *ELife*, 7. <https://doi.org/10.7554/eLife.37078>
- Tao, J. J., Wei, W., Pan, W. J., Lu, L., Li, Q. T., Ma, J. B., Zhang, W. K., Ma, B., Chen, S. Y., & Zhang, J. S. (2018). An Alfin-like gene from *Atriplex hortensis* enhances salt and drought tolerance and abscisic acid response in transgenic *Arabidopsis*. *Scientific Reports*, 8(1), 1–13. <https://doi.org/10.1038/s41598-018-21148-9>
- Valverde, F., Mouradov, A., Soppe, W., Ravenscroft, D., Samach, A., & Coupland, G. (2004). Photoreceptor Regulation of CONSTANS Protein in Photoperiodic Flowering. *Science*, 303(5660), 1003–1006. <https://doi.org/10.1126/science.1091761>

Wang, Lin, Yan, X., Li, Y., Wang, Z., Chhajed, S., Shang, B., Wang, Z., Choi, S. W., Zhao, H., Chen, S., & Zhang, X. (2022). PRP4KA phosphorylates SERRATE for degradation via 20 S proteasome to fine-tune miRNA production in Arabidopsis. *Science Advances*, 8(12), 8435. https://doi.org/10.1126/SCIADV.ABM8435/SUPPL_FILE/SCIADV.ABM8435_TABLES_S1_TO_S5.ZIP

Wang, Long, Zhou, C.-M., Mai, Y.-X., Li, L.-Z., Gao, J., Shang, G.-D., Lian, H., Han, L., Zhang, T.-Q., Tang, H.-B., Ren, H., Wang, F.-X., Wu, L.-Y., Liu, X.-L., Wang, C.-S., Chen, E.-W., Zhang, X.-N., Liu, C., & Wang, J.-W. (2019). A spatiotemporally regulated transcriptional complex underlies heteroblastic development of leaf hairs in Arabidopsis thaliana. *The EMBO Journal*, 38(8), e100063. <https://doi.org/10.15252/EMBJ.2018100063>

Wang, Z., Ma, Z., Castillo-González, C., Sun, D., Li, Y., Yu, B., Zhao, B., Li, P., & Zhang, X. (2018). SWI2/SNF2 ATPase CHR2 remodels pri-miRNAs via Serrate to impede miRNA production. *Nature*, 557(7706), 516–521. <https://doi.org/10.1038/s41586-018-0135-x>

Wei, W., Zhang, Y.-Q., Tao, J.-J., Chen, H.-W., Li, Q.-T., Zhang, W.-K., Ma, B., Lin, Q., Zhang, J.-S., & Chen, S.-Y. (2015). The Alfin-like homeodomain finger protein AL5 suppresses multiple negative factors to confer abiotic stress tolerance in Arabidopsis. *The Plant Journal*, 81(6), 871–883. <https://doi.org/10.1111/tpj.12773>

Werner, S., Bartrina, I., & Schmülling, T. (2021). Cytokinin regulates vegetative phase change in Arabidopsis thaliana through the miR172/TOE1-TOE2 module. *Nature Communications* 2021 12:1, 12(1), 1–11. <https://doi.org/10.1038/s41467-021-26088-z>

Wigge, P. A., Kim, M. C., Jaeger, K. E., Busch, W., Schmid, M., Lohmann, J. U., & Weigel, D. (2005).

Integration of spatial and temporal information during floral induction in Arabidopsis. *Science*, 309(5737), 1056–1059. https://doi.org/10.1126/SCIENCE.1114358/SUPPL_FILE/WIGGE.SOM.PDF

Wilson, M. D., Wang, D., Wagner, R., Breysens, H., Gertsenstein, M., Lobe, C., Lu, X., Nagy, A., Burke, R. D., Koop, B. F., & Howard, P. L. (2008). ARS2 Is a Conserved Eukaryotic Gene Essential for Early Mammalian Development . *Molecular and Cellular Biology*, 28(5), 1503–1514. https://doi.org/10.1128/MCB.01565-07/SUPPL_FILE/SUPPLEMENTAL_TABLE_A1.DOC

Wu, G., Park, M. Y., Conway, S. R., Wang, J.-W., Weigel, D., & Poethig, R. S. (2009). The sequential action of miR156 and miR172 regulates developmental timing in Arabidopsis. *Cell*, 138(4), 750. <https://doi.org/10.1016/J.CELL.2009.06.031>

Wu, G., & Poethig, R. S. (2006). Temporal regulation of shoot development in Arabidopsis thaliana by miR156 and its target SPL3. *Development (Cambridge, England)*, 133(18), 3539–3547. <https://doi.org/10.1242/DEV.02521>

Xie, D., Chen, M., Niu, J., Wang, L., Li, Y., Fang, X., Li, P., & Qi, Y. (2021). Phase separation of SERRATE drives dicing body assembly and promotes miRNA processing in Arabidopsis. *Nature Cell Biology*, 23(1), 32–39. <https://doi.org/10.1038/s41556-020-00606-5>

Xu, M., Hu, T., Zhao, J., Park, M. Y., Earley, K. W., Wu, G., Yang, L., & Poethig, R. S. (2016). Developmental Functions of miR156-Regulated SQUAMOSA PROMOTER BINDING PROTEIN-LIKE (SPL) Genes in Arabidopsis thaliana. *PLOS Genetics*, 12(8), e1006263. <https://doi.org/10.1371/JOURNAL.PGEN.1006263>

Yang, L., Liu, Z., Lu, F., Dong, A., & Huang, H. (2006a). SERRATE is a novel nuclear regulator in primary microRNA processing in Arabidopsis. *Plant Journal*, 47(6), 841–850. <https://doi.org/10.1111/j.1365-313X.2006.02835.x>

Yang, L., Liu, Z., Lu, F., Dong, A., & Huang, H. (2006b). SERRATE is a novel nuclear regulator in primary microRNA processing in Arabidopsis. *The Plant Journal*, 47(6), 841–850. <https://doi.org/10.1111/J.1365-313X.2006.02835.X>

Zhai, H., Bai, X., Zhu, Y., Li, Y., Cai, H., Ji, W., Ji, Z., Liu, X., Liu, X., & Li, J. (2010). A single-repeat R3-MYB transcription factor MYBC1 negatively regulates freezing tolerance in Arabidopsis. *Biochemical and Biophysical Research Communications*, 394(4), 1018–1023. <https://doi.org/10.1016/J.BBRC.2010.03.114>

Zhang, B., Wang, L., Zeng, L., Zhang, C., & Ma, H. (2015a). Arabidopsis TOE proteins convey a photoperiodic signal to antagonize CONSTANS and regulate flowering time. *Genes & Development*, 29(9), 975–987. <https://doi.org/10.1101/GAD.251520.114>

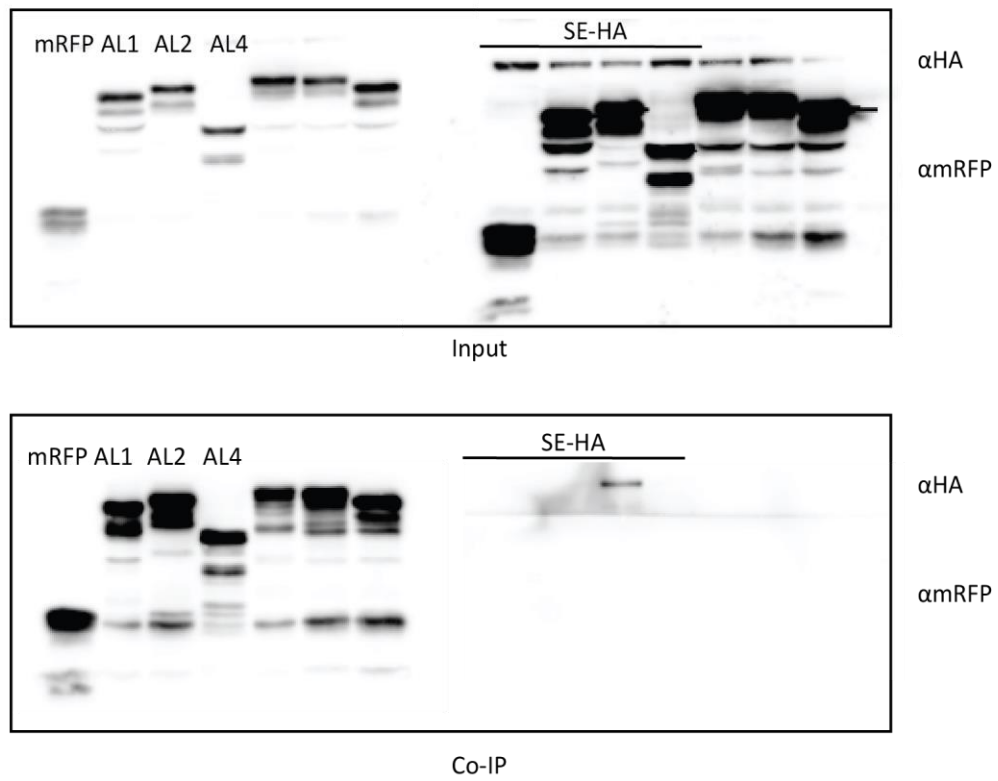
Zhang, B., Wang, L., Zeng, L., Zhang, C., & Ma, H. (2015b). Arabidopsis TOE proteins convey a photoperiodic signal to antagonize CONSTANS and regulate flowering time. *Genes & Development*, 29(9), 975–987. <https://doi.org/10.1101/GAD.251520.114>

Zhang, R., Calixto, C. P. G., Marquez, Y., Venhuizen, P., Tzioutziou, N. A., Guo, W., Spensley, M., Frey, N. F. dit, Hirt, H., James, A. B., Nimmo, H. G., Barta, A., Kalyna, M., & Brown, J. W. S. (2016). AtRTD2: A Reference Transcript Dataset for accurate quantification of alternative splicing and expression changes in Arabidopsis thaliana RNA-seq data. *BioRxiv*, 051938. <https://doi.org/10.1101/051938>

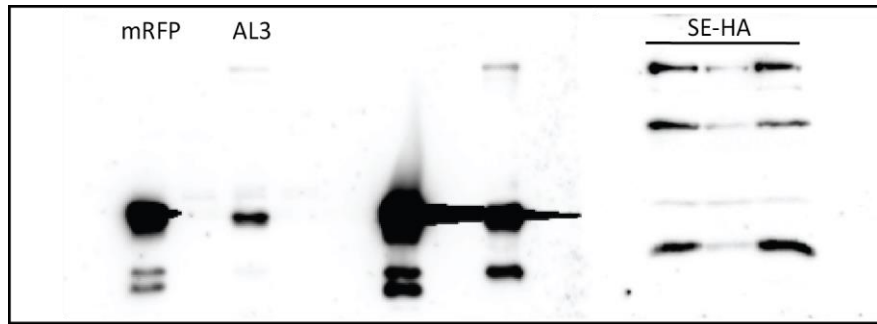
Zou, Y., Wang, S., & Lu, D. (2020). MiR172b-TOE1/2 module regulates plant innate immunity in an age-dependent manner. *Biochemical and Biophysical Research Communications*, 531(4), 503–507. <https://doi.org/10.1016/j.bbrc.2020.07.061>

Zou, Y., Wang, S., Zhou, Y., Bai, J., Huang, G., Liu, X., Zhang, Y., Tang, D., & Lu, D. (2018). Transcriptional Regulation of the Immune Receptor FLS2 Controls the Ontogeny of Plant Innate Immunity. *The Plant Cell*, tpc.00297.2018. <https://doi.org/10.1105/tpc.18.00297>

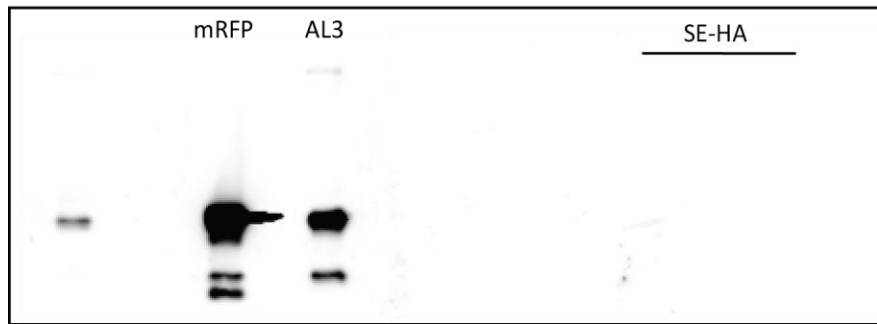
8 Supplementary Data



Supplementary Figure 1: Western blot images showing the Input and Co-IP for AL1, AL2 and AL4. These images are the full images for Figure 2.

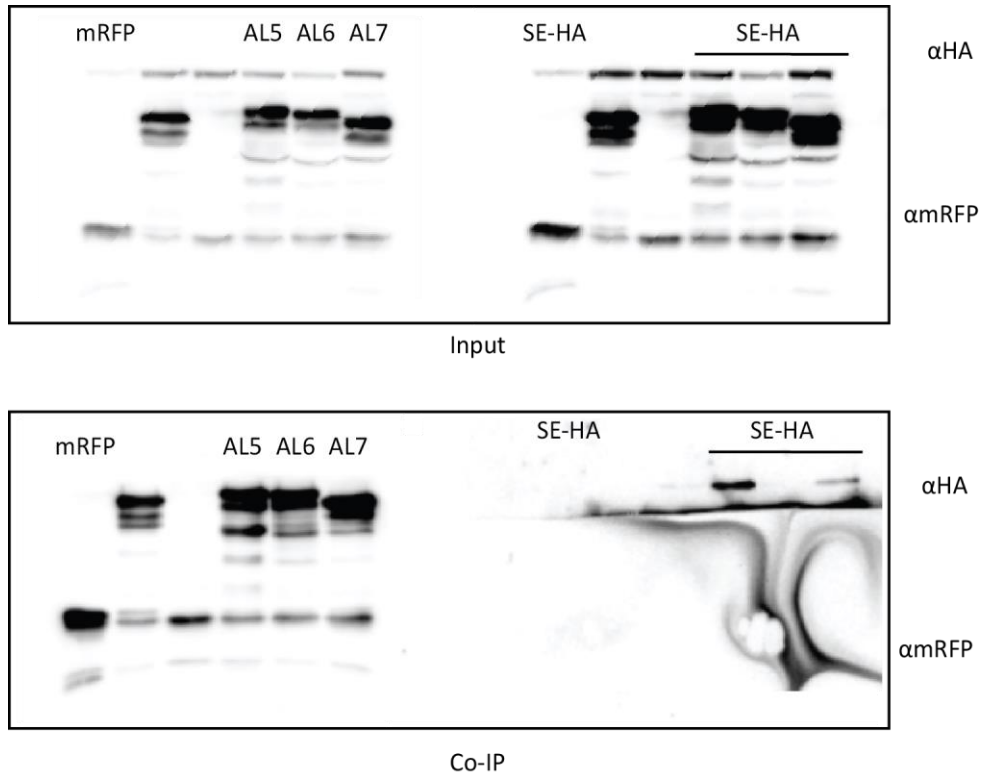


Input

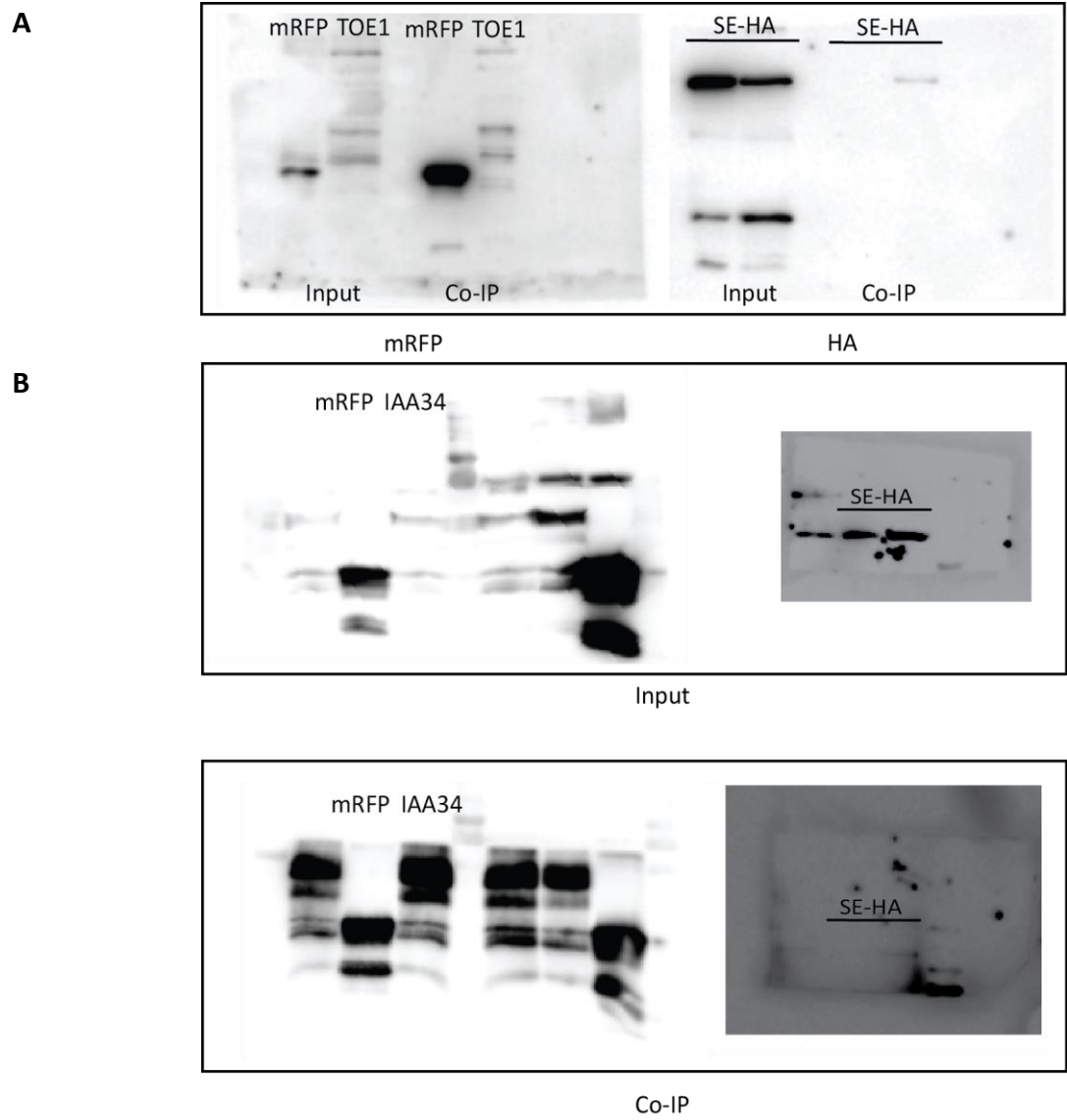


Co-IP

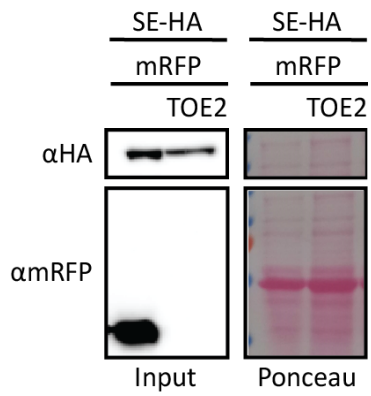
Supplementary Figure 2: Western blot images showing the Input and Co-IP for AL3. These images are the full images for Figure 2.



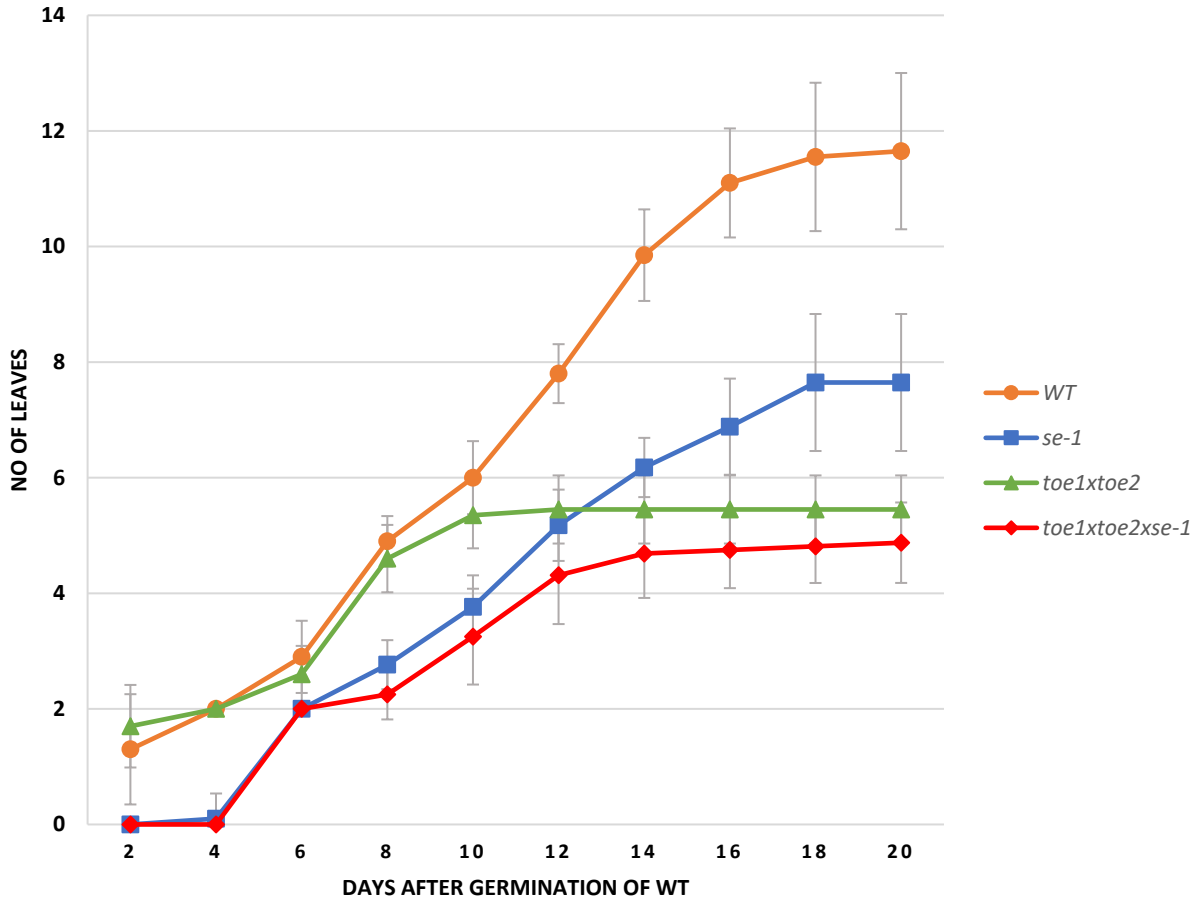
Supplementary Figure 3: Western blot images showing the Input and Co-IP for AL5, AL6 and AL7. These images are the full images for Figure 2.



Supplementary Figure 4: Complete western blot images showing the Input and Co-IP. These images are the full images for Figure 7. A) images of Co-IP from TOE1 B) Images of Co-IP from IAA34.

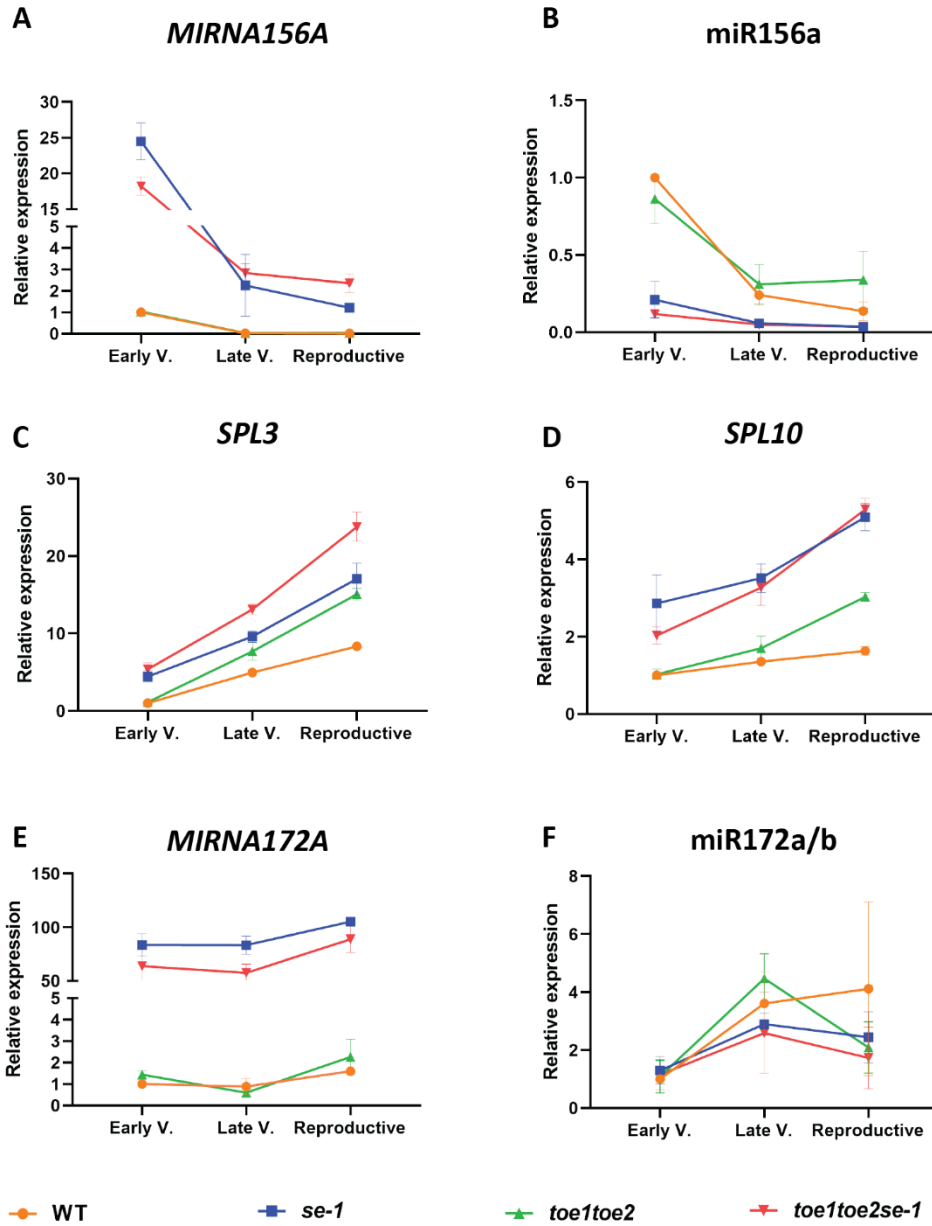


Supplementary Figure 5: Western blot images from tobacco leaves transformed with vectors containing TOE2-mRFP and SE-HA. No expression observed for TOE2-mRFP. Right column shows ponceau staining indicating the presence of proteins in the extract.

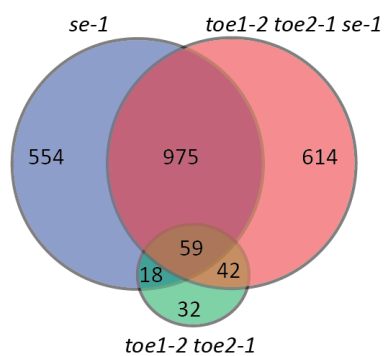
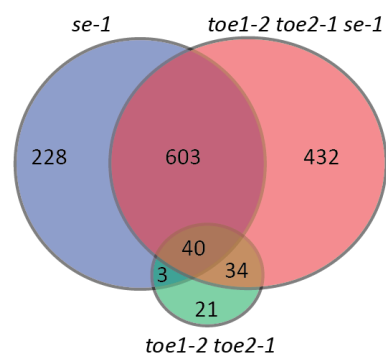
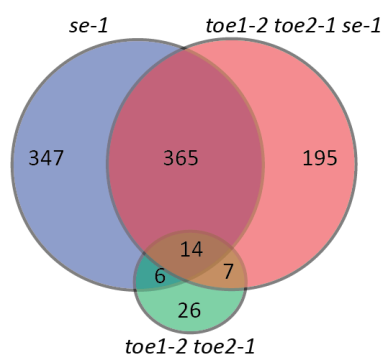
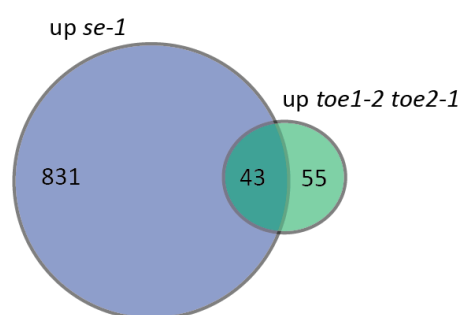
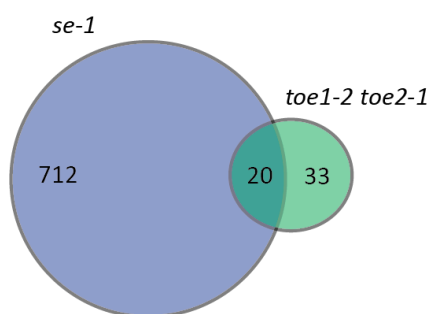
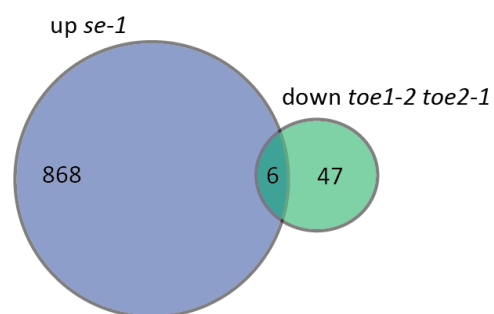
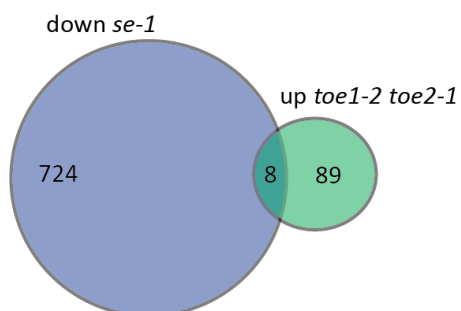


Supplementary Figure 6: Leaf initiation rate.

Comparison of leaf initiation rate of WT, *se-1 toe1-2 toe2-1*, *toe1-2 toe2-1 se-1* under long day conditions. Each point is an average of approximately 20 plants counted and whiskers show SD.



Supplementary Figure 7: Line graph showing the relative expression of genes and miRNAs. Relative expression of A) *MIRNA156a* B) *miR156a* C) *SPL3* D) *SPL10* E) *MIRNA172a* F) *miR172a/b*. Each data point indicates an average of three independent biological replicates with the lines indicating SD. "V." Stands for vegetative phase. qPCR was performed using 3 individual biological replicates with 2 technical replicates. Value of WT early vegetative phase was denoted as 1.

A DEGs**B Upregulated****C Downregulated****D Upregulated****E Downregulated****F****G**

Supplementary Figure 8: Venn diagrams of DEGs in *se-1*, *toe1-2 toe2-1* and triple mutant.

DEGs determined by setting a threshold at $p < 0.05$ and $\text{Log}_2 \text{FC} > \pm 1$. Venn diagram was drawn using Adobe Illustrator. Figures are graphical representation of the values.

| Genotype | Days after Germination |
|---------------------------|------------------------|
| WT | 19.7 ± 1.0 |
| <i>se-1</i> | 21.4 ± 1.6 |
| <i>toe1-2 toe2-1</i> | 15.2 ± 1.0 |
| <i>toe1-2 toe2-1 se-1</i> | 16.7 ± 1.2 |

Supplementary table 1: No of days until bolting for WT, *se-1*, *toe1-2 toe2-1* and *toe1-2 toe2-1 se-1*.

| No. | Name | Forward/Reverse | Sequence |
|------|-----------------------------|-----------------|---------------------------------|
| 44 | mir156-Forwardprimer | F | GCGGCGGTGACAGAAGAGAGT |
| 47 | RT-universal-Reverse-primer | R | GTGCAGGGTCCGAGGT |
| 48 | Tubulin | F | GAGCCTTACAACGCTACTCTGTCTGTC |
| 49 | Tubulin | R | ACACCAGACATAGTAGCAGAAATCAAG |
| 73 | SPL3 | F | ACGCTTAGCTGGACACAACGAGAGAAG |
| 74 | SPL3 | R | TGGAGAAACAGACAGAGACACAGAGGA |
| 99 | GW1-TOPO sequencing | F | GTTGCAACAAATTGATGAGCAATGC |
| 100 | GW2-TOPO sequencing | R | GTTGCAACAAATTGATGAGCAATTA |
| 180 | miR172a/b | F | CCGTCGAGAATCTTGATGATG |
| 304 | <i>se-1</i> | R | CTA CAA GCT CCT GTA ATC AAT AAC |
| 305 | <i>se-1</i> | F | CCA CCT GAA GTT GCT ATG CAG |
| 1413 | SPL10 | F | AAGGTGTGGGAGAATGCTCA |
| 1414 | SPL10 | R | TCAGATGAAATGACTAGGGAA |
| 2298 | AL7 | F | ATGGAAGGAATTCAGCATCC |
| 2299 | AL7 | R | TCAGGCTTTCATTTTCTTGCTGGTAG |
| 2300 | AL6 | R | TCAAGGTCTAGCTCTCTTGTTACTG |
| 2318 | AL6 | F | ATGGAGGGAATTACTIONCATCC |
| 2834 | LBb1.3 | | ATTTTGCCGATTTTCGGAAC |
| 2842 | TOE2 | F | ATGCTGGATCTCAATCTCGAC |
| 2843 | TOE2 | R | CTATGGTGGTGGTTGTGG |
| 3145 | IAA34 | F | ATGTATTGCAGCGATCCTCC |
| 3146 | IAA34 | R | TTAAAAGGGAAGTACAGCATCG |
| 3149 | WRKY49 | F | ATGGAAGAAGAAGGTTATCAGTG |

| | | | |
|-------------|--------------------|---|---------------------------|
| 3150 | WRKY49 | R | TCAAGAAGCTGTCAAAACACTG |
| 3151 | MYBC1 | F | ATGAGAGAAGATAATCCAAATTGG |
| 3152 | MYBC1 | R | TTAATTTCCGGCAGGGAAGAGC |
| 4927 | IAA32 | F | ATGGACCCAAACACACCTGC |
| 4928 | IAA32 | R | TTAAAAGGGAAGAAGAGCATCG |
| 4929 | TOE1 | F | ATGTTGGATCTTAACCTCAACG |
| 4930 | TOE1 | R | TTAAGGGTGTGGATAAAAGTAACC |
| 4931 | IAA34 crispr | F | attgAGACTACGGTGATTCACGTT |
| 4932 | IAA34 crispr | R | aaacCAACGTGAATCACCGTAGTCT |
| 4933 | IAA34 crispr | F | attgAGTTCATAGAAAGCGTGGAG |
| 4934 | IAA34 crispr | R | aaacCTCCACGCTTTCTATGAACT |
| 4937 | IAA32 crispr | F | attgCTAATGGGGTGGTGGGAAAA |
| 4938 | IAA32 crispr | R | aaacTTTTCCCACCACCCATTAG |
| 4939 | IAA32 crispr | F | attgCATTGAGGAACTAGTTGT |
| 4940 | IAA32 crispr | R | aaacACAAC TAGTTCCTCGAATG |
| 5067 | pDGE347 sequencing | F | AGCTCCATTAGAGCCCAAACC |
| 5260 | SMZ | F | ATGTTGGATC TTAACCTAAA |
| 5261 | SMZ | R | CTATGGATCAAAACAATTGG |
| 5262 | SNZ | F | ATGTTGGACC TCAACCTCGG |
| 5263 | SNZ | R | TCATGGATCAAAACAAGATA |
| 5266 | <i>toe1-2</i> | F | TAGGTGGTTTCGACACTGCTC |
| 5267 | <i>toe1-2</i> | R | CGAGGATCCATAAGGAAGAGG |
| 5268 | <i>toe2-1</i> | F | GAATTTGACAGCAGCTCGATC |
| 5269 | <i>toe2-1</i> | R | TGTTTATTTCAAATCGACGGC |
| 5444 | AL3 | F | ATGGAAGGTGGAGCTGCTCT |
| 5445 | AL3 | R | TTAAGCTCGAGCTCTTTTGTTGC |
| 5446 | AL4 | F | ATGGAAGCAGGTGGCGCGTA |
| 5447 | AL4 | R | TTAGGAACGAGCCCTTTTGTTG |

| | | | |
|-------------|--------------------|---|----------------------------|
| 5448 | AL5 | F | ATGGAAGGAGGAACTGCGCA |
| 5449 | AL5 | R | CTAGGGTCGTGCTCTTTTGT |
| 5450 | AL1 | F | ATGGCCGCTGAGTCTTCTAA |
| 5451 | AL1 | R | TCACTGTCTTCCTTTCTTAGTGCAGC |
| 5452 | AL2 | F | ATGGCCGCCGCAGCCGTTT |
| 5453 | AL2 | R | TCACTGTCTTCCTTTCTTTG |
| 5732 | AL4 genotyping | F | GCCGGCGAAAGTTTGGTTT |
| 5735 | AL4 genotyping | R | GATACACAGAAGCGAGCGGT |
| 5744 | AL7 genotyping | F | GTGACGATCTCTGGCACACT |
| 5745 | AL7 genotyping | R | GCTTCTACCTTGCCACCACT |
| 5746 | AL7 genotyping | F | TGCAAGAGTTCCTTTCGGGT |
| 5747 | AL7 genotyping | R | ACGTTTTCTCTTTCACAGGC |
| 5830 | <i>al5</i> mutant | F | TTCAATAAAGCACAGCACTGG |
| 5831 | <i>al5</i> mutant | R | TGGGTTGAGGAATCAAATCTG |
| 5832 | <i>al6</i> mutant | F | GAAAAGAAAAGACATCACCAACTG |
| 5833 | <i>al6</i> mutant | R | TTATGAATCGCACCAATCTGG |
| 5856 | TOE2 no stop codon | R | TGGTGGTGGTTGTGGGCGGTTCA |
| 5857 | TOE1 no stop codon | R | AGGGTGTGGATAAAAAGTAACCACG |
| 6007 | <i>al1-5'</i> | F | TGGAACCATTGATGCAGACCTC |
| 6008 | <i>al1-5'</i> | R | GAGCTCGTTTACCCGGATC |
| 6009 | <i>al1-3'</i> | F | TGGAAGAGAGCTATGAAGATGAAG |
| 6010 | <i>al1-3'</i> | R | CATGTCTCATACCCTCATTACTA |
| 6011 | <i>al2-5'</i> | F | ATGGGAAGTGAATCTACCAGCAG |
| 6012 | <i>al2-5'</i> | R | CTTCACATGAGAAGAGCCAGGAT |
| 6015 | <i>al3-5'</i> | F | AGATCGGGTCTCGTCAC |
| 6016 | <i>al3-5'</i> | R | GAACATAGATCGGAGAAGATAAC |
| 6017 | <i>al3-3'</i> | F | TGGGAATGCAGAGAACTTCAG |
| 6018 | <i>al3-3'</i> | R | CTAGCTGGAGTGATCTTCACAC |

| | | | |
|--------------|---------------|---|------------------------------|
| CR157 | <i>al4 3'</i> | F | attGAGCAAGGTGAAACACAGTG |
| CR158 | <i>al4 3'</i> | R | aaacCACTGTGTTTCACCTTGCTC |
| CR159 | <i>al4 5'</i> | F | attgACTCACCGGGATCACAAAGT |
| CR160 | <i>al4 5'</i> | R | aaacACTTTGTGATCCCGGTGAGT |
| CR169 | <i>al7 3'</i> | F | attGTGTGAGATTCAGAATGACG |
| CR170 | <i>al7 3'</i> | R | aaaCGTCATTCTGAATCTCACAC |
| CR171 | <i>al7 5'</i> | F | attGGTAACGAAATAACTCACCA |
| CR172 | <i>al7 5'</i> | R | aaacTGGTGAGTTATTTTCGTTACC |
| CR173 | <i>al1 5'</i> | F | attGCGAGGGTTAGAAGACTCAGCGG |
| CR174 | <i>Al1 5'</i> | R | aaacCCGCTGAGTCTTCTAACCCCTCGC |
| CR175 | <i>al1 3'</i> | F | attgTGTGTGAACGTTGGTACCATGGG |
| CR176 | <i>al1 3'</i> | R | aaacCCCATGGTACCAACGTTACACA |
| CR177 | <i>al2 5'</i> | F | attgCCTCTCATTGCGATTAAGACGGG |
| CR178 | <i>al2 5'</i> | R | aaacCCCGTCTTAATCGCAATGAGAGG |
| CR179 | <i>al2 3'</i> | F | attgTGGAGGTCATTACACAAATGAGG |
| CR180 | <i>al2 3'</i> | R | aaacCCTCATTGTGTAATGACCTCCA |
| CR181 | <i>al3 5'</i> | F | attGGTGGTGAGAGCTTTGACAATGG |
| CR182 | <i>al3 5'</i> | R | aaacCCATTGTCAAAGCTCTCACCACC |
| CR183 | <i>al3 3'</i> | F | attgCTCCACAAAGGGTTTCCCCGTGG |
| CR184 | <i>al3 3'</i> | R | aaacCCACGGGGAAACCCTTTGTGGAG |

Supplementary table 2: List of primers used in the study

| Plant number | Genotype | Remarks |
|--------------|---------------------------|---|
| SP1 | WT Col-0 | |
| SP7 | <i>se-1</i> | |
| SP16 | <i>toe1-2 toe2-1</i> | SALK_069677 and SALK_065370 |
| SP27 | <i>iaa32 iaa34</i> | CRISPR T1 generation. <i>iaa34</i> segregating |
| SP55 | <i>toe1-2 toe2-1 se-1</i> | Crossing of <i>toe1-2 toe2-1</i> with <i>se-1</i> |
| SP122 | <i>al5 al6</i> | SALK_075676 and SALK_040877 |
| SP159 | <i>al4 al5 al6</i> | CRISPR mutants |
| SP201 | <i>al4 al5 al6 al7</i> | CRISPR mutants |
| SP202 | <i>al4 al5 al6 al7</i> | CRISPR mutants |

Supplementary Table 3: List of transformants generated in this study. List of mutants used in this study.

| Number | Insert | Vector backbone | Remarks |
|--------|-----------------------|-----------------|---------------------|
| SP6 | WRKY49 | pGBKT7 | |
| SP7 | WOX9 | pGADT7 | |
| SP8 | WOX9 | pGBKT7 | |
| SP9 | MYBC1 | pGBKT7 | |
| SP22 | IAA34 | pCR8-GW-TOPO | Generated by Imke |
| SP36 | IAA34 | pGBKT7 | Generated by Imke |
| SP44 | IAA34 | pGADT7 | Generated by Imke |
| SP48 | TOE2 | pCR8-GW-TOPO | Generated by Imke |
| SP49 | TOE2 | pGBKT7 | |
| SP54 | TOE2 | pGWB421 | |
| SP55 | TOE2 | pGWB655 | |
| SP56 | IAA34 | pGWB655 | |
| SP57 | IAA34 | pGWB655 | |
| SP58 | TOE2 | pGWB655 | |
| SP105 | laa32 iaa34 5' and 3' | pDGE347 | |
| SP118 | TOE1 | pCR8-GW-TOPO | Generated by Thilo |
| SP122 | TOE1 | pGWB655 | Generated by Thilo |
| SP126 | IAA32 | pCR8-GW-TOPO | Generated by Thilo |
| SP127 | SNZ | pCR8-GW-TOPO | Generated by Thilo |
| SP128 | TOE1 | pGADT7 | Generated by Thilo |
| SP129 | IAA32 | pGADT7 | Generated by Thilo |
| SP130 | SNZ | pGADT7 | Generated by Thilo |
| SP131 | TOE1 | pGBKT7 | Generated by Thilo |
| SP132 | IAA32 | pGBKT7 | Generated by Thilo |
| SP133 | SNZ | pGBKT7 | Generated by Thilo |
| SP171 | AL1 | pCR8-GW-TOPO | |
| SP172 | AL2 | pCR8-GW-TOPO | Generated by Svenja |

| | | | |
|-------|--------------------|--------------|---------------------|
| SP173 | AL3 | pCR8-GW-TOPO | Generated by Svenja |
| SP174 | AL4 | pCR8-GW-TOPO | Generated by Svenja |
| SP175 | AL5 | pCR8-GW-TOPO | Generated by Svenja |
| SP180 | AL1 | pGADT7 | |
| SP181 | AL2 | pGADT7 | |
| SP182 | AL3 | pGADT7 | Generated by Svenja |
| SP183 | AL4 | pGADT7 | Generated by Svenja |
| SP184 | AL5 | pGADT7 | Generated by Svenja |
| SP185 | AL6 | pGADT7 | Generated by Svenja |
| SP186 | AL7 | pGADT7 | |
| SP195 | AL2 | pGWB655 | |
| SP196 | AL4 | pGWB655 | |
| SP197 | AL3 | pGWB655 | |
| SP198 | AL7 | pGWB655 | |
| SP199 | AL5 | pGWB655 | |
| SP212 | AL6 | pGWB655 | |
| SP219 | AL1 | pGBKT7 | |
| SP220 | AL1 | pGWB655 | |
| SP230 | al4, al7 5' and 3' | pDGE347 | |
| SP234 | TOE1 no stop | pCR8-GW-TOPO | |
| SP235 | TOE1 no stop | pGWB654 | |
| SP237 | TOE2 no stop gDNA | pCR8-GW-TOPO | |
| SP238 | TOE2 no stop gDNA | pGWB654 | |

Supplementary table 4: List of constructs generated in this study.

9 Curriculum Vitae

Personal Information

Shruti Sameer Pande

Born on 09.04.1994 in Jalgaon, India

School Education

| | |
|-----------|----------------------------------|
| 2000-2007 | Elementary School in Pune, India |
| 2007-2010 | Highschool in Pune, India |
| 2010-2012 | Junior College in Pune, India |

Higher Education

| | |
|-----------|--|
| 2012-2015 | B.Sc. in Biotechnology from University of Pune, Pune, India |
| 2015 | M.Sc. in Biochemistry and Molecular Biology from Universität Bremen, Germany. |
| 2017 | Internship to develop skillset in handling <i>Ceanorhabditis elegans</i> in Salcini Group from Biotech Research and Innovation Centre, University of Copenhagen, Denmark |
| 2017-2018 | Master thesis in Groß-Hardt Group from Universität Bremen, Title: Towards identification of factors affecting plant reproduction in <i>Arabidopsis Thaliana</i> |
| 2018-2022 | PhD thesis in Laubinger Group from Carl von Ossietzky Universität Oldenburg. Title: To Study and Evaluate the Interacting Partners of SERRATE in <i>Arabidopsis thaliana</i> . |

Publication

- 2021 Siadjeu C, Mayland-Quellhorst E, Pande S, Laubinger S, Albach DC. Transcriptome Sequence Reveals Candidate Genes Involving in the Post-Harvest Hardening of Trifoliolate Yam *Dioscorea dumetorum*. *Plants*. 2021; 10(4):787.

Scholarships

- 2016 DAAD scholarship for internship (3 months) in Biotechnology Research and Innovation Centre, University of Copenhagen. Title: Role of JMJD-5 in maintenance of germline identity in *Caenorhabditis elegans*.
- 2017 Biochemistry and Molecular Biology symposium, 2017
First prize for Poster Presentation. Title: "Role of JMJD-5 in maintenance of germline identity in *Caenorhabditis elegans*."

Im Selbstverlag herausgegeben von

Shruti Pande